

5-9-2015

# Synthesis and Characterization of C8 and N2 2'-Deoxyguanosine Adducts of 6-Nitrochrysene, A Cancer-Causing Agent

Kimberly R. Rebello

University of Connecticut - Storrs, [kimberlyrebello@sbcglobal.net](mailto:kimberlyrebello@sbcglobal.net)

---

## Recommended Citation

Rebello, Kimberly R., "Synthesis and Characterization of C8 and N2 2'-Deoxyguanosine Adducts of 6-Nitrochrysene, A Cancer-Causing Agent" (2015). *Master's Theses*. 780.  
[https://opencommons.uconn.edu/gs\\_theses/780](https://opencommons.uconn.edu/gs_theses/780)

This work is brought to you for free and open access by the University of Connecticut Graduate School at OpenCommons@UConn. It has been accepted for inclusion in Master's Theses by an authorized administrator of OpenCommons@UConn. For more information, please contact [opencommons@uconn.edu](mailto:opencommons@uconn.edu).

***Synthesis and Characterization of C8 and N<sup>2</sup> 2'-  
Deoxyguanosine Adducts of 6-Nitrochrysene,  
A Cancer-Causing Agent***

Kimberly Romana Rebello  
B. Sc., University of Connecticut, 2015

A Thesis Submitted in Partial Fulfillment  
for the Degree of Master of Science at the  
University of Connecticut

2015

Copyright by  
Kimberly Romana Rebello

2015

## APPROVAL PAGE

Master of Science Thesis

### Synthesis and Characterization of C8 and $N^2$ 2'-Deoxyguanosine Adducts of 6-Nitrochrysene, A Cancer-Causing Agent

Presented by  
Kimberly Romana Rebello, B. Sc.

Major Advisor Ashis K Basu

Dr. Ashis K. Basu

Associate Advisor Amy R. Howell

Dr. Amy R. Howell

Associate Advisor Angela Boza

Dr. Alfredo Angeles-Boza

University of Connecticut  
2015

### ***Dedication***

I dedicate my work to my parents, Kennedy and Corina Rebello. Their endless love and care give me the strength and confidence to complete everything I put my mind to. I will always appreciate all that they do and words cannot express my love and gratitude towards them.

### *Acknowledgements*

I would like to express my deep appreciation and gratitude for the mentorship, guidance, and support that was given to me by my advisor, Dr. Ashis Basu over these past four years. His confidence in me encouraged me to persevere in my work and without his help, I would not have been able to get both my Bachelor's and Master's degrees. He gave me the opportunity to develop as a chemist by giving me so much independence. I extend this thanks to the remainder of my advising committee: Dr. William Bailey, who taught me organic chemistry; Dr. Amy Howell, who continued my graduate studies in the same field; Dr. Alfredo Angeles-Boza, who assisted me with my final defense.

In particular, I want to thank my lab mates, who have made the last four years so much fun. I'm grateful to the graduate students who mentored me when I first entered college, Dr.'s Rajat Das, Savithri Weerasooriya, and Vijay Jasti. Their teaching and patience served to instill in me the fundamental principles of research, as well as the basics of bench work. I would also like to thank Arindom Chatterjee, who was a close friend and mentor throughout my final years. In addition, thank you to all the other graduate students for your support and advice: Dr.'s Varsha Pednekar, Paritosh Pande, and Chanchal Malik, along with Arindom Bose, Vidya Boyanapalli, Nadeeshani Jayathilake, Chaitra Veerabhadrapasurugi, Spandana Naldiga, and Brent Powell.

I would also like to express my gratitude for the undergraduates that worked alongside me in lab, Stuart Mehrens and Christopher Zins. Additionally, I thank those who were senior to me, Savas Tsikis, Ashley Clemens, Laura Baumann, and Samantha Gallagher. I wish the best of luck to the other undergraduates who were always willing to assist me, Vruksha Upadhyay and Hamsa Ganapathi.

Furthermore, I would like to acknowledge Michael Mercadante and Christopher Kelly, both of whom were dear friends for the past four years, always ready to offer a helping hand. Alongside them, I would like to thank my roommates, Selena Roy, and Hannah and Elizabeth Tripp. Their assistance, support, and

care have shaped the person I am today. I truly value their friendship; the many late nights spent working with them while laughing and joking with each other are the highlights of my college years.

Finally, I give my heartfelt gratitude to my parents, Kennedy and Corina Rebello, whom this thesis is dedicated to. They have always believed in me and without their love I would not be where I am today. Their support and strength helped me to overcome numerous setbacks and aided me to remain focused on my studies ahead.

## *Table of Contents*

Title	i
Copyright	ii
Approval	iii
Dedication	iv
Acknowledgements	v
Table of Contents	vii
List of Figures	viii
List of Tables	x
List of Schemes	x
List of Abbreviations	x
 Abstract	 xi
 I. Introduction	 1
1.1 DNA Damage	2
1.2 Polycyclic Aromatic Hydrocarbons	5
1.3 Metabolic Activation of 6-Nitrochrysene	6
1.4 Buchwald-Hartwig Palladium-Catalyzed Coupling Reactions	9
1.5 Solid Phase Oligonucleotide Synthesis	11
 II. Synthesis of the C8 Phosphoramidite Monomer of 8-(N-6-aminochrysene)-N <sup>2</sup> -DMF-5'-O-(4,4'-dimethoxytrityl)-2'-deoxyguanosine	 14
2.1 Scheme for the 6-NC C8-dG Phosphoramidite Monomer	15
2.2 Materials and Methods	16
2.3 Results and Discussion	28
 III. Synthesis of the N <sup>2</sup> Phosphoramidite Monomer of N <sup>2</sup> -(6-aminochrysene)-5'-O-(4,4'-dimethoxytrityl)-2'-deoxyguanosine	 30
3.1 Original Synthetic Scheme for the 6-NC N <sup>2</sup> -dG Adduct	31
3.2 Materials and Methods	33
3.3 Results and Discussion	41
3.4 Modified Synthetic Scheme for the 6-NC N <sup>2</sup> -dG Adduct	46
3.5 Materials and Methods	48
3.6 Results and Discussion	50
 IV. Conclusion and Future Work	 53
4.1 Conclusion	54
4.2 Future Work	55
 References	 57
 Appendix A: NMR and Mass Spectra for C8-CR-dG Adduct	 60
Appendix B: NMR and Mass Spectra for N <sup>2</sup> -CR-dG Adduct	94



## List of Figures

<b>Figure 1</b>	BER, Short and Long Patch Repair	3
<b>Figure 2</b>	NER, Process Scheme	3
<b>Figure 3</b>	Common Carcinogenic PAHs, (a) benzo[a]pyrene, (b) 6-nitrochrysene, (c) 2-nitrofluorene, (d) 3-nitrobenzanthrone	5
<b>Figure 4</b>	Regions of Polycyclic Aromatic Hydrocarbon Ring Systems	7
<b>Figure 5</b>	Polycyclic Aromatic Hydrocarbon Diol Epoxides	7
<b>Figure 6</b>	Metabolic Activation of 6-Nitrochrysene	8
<b>Figure 7</b>	General Outline of Buchwald-Hartwig Cross Coupling Reaction	9
<b>Figure 8</b>	Key C-N Bond Formation within dG Systems	9
<b>Figure 9</b>	Revised Catalytic Mechanism for the Buchwald-Hartwig Cross-Coupling	10
<b>Figure 10</b>	Racemic 2,2'-Bis(diphenylphosphino)-1,1'-binaphthalene	11
<b>Figure 11</b>	General Synthetic Outline for Phosphoramidite Monomer Prior to Solid Phase Synthesis	12
<b>Figure 12</b>	Cycle for Solid Phase Oligonucleotide Synthesis	13
<b>Figure 13</b>	General Outline of the Suzuki Coupling with Major Products	42
<b>Figure 14</b>	Final Oligomer for the C8-dG Adduct Incorporation	55
<b>Figure 15</b>	<sup>1</sup> H-NMR of 6-Nitrochrysene	61
<b>Figure 16</b>	<sup>1</sup> H-NMR of 6-Aminochrysene	62
<b>Figure 17</b>	<sup>13</sup> C-NMR of 6-Aminochrysene	63
<b>Figure 18</b>	<sup>1</sup> H-NMR of 8-Bromo-2'-deoxyguanosine	64
<b>Figure 19</b>	<sup>13</sup> C-NMR of 8-Bromo-2'-deoxyguanosine	65
<b>Figure 20</b>	<sup>1</sup> H-NMR of 8-Bromo-3',5'-O-bis( <i>tert</i> -butyldimethylsilyl)-2'-deoxyguanosine	66
<b>Figure 21</b>	<sup>13</sup> C-NMR of 8-Bromo-3',5'-O-bis( <i>tert</i> -butyldimethylsilyl)-2'-deoxyguanosine	67
<b>Figure 22</b>	<sup>1</sup> H-NMR of O <sup>6</sup> -Benzyl-8-bromo-3',5'-O-bis( <i>tert</i> -butyldimethylsilyl)-2'-deoxyguanosine	68
<b>Figure 23</b>	<sup>13</sup> C-NMR of O <sup>6</sup> -Benzyl-8-bromo-3',5'-O-bis( <i>tert</i> -butyldimethylsilyl)-2'-deoxyguanosine	69
<b>Figure 24</b>	<sup>1</sup> H-NMR of O <sup>6</sup> -Benzyl-8-bromo-3',5'-O-bis( <i>tert</i> -butyldimethylsilyl)-N <sup>2</sup> -dimethoxytrityl-2'-deoxyguanosine	70
<b>Figure 25</b>	<sup>13</sup> C-NMR of O <sup>6</sup> -Benzyl-8-bromo-3',5'-O-bis( <i>tert</i> -butyldimethylsilyl)-N <sup>2</sup> -dimethoxytrityl-2'-deoxyguanosine	71
<b>Figure 26</b>	<sup>1</sup> H-NMR of 8-(N-6-Aminochrysene)-O <sup>6</sup> -benzyl-3',5'-O-bis( <i>tert</i> -butyldimethylsilyl)-N <sup>2</sup> -dimethoxytrityl-2'-deoxyguanosine	72
<b>Figure 27</b>	<sup>13</sup> C-NMR of 8-(N-6-Aminochrysene)-O <sup>6</sup> -benzyl-3',5'-O-bis( <i>tert</i> -butyldimethylsilyl)-N <sup>2</sup> -dimethoxytrityl-2'-deoxyguanosine	73
<b>Figure 28</b>	Mass Spectrum of 8-(N-6-Aminochrysene)-O <sup>6</sup> -benzyl-3',5'-O-bis( <i>tert</i> -butyldimethylsilyl)-N <sup>2</sup> -dimethoxytrityl-2'-deoxyguanosine	74
<b>Figure 29</b>	<sup>1</sup> H-NMR of 8-(N-6-Aminochrysene)-O <sup>6</sup> -benzyl-3',5'-O-bis( <i>tert</i> -butyldimethylsilyl)-2'-deoxyguanosine	75
<b>Figure 30</b>	<sup>13</sup> C-NMR of 8-(N-6-Aminochrysene)-O <sup>6</sup> -benzyl-3',5'-O-bis( <i>tert</i> -butyldimethylsilyl)-2'-deoxyguanosine	76
<b>Figure 31</b>	Mass Spectrum of 8-(N-6-Aminochrysene)-O <sup>6</sup> -benzyl-3',5'-O-bis( <i>tert</i> -butyldimethylsilyl)-2'-deoxyguanosine	77
<b>Figure 32</b>	<sup>1</sup> H-NMR of 8-(N-6-Aminochrysene)-3',5'-O-bis( <i>tert</i> -butyldimethylsilyl)-2'-deoxyguanosine	78
<b>Figure 33</b>	<sup>13</sup> C-NMR of 8-(N-6-Aminochrysene)-3',5'-O-bis( <i>tert</i> -butyldimethylsilyl)-2'-deoxyguanosine	79
<b>Figure 34</b>	Mass Spectrum of 8-(N-6-Aminochrysene)-3',5'-O-bis( <i>tert</i> -butyldimethylsilyl)-2'-deoxyguanosine	80
<b>Figure 35</b>	<sup>1</sup> H-NMR of 8-(N-6-Aminochrysene)-3',5'-O-bis( <i>tert</i> -butyldimethylsilyl)-N <sup>2</sup> -DMF-2'-deoxyguanosine	81
<b>Figure 36</b>	<sup>13</sup> C-NMR of 8-(N-6-Aminochrysene)-3',5'-O-bis( <i>tert</i> -butyldimethylsilyl)-N <sup>2</sup> -DMF-2'-deoxyguanosine	82

<b>Figure 37</b>	Mass Spectrum of 8-(N-6-Aminochrysene)-3',5'-O-bis( <i>tert</i> -butyldimethylsilyl)-N <sup>2</sup> -DMF-2'-deoxyguanosine	83
<b>Figure 38</b>	<sup>1</sup> H-NMR of 8-(N-6-Aminochrysene)-N <sup>2</sup> -DMF-2'-deoxyguanosine	84
<b>Figure 39</b>	<sup>13</sup> C-NMR of 8-(N-6-Aminochrysene)-N <sup>2</sup> -DMF-2'-deoxyguanosine	85
<b>Figure 40</b>	Mass Spectrum of 8-(N-6-Aminochrysene)-N <sup>2</sup> -DMF-2'-deoxyguanosine	86
<b>Figure 41</b>	<sup>1</sup> H-NMR of 8-(N-6-Aminochrysene)-N <sup>2</sup> -DMF-5'-O-(4,4'-dimethoxytrityl)-2'-deoxyguanosine	87
<b>Figure 42</b>	<sup>13</sup> C-NMR of 8-(N-6-Aminochrysene)-N <sup>2</sup> -DMF-5'-O-(4,4'-dimethoxytrityl)-2'-deoxyguanosine	88
<b>Figure 43</b>	Mass Spectrum of 8-(N-6-Aminochrysene)-N <sup>2</sup> -DMF-5'-O-(4,4'-dimethoxytrityl)-2'-deoxyguanosine	89
<b>Figure 44</b>	<sup>1</sup> H-NMR of 8-(N-6-Aminochrysene)-N <sup>2</sup> -DMF-5'-O-(4,4'-dimethoxytrityl)-3'-cyanoethyl-2'-deoxyguanosine phosphoramidite	90
<b>Figure 45</b>	<sup>13</sup> C-NMR of 8-(N-6-Aminochrysene)-N <sup>2</sup> -DMF-5'-O-(4,4'-dimethoxytrityl)-3'-cyanoethyl-2'-deoxyguanosine phosphoramidite	91
<b>Figure 46</b>	<sup>31</sup> P-NMR of 8-(N-6-Aminochrysene)-N <sup>2</sup> -DMF-5'-O-(4,4'-dimethoxytrityl)-3'-cyanoethyl-2'-deoxyguanosine phosphoramidite	92
<b>Figure 47</b>	Mass Spectrum of 8-(N-6-Aminochrysene)-N <sup>2</sup> -DMF-5'-O-(4,4'-dimethoxytrityl)-3'-cyanoethyl-2'-deoxyguanosine phosphoramidite	93
<b>Figure 48</b>	<sup>1</sup> H-NMR of 1,2-Dihydronaphtho[2,1-b]furan-1,2-diol	95
<b>Figure 49</b>	<sup>13</sup> C-NMR of 1,2-Dihydronaphtho[2,1-b]furan-1,2-diol	96
<b>Figure 50</b>	Mass Spectrum of 1,2-Dihydronaphtho[2,1-b]furan-1,2-diol	97
<b>Figure 51</b>	<sup>1</sup> H-NMR of Naphtho[2,1-b]furan-2(1H)-one	98
<b>Figure 52</b>	<sup>13</sup> C-NMR of Naphtho[2,1-b]furan-2(1H)-one	99
<b>Figure 53</b>	Mass Spectrum of Naphtho[2,1-b]furan-2(1H)-one	100
<b>Figure 54</b>	<sup>1</sup> H-NMR of Ethyl 2-(2-hydroxynaphthalen-1-yl)acetate	101
<b>Figure 55</b>	<sup>13</sup> C-NMR of Ethyl 2-(2-hydroxynaphthalen-1-yl)acetate	102
<b>Figure 56</b>	Mass Spectrum of Ethyl 2-(2-hydroxynaphthalen-1-yl)acetate	103
<b>Figure 57</b>	<sup>1</sup> H-NMR of Ethyl 2-(2-(((trifluoromethyl)sulfonyl)oxy)naphthalen-1-yl)acetate	104
<b>Figure 58</b>	<sup>13</sup> C-NMR of Ethyl 2-(2-(((trifluoromethyl)sulfonyl)oxy)naphthalen-1-yl)acetate	105
<b>Figure 59</b>	<sup>19</sup> F-NMR of Ethyl 2-(2-(((trifluoromethyl)sulfonyl)oxy)naphthalen-1-yl)acetate	106
<b>Figure 60</b>	Mass Spectrum of Ethyl 2-(2-(((trifluoromethyl)sulfonyl)oxy)naphthalen-1-yl)acetate	107
<b>Figure 61</b>	<sup>1</sup> H-NMR of Ethyl 2-(2-(2-formylphenyl)naphthalen-1-yl)acetate	108
<b>Figure 62</b>	<sup>1</sup> H-NMR of Ethyl chrysene-5-carboxylate	109
<b>Figure 63</b>	<sup>13</sup> C-NMR of Ethyl chrysene-5-carboxylate	110
<b>Figure 64</b>	Mass Spectrum of Ethyl chrysene-5-carboxylate	111
<b>Figure 65</b>	<sup>1</sup> H-NMR of Chrysene-5-carboxylic acid	112
<b>Figure 66</b>	<sup>13</sup> C-NMR of Chrysene-5-carboxylic acid	113
<b>Figure 67</b>	<sup>1</sup> H-NMR of Chrysene-5-carboxamide	114
<b>Figure 68</b>	<sup>1</sup> H-NMR of 3',5'-O-Bis( <i>tert</i> -butyldimethylsilyl)-2'-deoxyguanosine	115
<b>Figure 69</b>	<sup>13</sup> C-NMR of 3',5'-O-Bis( <i>tert</i> -butyldimethylsilyl)-2'-deoxyguanosine	116
<b>Figure 70</b>	<sup>1</sup> H-NMR of O <sup>6</sup> -Benzyl-3',5'-O-bis( <i>tert</i> -butyldimethylsilyl)-2'-deoxyguanosine	117
<b>Figure 71</b>	<sup>13</sup> C-NMR of O <sup>6</sup> -Benzyl-3',5'-O-bis( <i>tert</i> -butyldimethylsilyl)-2'-deoxyguanosine	118
<b>Figure 72</b>	<sup>1</sup> H-NMR of Chrysen-5-ylmethanol	119
<b>Figure 73</b>	<sup>13</sup> C-NMR of Chrysen-5-ylmethanol	120
<b>Figure 74</b>	Mass Spectrum of Chrysen-5-ylmethanol	121
<b>Figure 75</b>	<sup>1</sup> H-NMR of Chrysene-5-carbaldehyde	122

### *List of Tables*

<b>Table 1</b>	Standardization of the Suzuki Coupling Reaction in the N <sup>2</sup> -dG Scheme	43
----------------	----------------------------------------------------------------------------------	----

### *List of Schemes*

<b>Scheme 1</b>	Synthetic Scheme for C8-CR-dG Phosphoramidite Monomer	15
<b>Scheme 2</b>	Original Synthetic Scheme for N <sup>2</sup> -CR-dG Phosphoramidite Monomer	31
<b>Scheme 3</b>	Modified Synthetic Scheme for N <sup>2</sup> -CR-dG Phosphoramidite Monomer	46

### *List of Abbreviations*

<b>6-AC</b>	6-aminochrysene	<b>LAH</b>	lithium aluminum hydride
<b>6-NC</b>	6-nitrochrysene	<b>MMTr</b>	4-monomethoxytrityl
<b>AP</b>	apurinic/apyrimidinic site	<b>N<sup>2</sup>-CR-dG</b>	N <sup>2</sup> -(6-aminochrysene)-5'-O-(4,4'-dimethoxytrityl)-3'-cyanoethyl-2'-deoxyguanosine phosphoramidite
<b>BER</b>	base excision repair	<b>NBS</b>	N-bromosuccinimide
<b>BINAP</b>	2,2'-bis(diphenylphosphino)-1,1'-binaphthyl	<b>NER</b>	nucleotide excision repair
<b>C8-CR-dG</b>	8-(N-6-Aminochrysene)-N <sup>2</sup> -DMF-5'-O-(4,4'-dimethoxytrityl)-3'-cyanoethyl-2'-deoxyguanosine phosphoramidite	<b>PAH</b>	polycyclic aromatic hydrocarbon
<b>DCM</b>	dichloromethane	<b>PAHDE</b>	polycyclic aromatic hydrocarbon diol epoxide
<b>DEAD</b>	diethyl azodicarboxylate	<b>PCC</b>	pyridinium chlorochromate
<b>dG</b>	2'-deoxyguanosine	<b>Pd<sub>2</sub>(dba)<sub>3</sub></b>	tris(dibenzylideneacetone)dipalladium (0)
<b>DIAD</b>	diisopropyl azodicarboxylate	<b>PDC</b>	pyridinium dichromate
<b>DMF</b>	dimethylformamide	<b>RNA</b>	ribonucleic acid
<b>DMTr</b>	4,4'-dimethoxytrityl	<b>TBDMS</b>	<i>tert</i> -butyldimethylsilyl
<b>DNA</b>	deoxyribonucleic acid	<b>TC-NER</b>	transcription-coupled nucleotide excision repair
<b><i>E. coli</i></b>	<i>Escherichia coli</i>	<b>TEA•3HF</b>	triethylamine trihydrofluoride
<b>GG-NER</b>	global genomic nucleotide excision repair	<b>TLS</b>	translesion synthesis
<b>HEK</b>	human embryonic kidney	<b>Triflate</b>	trifluoromethane sulfonate

### *Abstract*

Nitropolycyclic aromatic hydrocarbons are ubiquitous in the environment, and many compounds of this family are carcinogenic. 6-Nitrochrysene, a representative member of this group, is a suspected human carcinogen that has been shown to cause lung, breast, and other forms of cancer in rodents. It is believed that this derivative of chrysene causes cancer by forming DNA adducts, which, in turn, induce mutations in critical gene sequences. The goal of my research is to synthesize one or more of the major DNA adducts formed by 6-nitrochrysene, which will be introduced in DNA in order to study their biological effects.

The initiation step of the multi-step process that leads to cancer involves mutations in DNA via erroneous replication, which occurs when the body is unable to repair certain DNA damages. Accumulation of these mutations in critical genes triggers a series of biological events, ultimately making the cell an outlaw. Usually, there are specific processes the cell employs to repair DNA damages. Cancer-causing agents, such as 6-nitrochrysene, are metabolically activated in a cell to electrophilic species, which induce specific DNA damages resulting in a high frequency of mutations.

Understanding exactly how 6-nitrochrysene causes mutations will provide insight into how cancer by this chemical is initiated. In order to accomplish this, one must synthesize the damaged nucleoside and incorporate it into a DNA fragment. In this thesis, two new schemes are presented to prepare the 6-nitrochrysene-damaged DNA fragments.

I have completed the synthesis of the appropriately protected C8-dG 6-nitrochrysene adduct and its subsequent incorporation into an oligonucleotide by using a solid phase synthesis approach. This adducted oligonucleotide will be used for structural and biological studies.

I have also developed and refined a synthetic route towards the  $N^2$ -dG adduct. In this novel scheme, the precursor to the Buchwald-Hartwig coupling has been prepared, and the chrysene derivative is nearly complete. The subsequent steps are expected to proceed in good to excellent yield.

# **CHAPTER I**

## **INTRODUCTION**

## ***1.1 DNA Damages***

DNA acts as a carrier for all of the genetic information in an organism. When a cell undergoes replication, it is critical that the DNA undergoes faithful replication and pass the genetic information to the subsequent generation. The process of DNA replication is semi-conservative, since each strand of the double helix can act as a template for a new strand. This replication method gives the next generation one of the old strands, along with a newly synthesized strand. Due to the high fidelity of DNA polymerase, this process takes places with a very high degree of accuracy. However, the few errors that do occur allow for the mutations necessary to produce a variety of species through evolution.<sup>[1]</sup>

DNA possesses a number of nucleophilic centers in its structure and is therefore very susceptible to attack by various agents. These agents include, but are not limited to, ultraviolet light, natural and man-made chemicals, ionizing radiation, and reactive oxygen species.<sup>[2]</sup> All of these agents can induce DNA damages. The process by which the damage occurs can either be through direct reaction of the agent with DNA, or through metabolic processes within the cell which activate the agent and enable it to react with DNA. Chemical carcinogens are often metabolized by the cellular enzymes and are largely excreted. However, some of these metabolites may still react with DNA.<sup>[3-6]</sup>

If the cell is damaged, multiple pathways are pursued to rectify the damage or to avoid further damage to the organism. Among these is apoptosis, the process of programmed cell death. This can occur if the damage is great enough to induce a double strand break. There is also cell cycle checkpoint activation, which serves to halt the cell cycle at G1. Arrest of cell replication can occur through a variety of pathways, but it primarily proceeds through ubiquitination of key phosphatases to mark them for degradation. This triggers a series of cellular activities which serve to prevent the cell from transitioning to S phase.<sup>[3]</sup>

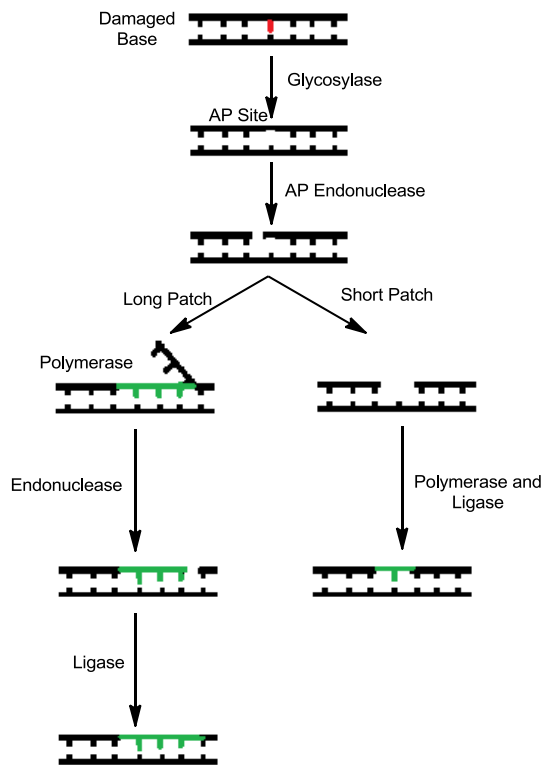


Figure 1: BER, Short and Long Patch Repair

BER. Current studies are attempting to determine what may be the deciding factor between these two pathways, but as of now, no decisive conclusion has been reached. Pol  $\beta$  is the primary DNA polymerase that repairs the strand in the short-patch pathway, although in its absence, pol  $\gamma$  can take over. In the long-patch pathway, pol  $\delta$  and pol  $\epsilon$  are the primary DNA polymerases; it should be noted that pol  $\beta$  can also take part in long-patch repair. In contrast, NER is employed to repair bulky or helix-distorting DNA adducts (Figure 2).<sup>[8]</sup> NER is initiated when a helical distortion is noted or when RNA polymerase stalls at some type of DNA lesion during transcription. The former initiation is referred to as GG-NER (global genomic NER) while the latter is referred to as TC-NER (transcription-coupled NER).

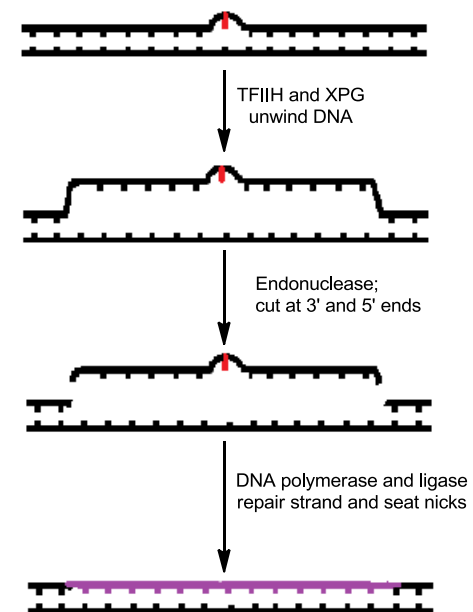


Figure 2: NER, Process Scheme



They differ only in their methods of identifying DNA damages. Thereafter, both pathways undergo the same process. DNA is unwound and a single-strand gap of 25-30 nucleotides around the damage is excised. DNA polymerases (usually pol  $\delta$ ,  $\epsilon$ , and/or  $\kappa$ ) are recruited to repair the strand, following which a ligase seals the nicks in the strand.

There is also a series of translesion synthesis (TLS) polymerases, which aid a cell in bypassing DNA lesions.<sup>[4,9]</sup> They restart stalled replications sites, but the major consequence of these polymerases are their higher rates of errors and aptitude for introducing mutations in the DNA sequence.<sup>[9a,c]</sup> The five known eukaryotic polymerases are Rev1, pol  $\zeta$ , pol  $\eta$ , pol  $\kappa$ , and pol  $\iota$ . These (with the exception of the pol  $\zeta$ , which is a B family polymerase) are part of the Y family of polymerases which are modified with specialized structures to allow for the ability to read through bulky lesions, insert bases opposite them, and carry out further extension.<sup>[9b]</sup> Their function is not to repair the damage, but to simply bypass the lesion. This allows for survival through DNA replication as opposed to maintaining the accuracy of the genetic information. Based on this, it is not surprising that DNA damage tolerance is often a mutagenic process.<sup>[9d]</sup> Replicative DNA polymerases make one error in  $10^6$ - $10^8$  bases, while TLS polymerases make errors once every  $10$ - $10^3$  bases. This reduced fidelity is likely due in part to some of the polymerases not using canonical Watson-Crick base pairing (ex. pol  $\iota$  and Rev1), whereas some do not undergo an induced fit upon nucleotide binding and may involve a limited contact with the template base. Altogether, cells' development of TLS polymerases to bypass DNA lesions and allow for restarting of stalled replication forks comes at the cost of higher mutational frequencies. Elaborate regulatory mechanisms are in place to limit the amount of mutations introduced during replication and this subject is still being investigated.<sup>[9e]</sup>

## 1.2 Polycyclic Aromatic Hydrocarbons

Polycyclic aromatic hydrocarbons (PAHs) are a family of compounds comprising hydrocarbons in multiple aromatic rings (Figure 3).<sup>[6]</sup> This family has been studied extensively and a number of its members have been associated with various carcinogenic effects in biological systems.<sup>[10]</sup> The

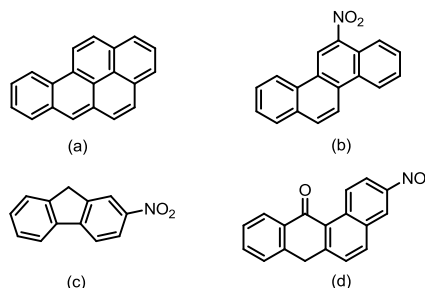


Figure 3: Common Carcinogenic PAHs, (a) benzo[a]pyrene, (b) 6-nitrochrysene, (c) 2-nitrofluorene, (d) 3-nitrobenzanthrone

first chemical carcinogen discovered was benzo[a]pyrene, one of the many chemical carcinogens present in cigarette smoke. Since then, the EPA has classified several PAHs as probable human carcinogens: benz[a]anthracene, benzo[a]pyrene, benzo[b]fluoranthene, benzo[k]fluoranthene, chrysene, dibenz[a,h]anthracene, and indeno[1,2,3-cd]pyrene. All of these are on the EPA's list of priority pollutants and are often targeted for measurement in environmental samples.<sup>[11,12]</sup>

A subfamily of the PAHs is the nitro-PAHs. Nitropolycyclic aromatic hydrocarbons were first studied intensively when 4-nitroquinoline-1-oxide (4-NQO) was reported as a potent carcinogen.<sup>[11]</sup> After the finding that this compound is carcinogenic, a number of other nitro-PAHs were found to be carcinogenic. In fact, the nitrated versions of the original PAHs proved to be even more carcinogenic than their unsubstituted counterparts. Members of this subfamily are easily found in various environmental samples, thereby warranting the extensive studies on their potential biological effects.

The original PAHs are capable of reacting with nitrogen oxides to form NO<sub>2</sub>-PAHs; this was first reported by Pitts et al.<sup>[11a]</sup> and Jager.<sup>[11b]</sup> These reactions proceed under conditions akin to polluted air and combustion processes. As such, it is not surprising that the nitro-PAHs are commonly found in diesel exhaust and cigarette smoke, along with coal fly ash, industrial waste, and refined oil products. Additionally, some have also been found in the charred portion of certain grilled foods. As is clearly demonstrated, human exposure to these compounds can occur through a variety of routes.

Multiple studies focusing on the public exposure to these carcinogens determine that several occupational groups are at a considerably higher risk for developing associated cancers.<sup>[5]</sup> These include coke oven workers, steelworkers, furnace workers, asphalt workers, and the general public in cities with a high degree of air pollution. The occupational risks are directly associated with the complex mixtures containing PAHs that these workers encounter on a day-to-day basis, which may include coal tar pitch, coke oven tar, and crumb rubber asphalt.<sup>[6]</sup> As expected, smokers also belong to a high exposure population.

### ***1.3 Metabolic Activation of 6-Nitrochrysene***

Human exposure to these carcinogens occurs primarily through inhalation but also by ingestion and dermal contact. Once introduced into the body, the polycyclic aromatic hydrocarbons are capable of being biologically activated through metabolism.<sup>[13,14]</sup> The process of metabolism of each of the PAHs usually results eventually in what is referred to as the “ultimate carcinogen”, the most reactive and mutagenic derivative of the PAH.<sup>[13a]</sup> Usually, the original PAH – such as pyrene or chrysene – is not nearly as carcinogenic as some of its derivatives.

Chrysene in particular is notably less carcinogenic than its nitrated form.<sup>[13b-d]</sup> It is commonly found in exhaust mixtures of high temperature, such as coke oven exhaust or consumed engine oil. Although the abundance of 6-nitrochrysene is far reduced compared to other members of its family, it is the most potent tumor-inducing agent in animal studies among all tested nitroaromatic compounds.<sup>[13]</sup> It also exhibits one of the highest carcinogenic potencies in experimental animals among a broad spectrum of PAH metabolites.

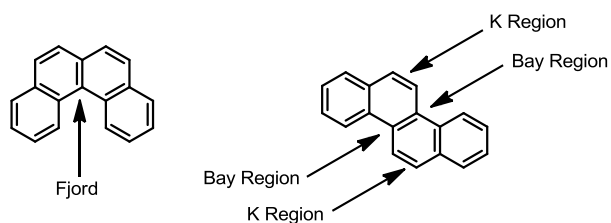


Figure 4: Regions of Polycyclic Aromatic Hydrocarbon Ring Systems

There are various pathways of metabolic activation for a given PAH. These include (1) metabolic oxidation using cytochrome P450 to form PAH radical cations, (2) creation of PAH-o-quinones via dihydrodiol dehydrogenase, and (3) formation of dihydrodiol epoxides via cytochrome p450 enzymes. Most commonly, metabolic activation occurs through the formation of bay-region dihydrodiol epoxides.<sup>[15]</sup> These species are extremely reactive and can covalently bind to DNA to form the DNA damages discussed earlier. The PAH diol epoxides (PAHDE) are further classified into groups based on the surrounding rings. There can be fjord, bay, and k-region modifications (Figure 4).<sup>[16]</sup> Both the bay and fjord complexes can form PAHDEs while the K region forms (predominantly) the epoxide (Figure 5). The PAHs with a fjord region typically show a high rate of tumorigenicity. Due to the placement of the epoxide and hydroxyl moieties, the planarity of the ring system cannot be maintained. These species are very reactive and tend to preferentially bind to adenines. In contrast, PAHs with a bay region are less reactive than the fjord region compounds. Due to the location of the hydroxyl and epoxide moieties on the outer ring, the entire compound is able to remain planar. As a consequence of reduced activity, these derivatives are generally seen binding to guanine bases upon DNA adduct formation.

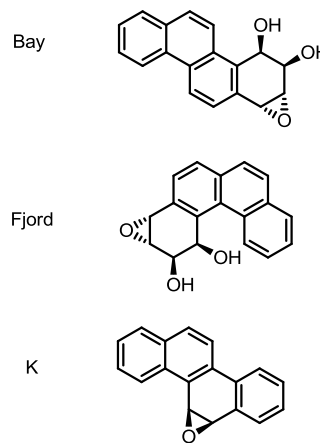


Figure 5: Polycyclic Aromatic Hydrocarbon Diol Epoxides

The metabolic pathway of 6-NC is shown in Figure 6 (adapted from Boyiri *et al.*).<sup>[14c]</sup> There are two predominant routes through which 6-NC can be metabolized: dihydroxylation and reduction.<sup>[17]</sup> The dihydroxylative pathway produces a variety of activated products through combinations of ring epoxidation and nitroreduction. The ring epoxidation occurs rapidly after dihydroxylation due to the availability of the double bond in the ring that lost its aromaticity.

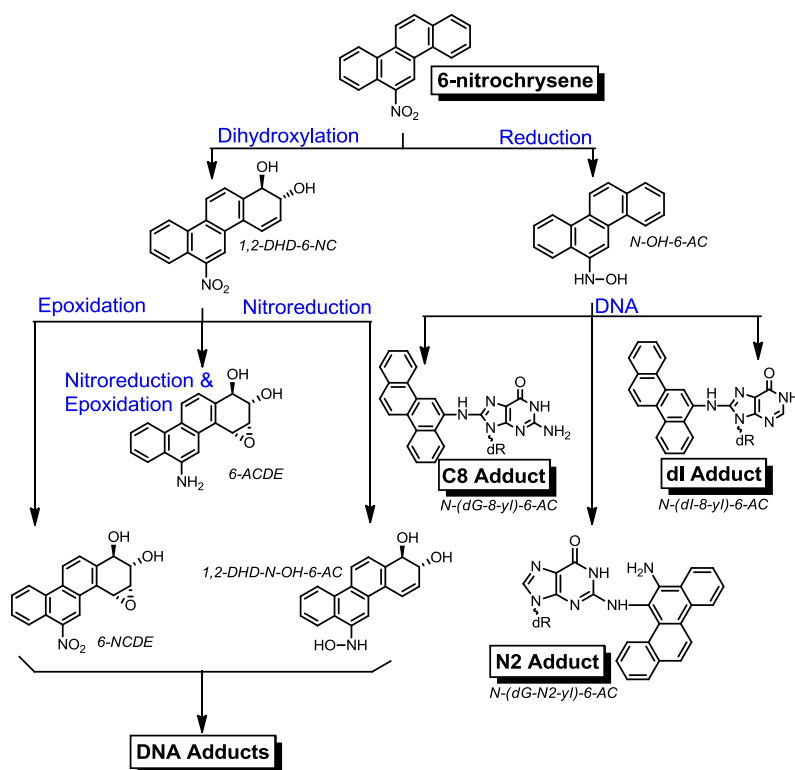
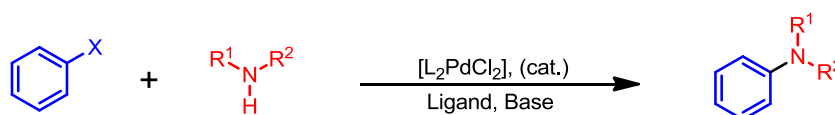


Figure 6: Metabolic Activation of 6-Nitrochrysene

The diol-epoxides comprise the set of the most reactive 6-nitrochrysene derivatives. These have been associated with multiple cases of malignant liver and lung cancers.<sup>[14]</sup> The other route occurs through reduction, producing *N*-hydroxyaminochrysene. This derivative is capable of forming a variety of adducts as listed in Figure 6. Among these, are the *N*-(deoxyguanosine-8-yl)-6-aminochrysene (C8-dG adduct), 5-(deoxyguanosine-*N*<sup>2</sup>-yl)-6-aminochrysene (*N*<sup>2</sup>-dG adduct), and *N*-(deoxyinosin-8-yl)-6-aminochrysene (C8-dI adduct). The latter adduct is believed to arise from deamination of the C8-dG adduct.

### 1.4 Buchwald-Hartwig Palladium Catalyzed Coupling Reactions

The key reaction in these syntheses is the formation of a C-N bond connecting the polycyclic aromatic hydrocarbon to the guanine base (see Reference 18 for a list of syntheses that employ this approach for similar substrates). This is accomplished via a Buchwald-Hartwig coupling reaction (Figure 7<sup>[19]</sup>). This produces a new carbon-nitrogen bond between the carcinogen and the DNA base.<sup>[20]</sup>



X = Cl, Br, I, OTf; R<sup>1</sup>, R<sup>2</sup> = 1° or 2° aromatic/aliphatic

Figure 7: General Outline of Buchwald-Hartwig Cross Coupling Reaction

The attachment points for each adduct vary. As such, the coupling reactants are modified to suit individual adducts. The C8-dG adducts are connected at the C8 position of the guanine base. The aryl carcinogen undergoes amination and the guanine base is brominated. To create the N<sup>2</sup>-dG adduct, the aryl carcinogen must have a leaving group such as a halogen or trifluoromethanesulfonate (triflate) to react with the free amine already present on the guanine base (Figure 8).

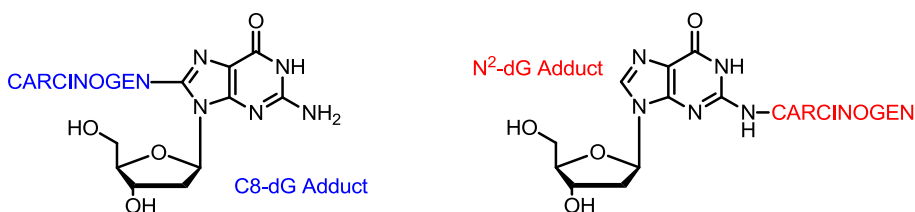


Figure 8: Key C-N Bond Formation within dG Syntheses

The general mechanism for this reaction was originally thought to be akin to other palladium-catalyzed coupling reactions, which includes: oxidative insertion and reductive elimination, and the coupled C-N

bond is formed.<sup>[19, 20a]</sup> This implies that the original palladium catalyst begins in the zero oxidation state. The first step of the catalytic cycle is oxidative insertion of the aryl halide or triflate, resulting in the palladium increasing to a +2 oxidation state. Upon direct attack of the amine on the palladium, the halide or triflate leaves and react with the strong base present in solution. Finally, upon reductive elimination, the palladium catalyst returns to its zero oxidation state while producing the desired C-N bond. This is the process presented in older literature such as Singh et al.<sup>[21]</sup>

More recently, the Hartwig, Blackmond, and Buchwald groups published a correction to this mechanism.<sup>[22]</sup> After several structural and kinetic studies, they posited the mechanism shown in Figure 9. Here, there is a “dead-end step” with the equilibrium forming Pd(BINAP)<sub>2</sub>. *In situ*, this complex forms and later dissociates to enter the catalytic cycle. Based on their studies, they believe that this is the palladium source that undergoes oxidative addition with the aryl halide. Then, upon addition of the base, the catalytic cycle proceeds as expected with the coordination of the amine with the Pd(II) complex. This is, of course, followed by reductive elimination of the desired product and regeneration of the Pd(BINAP)

complex which can resume the catalytic cycle.

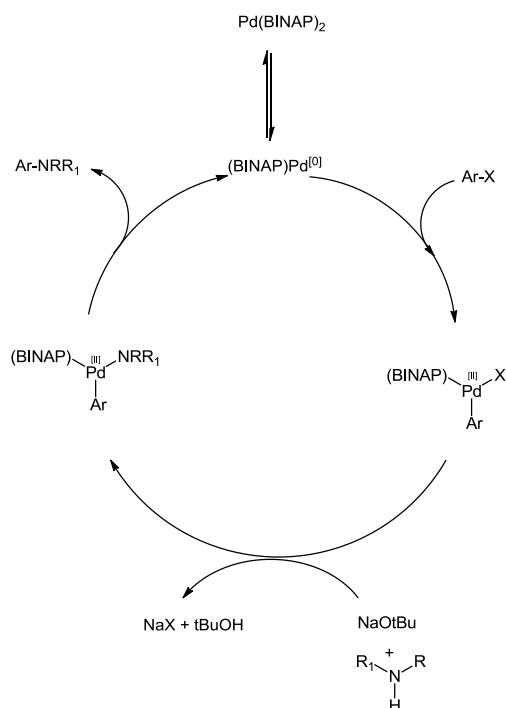


Figure 9: Revised Catalytic Mechanism for the Buchwald-Hartwig Cross-Coupling

the base used in all the syntheses presented here. The ligand and metal catalyst work together in a complex *in situ*. The chelating ligand chosen for the coupling of guanine with varying chrysene derivatives was 2,2'-bis(diphenylphosphino)-1,1'-binaphthyl (BINAP), depicted in Figure 10. Finally, the palladium catalyst used was tris(dibenzylideneacetone)dipalladium(0), Pd<sub>2</sub>dba<sub>3</sub>. These two choices are the most common choices for couplings of this nature, and were the first chosen for these syntheses. Since the reactions proceeded in good yield, other combinations of bases, ligands, and catalysts were not attempted.

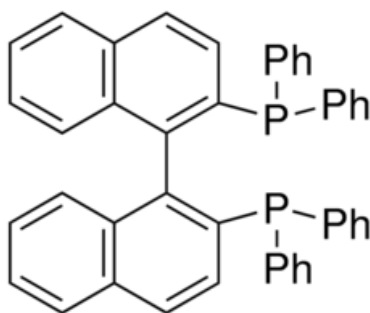


Figure 10: Racemic 2,2'-Bis(diphenylphosphino)-1,1'-binaphthalene

### 1.5 Solid-Phase Oligonucleotide Synthesis

Ultimately, the DNA adducts prepared must undergo solid-phase oligonucleotide synthesis.<sup>[23]</sup> This is a process to create a very specific oligonucleotide, containing the specially prepared DNA adduct monomer. Generally speaking, the oligomer chosen for my work was taken from the *p53* tumor suppressor gene, and the length of the oligomer chosen was based on the type of biological study that will be performed. However, in order to properly incorporate the DNA adduct into the oligonucleotide, it must be prepared with appropriate protecting groups.

Specifically in terms of a deoxyguanosine adduct, the 3'- and 5'-OH groups must be protected along with the *N*<sup>2</sup> amino group (Figure 11). It should be noted that, in the case of the *N*<sup>2</sup>-dG adducts, the *N*<sup>2</sup>



protection is omitted since the carcinogen is present at that position. The 5'-OH must be protected with an acid labile group. Traditionally, this has always been an MMTr<sup>[24a]</sup> or DMTr<sup>[24b]</sup> group. Since the DMTr protecting group has far more selectivity towards primary hydroxyls over secondary hydroxyls, its use has become more prevalent. The 3'-OH group is always protected with a phosphoramidite group.<sup>[23]</sup> This group is specific for oligonucleotide synthesis and allows for the generation of the phosphodiester linkage between the ribose sugars and is capable of undergoing oxidation to produce the sugar-phosphate backbone. Finally, the  $N^2$  amine on the guanosine base must be protected with a base labile group.<sup>[23]</sup> Historically, this was accomplished *via* an isobutyryl protection.<sup>[25]</sup> In recent years, a shift towards a DMF acetal protection has occurred since the latter group is far more labile during the deprotection step of the solid phase synthesis.<sup>[26]</sup> In the example presented in Figure 11, a DMF acetal group is present on the undamaged deoxyguanosine base.

Upon appropriate protection of the DNA adduct, the singular base is put through solid-phase oligonucleotide synthesis. This is a cyclic process that couples a series of individual bases to each other, resulting in the desired oligomer.<sup>[23]</sup> As represented

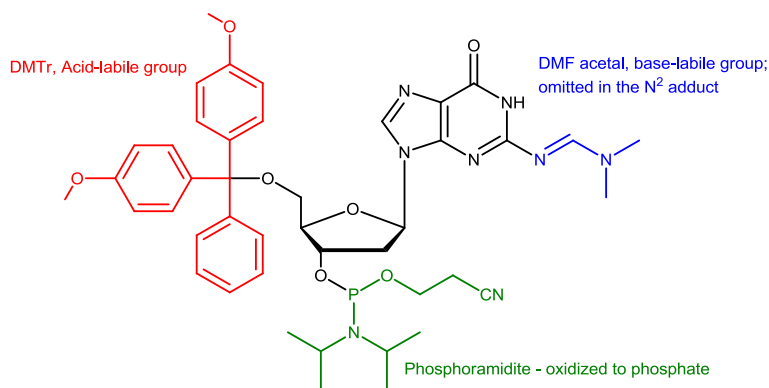


Figure 11: General Synthetic Outline for Phosphoramidite Monomer Prior to Solid Phase Synthesis

in Figure 12, the cycle begins with a protected base. The first step is detritylation, where the DMTr group on the 5'-OH is removed with a dilute acid. The free hydroxyl is then able to undergo coupling with the next base. This occurs through nucleophilic attack on the phosphorus of the incoming base and loss of a diisopropyl amine. The resulting bond is a phosphate linkage between two ribose sugars. The coupling step is generally expected to proceed in excellent yield (in the vicinity of 99.5%), but it is unreasonable to expect full conversion. As such, it is expected that there are some remaining 5'-OH groups that haven't coupled with the next base in the sequence. They cannot be allowed to continue to the next step in the

cycle, otherwise, they would form an oligomer with a deletion mutation. To avoid this, a capping step is introduced at this point in the cycle. Capping is essentially a process to “protect” the 5'-OH group, and prevent it from reacting further. It is usually accomplished *via* an *N*-methylimidazole or acetate group. The final step is oxidation of the phosphorus in the newest base was introduced to the oligomer; as seen in Figure 12, a double bond to an additional oxygen atom is observed. Once this has been completed, the *n*-mer will continue onto the next cycle for introduction of the next base. This process continues until the desired oligomer has been produced.

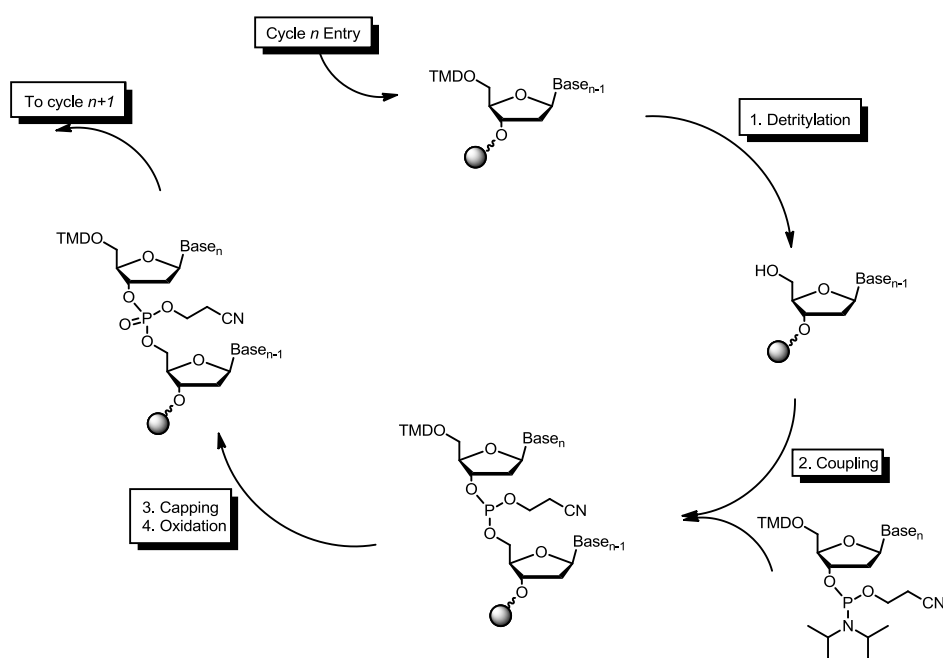
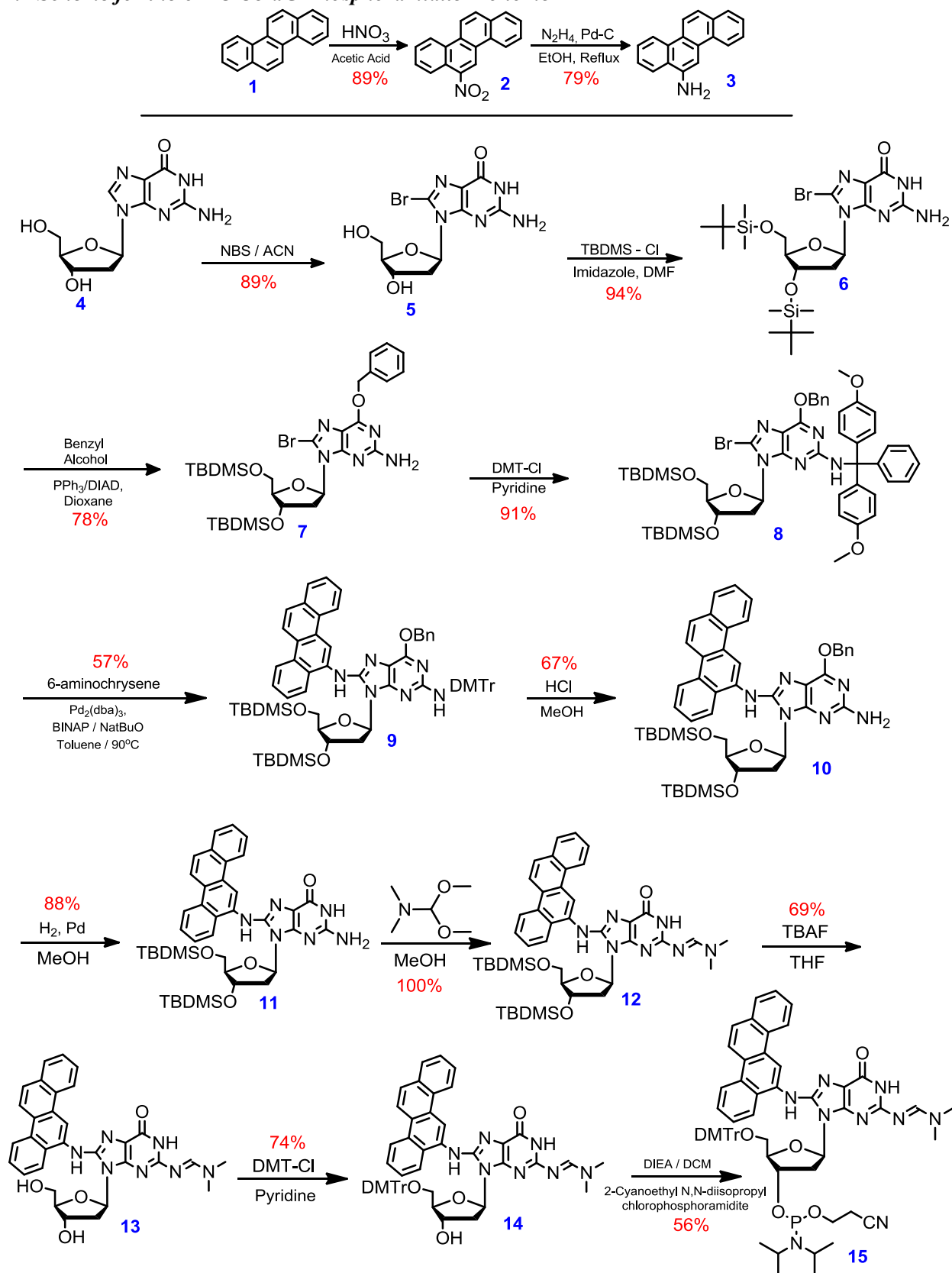


Figure 12: Cycle for Solid Phase Oligonucleotide Synthesis

## CHAPTER II

# SYNTHESIS OF THE C8 PHOSPHORAMIDITE MONOMER OF 8-(*N*-6-AMINOCHRYSENE)-*N*<sup>2</sup>-DMF-5'- O-(4,4'-DIMETHOXYTRITYL)-2'- DEOXYGUANOSINE

## 2.1 Scheme for the 6-NC C8-dG Phosphoramidite Monomer



## ***2.2 Materials and Methods***

### **MATERIALS**

Bulk solvents and chemicals were purchased either from Sigma Aldrich (St. Louis, MO) or Fisher Scientific (Clifton, NJ). Deuterated solvents were purchased from Cambridge Isotope Laboratories (Andover, MA). The 2'-deoxyguanosine was purchased from Berry and Associates (Dexter, MI). Every reagent used was obtained in the highest purity available. Both flash chromatography silica gel and gravitational chromatography silica gel were purchased from Sorbent Technology (Norcross, GA).

### **SPECTROSCOPIC METHODS**

NMR: NMR spectra were recorded as indicated on a Bruker 300, 400, or 500 MHz spectrometer.  $^1\text{H}$  chemical shifts are reported in parts per million relative to the residual chloroform ( $\delta$  7.26 ppm) or dimethyl sulfoxide ( $\delta$  2.50 ppm) peak. The  $^{13}\text{C}$ -NMR values were referenced to the residual chloroform ( $\delta$  77.1 ppm) or dimethyl sulfoxide ( $\delta$  39.52 ppm) peak. The  $^{31}\text{P}$ -NMR shifts are reported as obtained from the spectrometer. The  $^{19}\text{F}$ -NMR values are reported as obtained from the spectrometer.  $^1\text{H}$ -NMR shifts are reported as chemical shift  $\delta$ , multiplicity(s, singlet; d, doublet; t, triplet; q, quartet; m, multiplet; br., broad), relative integral, and assignment.

## PROCEDURES

**6-Nitrochrysene (2)** – In a 50 mL round bottom flask equipped with a stirbar was taken chrysene (**1**, 1.00 g, 4.384 mmol) in glacial acetic acid (28 mL). The solution was stirred briefly in an oil bath at 40 °C. To it a solution of fuming nitric acid (0.8 mL, 18.019 mmol) and concentrated sulfuric acid (1.0 mL, 18.760 mmol) in glacial acetic acid (8 mL) was slowly added dropwise. The reaction was allowed to stir for 20 mins at 40°C; within 5-10 mins, the reaction mixture turned yellow. After 20 mins, the solution was allowed to cool to room temperature and the solution was filtered. The precipitate was washed with acetic acid and allowed to dry over vacuum for 2 h. Following this, the compound was further dried in an oven for 30 mins to afford the pure compound as a pale yellow solid (1.0701 g, 89% yield).

<sup>1</sup>H-NMR (400 MHz, DMSO-d<sub>6</sub>) δ ppm 7.68-8.01 (m, 4H, C<sub>1</sub>-H, C<sub>2</sub>-H, C<sub>16</sub>-H, C<sub>17</sub>-H), 7.93 (m, 2H, C<sub>12</sub>-H, C<sub>15</sub>-H), 8.37 (t, 1H, C<sub>6</sub>-H), 8.89-8.95 (m, 1H, C<sub>11</sub>-H), 9.01 (t, 1H, C<sub>18</sub>-H), 9.17 (m, 1H, C<sub>3</sub>-H), 9.60 (s, 1H, C<sub>9</sub>-H)

**6-Aminochrysene (3)** – In a 25 mL round bottom flask equipped with a stirbar was taken **2** (100 mg, 0.366 mmol). The flask was placed under a N<sub>2</sub> atmosphere, and to it was added ethanol (8.5 mL). The flask was purged with N<sub>2</sub> for 30 mins. At this time, hydrazine monohydrate (0.6 mL, 5.803 mmol) was added to the flask, and the flask was purged for an additional 30 mins. After this, 10% wt palladium on carbon (1.3 mg, 0.0265 mmol) was added to the flask, and the reaction was heated at reflux for 15 h. After this time, the reaction flask was allowed to cool to room temperature, and the solvent was evaporated. The crude product was loaded onto a silica gel plug and the desired compound eluted in neat dichloromethane. The solvent was removed via rotary evaporation to afford the pure compound as a pale yellow solid (70.6 mg, 79% yield).

<sup>1</sup>H-NMR (400 MHz, DMSO-d<sub>6</sub>) δ ppm 6.03 (s, 2H, NH<sub>2</sub>), 7.60-7.78 (m, 5H, C<sub>1</sub>-H, C<sub>2</sub>-H, C<sub>9</sub>-H, C<sub>16</sub>-H, C<sub>17</sub>-H), 7.95 (m, 1H, C<sub>11</sub>-H), 8.12 (m, 2H, C<sub>12</sub>-H, C<sub>15</sub>-H), 8.59-8.67 (dd, 1H, C<sub>6</sub>-H), 8.89 (d, 1H, C<sub>18</sub>-H), 8.95 (d, 1H, C<sub>3</sub>-H)

<sup>13</sup>C-NMR (101 MHz, DMSO-d<sub>6</sub>) δ ppm 100.77, 121.08, 122.24, 122.72, 123.41, 123.69, 124.31, 124.60, 126.13, 126.54, 126.90, 127.42, 128.96, 129.33, 131.50, 131.67, 132.98, 144.51.

**8-Bromo-2'-deoxyguanosine (5)** – In a 500 mL Erlenmeyer flask equipped with a stirbar was taken 2'-deoxyguanosine monohydrate, **4** (6.50 g, 24.323 mmol) suspended in 80% aqueous acetonitrile (300 mL) at room temperature. Freshly recrystallized *N*-bromosuccinimide (6.493 g, 36.483 mmol) was added to the stirring mixture in three aliquots over 30 mins. The reaction mixture was then stirred for an additional 30 mins. After this time, the reaction mixture was filtered through a Büchner funnel. The product was washed with acetone to give 7.504 g (89% yield) of the product as a white flaky solid.

<sup>1</sup>H-NMR (400 MHz, DMSO-d<sub>6</sub>) δ ppm 2.07-2.13 (ddd, 1H, C<sub>13</sub>-H), 3.12-3.19 (ddd, 1H, C<sub>13</sub>-H'), 3.33 (br. s, 1H, O<sub>17</sub>-H), 3.48-3.52 (dd, 1H, C<sub>18</sub>-H), 3.60-3.64 (dd, 1H, C<sub>18</sub>-H'), 3.78-3.82 (q, 1H, C<sub>12</sub>-H), 4.38-4.41 (m, 1H, C<sub>16</sub>-H), 4.84 (br. s, 1H, O<sub>19</sub>-H), 6.14-6.17 (t, 1H, C<sub>14</sub>-H), 6.48 (br. s, 2H, N<sub>10</sub>-2H), 10.78 (s, 1H, N<sub>1</sub>-H)

<sup>13</sup>C-NMR (101 MHz, DMSO-d<sub>6</sub>) δ ppm 36.46 (C<sub>13</sub>), 62.05 (C<sub>18</sub>), 71.03 (C<sub>12</sub>), 85.06 (C<sub>14</sub>), 87.90 (C<sub>16</sub>), 117.49 (C<sub>5</sub>), 120.53 (C<sub>7</sub>), 151.98 (C<sub>4</sub>), 153.32 (C<sub>2</sub>), 155.42 (C<sub>6</sub>)

**8-Bromo-3',5'-O-bis(tert-butyldimethylsilyl)-2'-deoxyguanosine (6)** – In a 25 mL round bottom flask equipped with a stirbar was taken **5** (907 mg, 2.62 mmol) and imidazole (852 mg, 12.52 mmol) in dry DMF (10 mL) at room temperature. To the stirring reaction mixture was added *tert*-butyldimethylsilyl chloride (1.085 g, 7.2 mmol). The solution turned transparent within 5 mins and was allowed to continue

stirring for 8 hrs. Once this time elapsed, the reaction was quenched with methanol. The solution was evaporated and diluted with deionized water (25 mL) and methylene chloride (25 mL). The layers were separated and the aqueous layer extracted with methylene chloride (2 x 25 mL). The crude product was purified by silica gel flash column chromatography with a step gradient of methanol (0-10%) in methylene chloride as the mobile phase. The product was isolated as a white solid (1.42 g, 94% yield).

<sup>1</sup>H-NMR (400 MHz, DMSO-d<sub>6</sub>) δ ppm -0.04 (s, 3H, C<sub>23</sub>-3H), -0.02 (s, 3H, C<sub>24</sub>-3H), 0.09 (s, 6H, C<sub>29</sub>-3H, C<sub>30</sub>-3H), 0.81 (s, 9H, C<sub>32</sub>-3H, C<sub>33</sub>-3H, C<sub>34</sub>-3H), 0.87 (s, 9H, C<sub>25</sub>-3H, C<sub>26</sub>-3H, C<sub>27</sub>-3H), 2.10-2.16 (ddd, 1H, C<sub>13</sub>-H), 3.35-3.41 (ddd, 1H, C<sub>13</sub>-H'), 3.61-3.67 (m, 1H, C<sub>12</sub>-H), 3.73-3.79 (m, 2H, C<sub>18</sub>-2H), 4.58 (m, 1H, C<sub>16</sub>-H), 6.13-6.16 (t, 1H, C<sub>14</sub>-H), 6.46 (br. s, 2H, N<sub>10</sub>-2H), 10.87 (s, 1H, N<sub>1</sub>-H)

<sup>13</sup>C-NMR (101 MHz, DMSO-d<sub>6</sub>) δ ppm -5.50 (C<sub>29</sub>, C<sub>30</sub>), -4.94 (C<sub>23</sub>), -4.77 (C<sub>24</sub>), 17.63 (C<sub>31</sub>), 17.90 (C<sub>22</sub>), 25.63 (C<sub>32</sub>, C<sub>33</sub>, C<sub>34</sub>), 25.69 (C<sub>25</sub>, C<sub>26</sub>, C<sub>27</sub>), 36.07 (C<sub>13</sub>), 62.82 (C<sub>18</sub>), 72.38 (C<sub>12</sub>), 84.68 (C<sub>14</sub>), 87.12 (C<sub>16</sub>), 117.46 (C<sub>5</sub>), 120.40 (C<sub>7</sub>), 152.10 (C<sub>4</sub>), 153.38 (C<sub>2</sub>), 155.46 (C<sub>6</sub>)

***O<sup>6</sup>-Benzyl-8-bromo-3',5'-O-bis(tert-butyldimethylsilyl)-2'-deoxyguanosine (7)*** – In a 50 mL round bottom flask equipped with a stirbar was taken **6** (1.0 g, 1.74 mmol) and triphenylphosphine (800 mg, 3.04 mmol). The flask was placed under an N<sub>2</sub> atmosphere, and to it was added dry dioxane (20 mL). To the stirring reaction mixture at room temperature, benzyl alcohol (0.316 mL, 3.05 mmol) was added. Diisoproyl azodicarboxylate (0.600 mL, 3.09 mmol) was added dropwise to the stirring mixture, which turned to a transparent yellow within 15 mins. The reaction was allowed to continue stirring at room temperature for 8 h under the N<sub>2</sub> atmosphere. After this time, the solvent was evaporated. The crude compound was purified by silica gel flash column chromatography with a step gradient of ethyl acetate (0-15%) in hexanes as the mobile phase. The product was isolated as a light yellow solid (0.903 g, 78 % yield).



<sup>1</sup>H-NMR (400 MHz, CDCl<sub>3</sub>) δ ppm -0.03 (s, 3H, C<sub>37</sub>-3H), 0.01 (s, 3H, C<sub>38</sub>-3H), 0.14 (s, 6H, C<sub>29</sub>-3H, C<sub>30</sub>-3H), 0.84 (s, 9H, C<sub>39</sub>-3H, C<sub>40</sub>-3H, C<sub>41</sub>-3H), 0.93 (s, 9H, C<sub>31</sub>-3H, C<sub>32</sub>-3H, C<sub>33</sub>-3H), 2.13-2.18 (ddd, 1H, C<sub>13</sub>-H), 3.50-2.56 (ddd, 1H, C<sub>13</sub>-H'), 3.67-3.71 (dd, 1H, C<sub>17</sub>-H), 3.83-3.93 (m, 2H, C<sub>12</sub>-H, C<sub>17</sub>-H), 4.78 (dt, 1H, C<sub>16</sub>-H), 5.51 (s, 2H, C<sub>19</sub>-2H), 6.25 (t, 1H, C<sub>14</sub>-H), 6.28 (br. s, 2H, N<sub>10</sub>-2H), 7.28-7.36 (m, 3H, C<sub>21</sub>-H, C<sub>23</sub>-H, C<sub>25</sub>-H), 7.46 (m, 2H, C<sub>22</sub>-H, C<sub>24</sub>-H)

<sup>13</sup>C-NMR (101 MHz, CDCl<sub>3</sub>) δ ppm -5.45 (C<sub>37</sub>, C<sub>38</sub>), -4.66 (C<sub>29</sub>, C<sub>30</sub>), 18.00 (C<sub>36</sub>), 18.30 (C<sub>28</sub>), 21.90 (C<sub>39</sub>, C<sub>40</sub>, C<sub>41</sub>), 25.80 (C<sub>31</sub>, C<sub>32</sub>, C<sub>33</sub>), 36.41 (C<sub>13</sub>), 62.64 (C<sub>17</sub>), 68.10 (C<sub>19</sub>), 72.30 (C<sub>12</sub>), 85.71 (C<sub>16</sub>), 87.37 (C<sub>14</sub>), 116.42 (C<sub>5</sub>), 126.90 (C<sub>7</sub>), 128.00 (C<sub>23</sub>), 128.27 (C<sub>25</sub>), 128.33 (C<sub>21</sub>), 128.47 (C<sub>24</sub>), 128.51 (C<sub>22</sub>), 136.12 (C<sub>20</sub>), 154.41 (C<sub>4</sub>), 158.38 (C<sub>2</sub>), 159.81 (C<sub>6</sub>)

***O<sup>6</sup>-Benzyl-8-bromo-3',5'-O-bis(tert-butyldimethylsilyl)-N<sup>2</sup>-dimethoxytrityl-2'-deoxyguanosine (8)*** – In a 25 mL round bottom flask equipped with a stirbar was taken **7** (1.20 g, 1.80 mmol) in dry pyridine (15 mL). To this, was added some crystals of 4-dimethylaminopyridine. 4,4-Dimethoxytrityl chloride (0.92 g, 2.70 mmol) was added to the solution at room temperature and the reaction mixture was allowed to continue stirring for 12 hrs. The reaction was checked for completion by TLC (80/20 Hexanes/EtOAc, v/v). The solvent was evaporated and purified by aluminum oxide column chromatography with a step gradient of ethyl acetate (0-10%) in hexanes as the mobile phase. The product was isolated as a transparent solid (1.58 g, 91% yield).

<sup>1</sup>H-NMR (400 MHz, DMSO-d<sub>6</sub>) δ ppm -0.11 (s, 3H, C<sub>48</sub>-3H), -0.05 (s, 3H, C<sub>47</sub>-3H), 0.10 (s, 6H, C<sub>56</sub>-3H, C<sub>57</sub>-3H), 0.77 (s, 9H, C<sub>53</sub>-3H, C<sub>54</sub>-3H, C<sub>55</sub>-H), 0.87 (s, 9H, C<sub>49</sub>-3H, C<sub>50</sub>-3H, C<sub>51</sub>-3H), 3.32 (s, 2H, N<sub>10</sub>-H, C<sub>12</sub>-H), 3.51-3.56 (m, 2H, C<sub>13</sub>-H, C<sub>18</sub>-H), 3.68 (s, 6H, C<sub>41</sub>-3H, C<sub>43</sub>-3H), 3.72-3.76 (m, 2H, C<sub>16</sub>-H, C<sub>18</sub>-H), 4.81 (br. s, 2H, C<sub>58</sub>-2H), 6.07 (t, 1H, C<sub>14</sub>-H), 6.79-6.85 (d, 4H, C<sub>26</sub>-H, C<sub>28</sub>-H, C<sub>36</sub>-H, C<sub>38</sub>-H), 6.87-6.91 (m, 1H, C<sub>62</sub>-H), 7.14-7.24 (m, 6H, C<sub>30</sub>-H, C<sub>34</sub>-H, C<sub>60</sub>-H, C<sub>61</sub>-H, C<sub>63</sub>-H, C<sub>64</sub>-H), 7.26-7.28 (d, 4H, C<sub>25</sub>-H, C<sub>29</sub>-H, C<sub>35</sub>-H, C<sub>39</sub>-H), 7.30-7.32 (m, 3H, C<sub>31</sub>-H, C<sub>32</sub>-H, C<sub>33</sub>-H)

<sup>13</sup>C-NMR (101 MHz, DMSO-d<sub>6</sub>) δ ppm -4.92 (C<sub>57</sub>), -4.79 (C<sub>56</sub>), -4.16 (C<sub>48</sub>), -4.02 (C<sub>47</sub>), 18.43 (C<sub>52</sub>), 18.56 (C<sub>46</sub>), 26.33 (C<sub>53</sub>, C<sub>54</sub>, C<sub>55</sub>), 26.36 (C<sub>49</sub>, C<sub>50</sub>, C<sub>51</sub>), 35.83 (C<sub>13</sub>), 55.66 (C<sub>41</sub>, C<sub>43</sub>), 62.83 (C<sub>12</sub>), 67.64 (C<sub>58</sub>), 70.24 (C<sub>18</sub>), 72.80 (C<sub>21</sub>), 85.95 (C<sub>16</sub>), 87.33 (C<sub>14</sub>), 113.57 (C<sub>26</sub>, C<sub>28</sub>, C<sub>36</sub>, C<sub>38</sub>), 115.63 (C<sub>5</sub>), 127.06 (C<sub>7</sub>), 128.26 (C<sub>32</sub>), 128.68 (C<sub>60</sub>, C<sub>62</sub>, C<sub>64</sub>), 128.72 (C<sub>31</sub>, C<sub>33</sub>), 129.05 (C<sub>25</sub>, C<sub>29</sub>, C<sub>35</sub>, C<sub>39</sub>), 129.08 (C<sub>61</sub>, C<sub>63</sub>), 130.37 (C<sub>30</sub>, C<sub>34</sub>), 136.72 (C<sub>59</sub>), 138.32 (C<sub>22</sub>, C<sub>24</sub>), 138.41 (C<sub>23</sub>), 146.41 (C<sub>2</sub>), 154.59 (C<sub>4</sub>), 157.66 (C<sub>6</sub>), 158.37 (C<sub>27</sub>, C<sub>37</sub>)

***8-(N-6-Aminochrysene)-O<sup>6</sup>-benzyl-3',5'-O-bis(tert-butyldimethylsilyl)-N<sup>2</sup>-dimethoxytrityl-2'-***

***deoxyguanosine (9)*** – In a 25 mL round bottom flask equipped with a stirbar was taken **8** (531 mg, 0.548 mmol), 6-aminochrysene (**3**, 200 mg, 0.822 mmol), tris(dibenzylideneacetone)dipalladium(0) (Pd<sub>2</sub>(dba)<sub>3</sub>, 20 mg, 0.0219 mmol), and rac-2,2'-bis(diphenylphosphino)-1,1'-binaphthyl (BINAP, 40 mg, 0.0636 mmol), in dry toluene (5 mL). The solution was degassed by purging argon for one hour. The solution was then heated at 90°C for one hour. At this point, sodium *tert*-butoxide (79 mg, 0.823 mmol) was added, and the solution heated at 100°C for an additional hour. The reaction was cooled, diluted with ether (10 mL), and successively filtered through Celite®. The filtrate was evaporated and purified by alumina oxide column chromatography with a step gradient of EtOAc (0-15%) in hexanes as the mobile phase. The product was isolated as a dark yellow-green solid (354 mg, 57% yield).

<sup>1</sup>H-NMR (400 MHz, CDCl<sub>3</sub>) δ ppm -0.27 (s, 3H, CH<sub>3</sub>), -0.19 (s, 3H, CH<sub>3</sub>), 0.12 (s, 6H, 2 x CH<sub>3</sub>), 0.64 (s, 9H, *t*-Bu-9H), 0.94 (s, 9H, *t*-Bu-9H), 2.26 (m, 1H, C<sub>2'</sub>-H), 2.88 (br. s, 1H, C<sub>2'</sub>-H), 3.80 (s, 6H, 2 x OMe), 3.82-3.95 (m, 2H, C<sub>5'</sub>-2H), 4.15 (q, 1H, C<sub>3'</sub>-H), 4.50 (br. s, 1H, C<sub>4'</sub>-H), 5.08 (br. s, 2H, Bn-CH<sub>2</sub>), 6.10 (s, 1H, N<sup>2</sup>-H), 6.22 (br. s, 1H, C<sub>1'</sub>-H), 6.80 (d, 4H, DMTr-4H), 7.14-7.25 (m, 9H, DMTr-9H), 7.29-7.44 (m, 5H, OBn-5H), 7.57-7.74 (m, 4H, CR-4H), 7.91-8.01 (m, 2H, CR-2H), 8.11 (d, 1H, CR-H), 8.37 (br. s, 1H, CR-H), 8.66 (d, 1H, CR-H), 8.77 (d, 1H, CR-H), 8.83 (d, 1H, CR-H), 9.52 (br. s, 1H, N<sup>8</sup>-H)

$^{13}\text{C}$ -NMR (101 MHz,  $\text{CDCl}_3$ )  $\delta$  ppm -5.78, -5.70, -4.74, -4.58, 18.00, 18.23, 25.66, 25.81, 55.14, 55.23, 63.15, 70.14, 72.59, 112.78, 112.81, 113.16, 120.88, 123.85, 126.29, 126.37, 127.51, 127.83, 128.12, 128.23, 129.02, 129.11, 130.19, 130.25, 130.40, 131.44, 132.37, 158.00

ESI-MS (positive mode):  $m/z$  calcd for  $\text{C}_{68}\text{H}_{76}\text{N}_6\text{O}_6\text{Si}_2\text{H}^+$  1129.5, observed 1129.9 Da  $[\text{M}+\text{H}]^+$

**8-(N-6-Aminochrysene)-O<sup>6</sup>-benzyl-3',5'-O-bis(tert-butyldimethylsilyl)-2'-deoxyguanosine (10)** – In a 100 mL round bottom flask equipped with a stirbar was taken **9** (1.976 g, 1.746 mmol). The compound was dissolved in a minimal amount of methylene chloride (10 mL) and reacted with 0.01M methanolic HCl (20 mL, 0.175 mmol). The mixture was stirred for 16 h and monitored by TLC (neat DCM). Upon completion of the reaction, the solvent was evaporated and purified by silica gel flash column chromatography with a gradient of methanol (0-5%) in dichloromethane as the mobile phase. The product was isolated as a yellow solid (0.9697 g, 67% yield).

$^1\text{H}$ -NMR (400 MHz,  $\text{CDCl}_3$ )  $\delta$  ppm -0.27 (s, 3H,  $\text{CH}_3$ ), -0.19 (s, 3H,  $\text{CH}_3$ ), 0.17 (s, 6H, 2 x  $\text{CH}_3$ ), 0.63 (s, 9H, *t*-Bu-9H), 0.97 (s, 9H, *t*-Bu-9H), 2.40 (ddd, 1H,  $\text{C}_2$ -H), 3.15 (ddd, 1H,  $\text{C}_2$ -H), 3.85 (m, 1H,  $\text{C}_5$ -H), 3.98 (m, 1H,  $\text{C}_5$ -H), 4.17 (q, 1H,  $\text{C}_4$ -H), 4.64 (m, 1H,  $\text{C}_3$ -H), 4.78 (br. s, 2H, OBn-2H), 5.63 (br. s, 2H,  $\text{N}^2$ -2H), 6.47 (t, 1H,  $\text{C}_1$ -H), 7.28-7.36 (m, 3H, OBn-Ar-3H), 7.52 (d, 2H, OBn-Ar-2H), 7.61-7.75 (m, 4H, CR-4H), 7.93-7.99 (m, 2H, CR-2H), 8.14 (d, 1H, CR-H), 8.35 (br. s, 1H, CR-H), 8.67 (d, 1H, CR-H), 8.79-9.00 (m, 2H, CR-2H), 9.48 (s, 1H,  $\text{N}^8$ -H)

$^{13}\text{C}$ -NMR (101 MHz,  $\text{CDCl}_3$ )  $\delta$  ppm -5.93, -5.86, -4.87, -4.70, 17.86, 18.09, 25.49, 25.63, 39.16, 53.26, 62.92, 67.99, 72.24, 77.06, 85.01, 87.85, 112.55, 113.37, 120.75, 121.46, 123.69, 125.21, 125.86, 126.14, 126.17, 126.39, 126.89, 127.52, 127.86, 128.07, 128.11, 128.78, 130.23, 131.32, 132.22, 133.67, 136.89, 148.58, 153.86, 157.04, 158.06

ESI-MS (positive mode):  $m/z$  calcd for  $\text{C}_{47}\text{H}_{58}\text{N}_6\text{O}_4\text{Si}_2\text{H}^+$  827.4, observed 827.7 Da  $[\text{M}+\text{H}]^+$

**8-(*N*-6-Aminochrysene)-3',5'-*O*-bis(*tert*-butyldimethylsilyl)-2'-deoxyguanosine (11)** – In a 50 mL round bottom flask equipped with a stirbar was taken **10** (0.9697 g, 1.169 mmol) in anhydrous methanol (20 mL). The resulting solution was purged with N<sub>2</sub> for 30 mins. At this point, palladium black (125 mg, 1.169 mmol) was added to the stirring solution. The reaction was purged with H<sub>2</sub> for an additional 2 h and then left to stir under a hydrogen atmosphere for 12 h. The reaction mixture was monitored by TLC (90:10 DCM/MeOH v/v). Once the reaction was complete, the solvent was evaporated and the crude product purified via silica gel flash column chromatography with a step gradient of methanol (0-10%) in dichloromethane. The final product was isolated as a white solid (755 mg, 88% yield).

<sup>1</sup>H-NMR (400 MHz, CDCl<sub>3</sub>) δ ppm -0.29 (s, 3H, CH<sub>3</sub>), -0.22 (s, 3H, CH<sub>3</sub>), 0.14 (s, 3H, CH<sub>3</sub>), 0.15 (s, 3H, CH<sub>3</sub>), 0.60 (s, 9H, *t*-Bu-9H), 0.95 (s, 9H, *t*-Bu-9H), 1.64 (m, 1H, C<sub>2</sub>-H), 2.40 (m, 1H, C<sub>2</sub>-H), 3.10 (m, 1H, C<sub>3</sub>-H), 3.82-3.86 (m, 1H, C<sub>5</sub>-H), 3.97-4.00 (m, 1H, C<sub>5</sub>-H), 4.60 (m, 1H, C<sub>4</sub>-H), 5.14 (s, 1H, N<sup>1</sup>-H), 5.60 (s, 2H, N<sup>2</sup>-2H), 6.46 (t, 1H, C<sub>1</sub>-H), 7.60-7.76 (m, 4H, CR-4H), 7.94-7.99 (m, 2H, CR-2H), 8.13 (d, 1H, CR-H), 8.39 (br. s, 1H, CR-H), 8.68 (d, 1H, CR-H), 8.77 (d, 1H, CR-H), 8.84 (d, 1H CR-H), 9.38 (s, 1H, N<sup>8</sup>-H)

<sup>13</sup>C-NMR (101 MHz, CDCl<sub>3</sub>) δ ppm -5.57, -5.47, -4.50, -4.33, 18.24, 18.50, 25.86, 26.00, 29.93, 39.63, 53.68, 63.33, 68.85, 72.67, 77.08, 77.47, 85.36, 88.34, 100.23, 114.15, 121.15, 122.05, 123.96, 124.07, 126.47, 126.64, 126.89, 128.02, 128.29, 128.48, 128.56, 130.59, 131.73, 132.60

ESI-MS (positive mode): *m/z* calcd for C<sub>40</sub>H<sub>52</sub>N<sub>6</sub>O<sub>2</sub>Si<sub>2</sub>H<sup>+</sup> 737.4, observed 737.4 Da [M+H]<sup>+</sup>

**8-(*N*-6-Aminochrysene)-3',5'-*O*-bis(*tert*-butyldimethylsilyl)-*N*<sup>2</sup>-DMF-2'-deoxyguanosine (12)** – In a 50 mL round bottom flask equipped with a stirbar was taken **11** (755 mg, 1.024 mmol). The flask was placed under a N<sub>2</sub> atmosphere. To it was added anhydrous methanol (15 mL) and the solution was purged for 15 mins with N<sub>2</sub>. After, *N,N*-dimethylformamide dimethyl acetal (0.6 mL, 4.097 mmol) was slowly added dropwise to the solution. The solution was stirred for 40 hr. After the reaction was

complete, the solvent was evaporated, and the crude product was purified via silica gel flash column chromatography with a step gradient of methanol (0-10%) in dichloromethane to give the pure product as a yellow solid in quantitative yield (811 mg, 100% yield).

$^1\text{H-NMR}$  (400 MHz,  $\text{CDCl}_3$ )  $\delta$  ppm -0.35 (s, 3H,  $\text{CH}_3$ ), -0.25 (s, 3H,  $\text{CH}_3$ ), 0.09 (s, 6H, 2 x  $\text{CH}_3$ ), 0.57 (s, 9H, *t*-Bu-9H), 0.91 (s, 9H, *t*-Bu-9H), 2.27-2.32 (ddd, 1H,  $\text{C}_2$ -H), 2.78-2.85 (ddd, 1H,  $\text{C}_2$ -H), 3.07 (s, 3H, DMF- $\text{CH}_3$ ), 3.13 (s, 3H, DMF- $\text{CH}_3$ ), 3.82-3.86 (m, 1H,  $\text{C}_5$ -H), 3.92-3.96 (m, 1H,  $\text{C}_5$ -H), 4.11 (q, 1H,  $\text{C}_4$ -H), 4.50 (m, 1H,  $\text{C}_3$ -H), 6.49 (t, 1H,  $\text{C}_1$ -H), 7.56-7.68 (m, 4H, CR-4H), 7.88-7.93 (m, 2H, CR-2H), 8.08 (d, 1H, CR-H), 8.20 (br. s, 1H,  $\text{N}^1$ -H), 8.54 (s, 1H, CR-H), 8.61 (s, 1H, CR-H), 8.76 (t, 2H, CR-2H), 9.18 (br. s, 1H,  $\text{N}^8$ -H)

$^{13}\text{C-NMR}$  (101 MHz,  $\text{CDCl}_3$ )  $\delta$  ppm -5.81, -5.72, -4.73, -4.60, 17.94, 18.27, 25.63, 25.73, 31.39, 35.16, 36.43, 39.82, 41.26, 63.25, 72.68, 84.78, 88.03, 114.41, 120.83, 121.98, 123.72, 124.00, 125.50, 126.07, 126.17, 126.30, 126.44, 126.48, 128.13, 128.89, 130.28, 131.46, 132.27, 133.89, 147.58, 148.93, 154.68, 157.26, 162.47

ESI-MS (positive mode):  $m/z$  calcd for  $\text{C}_{43}\text{H}_{57}\text{N}_7\text{O}_4\text{Si}_2\text{H}^+$  792.4, observed 792.6 Da  $[\text{M}+\text{H}]^+$ .

**8-(*N*-6-Aminochrysene)- $\text{N}^2$ -DMF-2'-deoxyguanosine (13)** – In a 50 mL round bottom flask was taken **12** (811 mg, 1.024 mmol). The flask was placed under a  $\text{N}_2$  atmosphere and to it was added anhydrous tetrahydrofuran (25 mL). To the stirring solution was added 1M tetrabutylammonium fluoride in tetrahydrofuran (4.2 mL, 4.116 mmol). The reaction mixture immediately turned red after this addition. The solution was allowed to stir for 15 h under  $\text{N}_2$ . After this time, the solvent was evaporated and the crude product was purified via silica gel flash column chromatography with methanol (0-20%) in dichloromethane as the mobile phase. The pure product was afforded as a pale yellow solid (312.3 mg, 54% yield).

<sup>1</sup>H-NMR (400 MHz, DMSO-d<sub>6</sub>) δ ppm 2.22 (ddd, 1H, C<sub>2'</sub>-H), 2.98-3.05 (m, 1H, C<sub>2'</sub>-H), 3.05 (s, 3H, DMF-CH<sub>3</sub>), 3.18 (s, 3H, DMF-CH<sub>3</sub>), 3.65-3.70 (m, 1H, C<sub>5'</sub>-H), 3.79-3.85 (m, 1H, C<sub>5'</sub>-H), 3.94 (m, 1H, C<sub>4'</sub>-H), 4.51 (m, 1H, C<sub>3'</sub>-H), 5.32 (d, 1H, C<sub>3'</sub>-OH), 5.44 (t, 1H, C<sub>5'</sub>-OH), 6.50 (t, 1H, C<sub>1'</sub>-H), 7.66-7.80 (m, 4H, CR-3H and DMF-CH), 8.03-8.10 (m, 2H, CR-2H), 8.19 (d, 1H, CR-H), 8.56 (s, 1H, N<sup>1</sup>-H), 8.72 (m, 2H, CR-2H), 8.86 (d, 1H, CR-H), 9.00 (m, 2H, CR-2H), 11.23 (s, 1H, N<sup>8</sup>-H)

<sup>13</sup>C-NMR (101 MHz, DMSO-d<sub>6</sub>) δ ppm 13.71, 18.68, 19.72, 23.62, 30.79, 34.94, 46.87, 49.18, 54.99, 58.23, 62.02, 67.58, 71.86, 84.10, 88.12, 114.15, 116.78, 121.66, 123.82, 124.11, 125.79, 126.61, 126.81, 127.09, 127.17, 127.49, 128.15, 128.75, 128.90, 130.17, 131.68, 132.66, 136.62, 147.72, 149.71, 156.49, 157.56, 158.20

ESI-MS (positive mode): *m/z* calcd for C<sub>31</sub>H<sub>29</sub>N<sub>7</sub>O<sub>4</sub>H<sup>+</sup> 564.2, observed 586.3 Da [M+Na]<sup>+</sup>.

**8-(N-6-Aminochrysene)-N<sup>2</sup>-DMF-5'-O-(4,4'-dimethoxytrityl)-2'-deoxyguanosine (14)** – The product **13** of the preceding reaction was thrice azeotroped with anhydrous pyridine. In a 50 mL round bottom flask equipped with a stirbar was taken **13** with 4-dimethylaminopyridine (DMAP, 5 mg, catalytic amt.). The flask was placed under an argon atmosphere, and to it was added anhydrous pyridine (3 mL). To the stirring solution was added 4,4'-dimethoxytrityl chloride (110 mg, 0.325 mmol). The reaction mixture immediately turned a deep orange-yellow. Within one hour, the reaction mixture darkened to green. Over the following 2 hr, the reaction mixture became brown. The reaction was monitored via TLC (94:5:1 DCM/MeOH/NEt<sub>3</sub>). The reaction was stopped after 25 h and dried under nitrogen. The crude product was purified via silica gel column chromatography (0-5 % methanol in methylene chloride containing 1% NEt<sub>3</sub>). The product began eluting at approximately 5%. The pure product was isolated as a pale yellow solid (138 mg, 80% yield).

<sup>1</sup>H-NMR (400 MHz, CDCl<sub>3</sub>) δ ppm 2.83 (m, 1H, C<sub>2'</sub>-H), 3.08 (s, 3H, DMF-CH<sub>3</sub>), 3.24 (s, 3H, DMF-CH<sub>3</sub>), 3.27-3.32 (m, 2H, C<sub>5'</sub>-2H), 3.45 (s, 3H, DMTr-OMe), 3.48 (s, 3H, DMTr-OMe), 3.71 (m, 1H, C<sub>4'</sub>-H), 4.80 (m, 1H, C<sub>3'</sub>-H), 5.29 (s, 1H, C<sub>3'</sub>-OH), 6.34 (d, 2H, DMTr-2H), 6.38 (d, 2H, DMTr-2H), 6.74 (t,

<sup>1</sup>H, C<sub>1'</sub>-H), 7.01 (t, 3H, DMTr-3H), 7.07 (d, 2H, DMTr-2H), 7.11 (d, 2H, DMTr-2H), 7.41-7.56 (m, 4H, DMF-H, CR-3H), 7.65-7.72 (m, 2H, DMTr-2H), 7.83 (s, 1H, N<sub>8</sub>-H), 7.87-7.94 (m, 4H, CR-4H), 8.35 (s, 1H, CR-H), 8.58 (d, 1H, CR-H), 8.74 (m, 2H, CR-2H).

<sup>13</sup>C-NMR (101 MHz, CDCl<sub>3</sub>) δ ppm 13.22, 14.38, 19.26, 22.86, 23.58, 29.17, 33.81, 34.70, 38.69, 41.06, 54.41, 54.46, 58.51, 71.03, 83.35, 85.61, 86.01, 112.26, 115.52, 116.74, 119.98, 122.79, 123.46, 125.57, 126.20, 126.28, 126.44, 126.55, 127.16, 127.85, 128.12, 128.40, 129.24, 129.57, 130.58, 131.45, 133.80, 134.37, 142.72, 148.45, 149.50, 154.74, 156.38, 157.64, 157.72, 169.86.

ESI-MS (positive mode): *m/z* calcd for C<sub>52</sub>H<sub>47</sub>N<sub>7</sub>O<sub>6</sub>H<sup>+</sup> 866.4, observed 888.6 Da [M+Na]<sup>+</sup>.

***8-(N-6-amino-chrysene)-N<sup>2</sup>-DMF-5'-O-(4,4'-dimethoxytrityl)-3'-cyanoethyl-2'-deoxyguanosine***

**phosphoramidite (15)** – The entirety of the reaction was completed in a glovebag. In a 50 mL round bottom flask equipped with a stirbar was taken **14** (225 mg, 0.260 mmol) after having been dried thoroughly. The flask was placed under an argon atmosphere, and the product of the previous reaction was dissolved in anhydrous methylene chloride (3 mL). To the stirring solution was added anhydrous *N,N*-diisopropylethylamine (94 μL, 0.538 mmol), followed by 2-cyanoethyl-*N,N*-diisopropylchlorophosphoramidite (60 μL, 0.260 mmol). The reaction mixture was allowed to stir for 15 mins. At this time, additional anhydrous *N,N*-diisopropylethylamine (94 μL, 0.538 mmol) was added to the solution. The reaction was allowed to stir for an additional 15 mins, at which time it was stopped. The solution was diluted with methylene chloride (15 mL) and saturated sodium bicarbonate (20 mL). The organic layer was retained and the aqueous layer further extracted with methylene chloride (2 x 20 mL). The organic layers were combined and washed with brine (1 x 25 mL). The organic layer was dried over sodium sulfate and the solvent removed by rotary evaporation to give the crude product as a yellow-brown solid. This was dissolved in minimal methylene chloride (2 mL) and added dropwise to a stirring solution of hexanes (200 mL). The resulting precipitate was filtered out and collected. Any remaining free phosphorus was removed *via* basified silica gel flash column chromatography with a step gradient of

methanol (0-2%) in methylene chloride containing 1% triethylamine. The product was isolated as a pale yellow solid (145 mg, 52% yield).

$^1\text{H}$  NMR (500 MHz,  $\text{CDCl}_3$ , two diastereomers)  $\delta$  1.27 (m, 12H, 4 x  $^i\text{Pr-CH}_3$ ), 1.71 (m, 1H,  $\text{C}_2\text{-H}$ ), 2.36 (t, 1H,  $-\text{CH}_2\text{CN}$ ), 2.52 (t, 1H,  $-\text{CH}_2\text{CN}$ ), 2.60-2.66 (m, 1H,  $\text{P-O-CH}_2$ ), 2.75 (td, 1H,  $\text{P-O-CH}_2$ ), 3.08 (s, 3H,  $\text{DMF-CH}_3$ ), 3.13 (s, 3H,  $\text{DMF-CH}_3$ ), 3.30 (m, 1H,  $\text{C}_2\text{-H}$ ), 3.34-3.42 (m, 2H,  $\text{C}_5\text{-2H}$ ), 3.47 (s, 3H,  $\text{DMTr-OCH}_3$ ), 3.48 (s, 3H,  $\text{DMTr-OCH}_3$ ), 3.70 (m, 1H,  $\text{C}_4\text{-H}$ ), 4.09-4.23 (m, 1H,  $\text{P-N-CH}$ ), 4.30 (m, 1H,  $\text{C}_3\text{-H}$ ), 4.73-4.84 (m, 1H,  $\text{P-N-CH}$ ), 6.43 (m, 4H,  $\text{DMTr-4H}$ ), 6.53 (t, 1H,  $\text{C}_1\text{-H}$ ), 7.06 (m, 3H,  $\text{DMTr-3H}$ ), 7.09-7.16 (m, 5H,  $\text{DMTr-5H}$ ), 7.29 (m, 2H,  $\text{DMTr-H}$ ,  $\text{CR-H}$ ), 7.43 (m, 2H,  $\text{CR-H}$ ,  $\text{DMTr-H}$ ), 7.51 (t, 1H,  $\text{CR-H}$ ), 7.65 (t, 1H,  $\text{CR-H}$ ), 7.86 (m, 2H,  $\text{N}^1\text{-H}$ ,  $\text{CR-H}$ ), 7.94 (d, 1H,  $\text{CR-H}$ ), 8.10 (dd, 1H,  $\text{CR-H}$ ), 8.56 (s, 1H,  $\text{DMF-CH}$ ), 8.59 (dd, 1H,  $\text{CR-H}$ ), 8.65 (d, 1H,  $\text{CR-H}$ ), 8.76 (d, 1H,  $\text{CR-H}$ ), 8.82 (br. s, 1H,  $\text{N}^8\text{-H}$ )

$^{13}\text{C}$  NMR (101 MHz,  $\text{CDCl}_3$ , two diastereomers)  $\delta$  11.44, 14.13, 18.78, 20.11, 20.16, 20.20, 22.67, 22.93, 23.00, 23.02, 24.52, 24.60, 25.31, 31.61, 34.69, 35.12, 41.18, 43.29, 43.38, 45.32, 45.37, 54.94, 54.96, 58.14, 58.18, 77.24, 84.02, 86.59, 86.63, 112.85, 112.87, 112.93, 120.76, 122.29, 123.62, 124.02, 126.19, 126.40, 127.73, 128.37, 128.90, 129.79, 129.87, 129.94, 158.37

$^{31}\text{P}$  NMR (x MHz,  $\text{CDCl}_3$ , two diastereomers)  $\delta$  148.61, 149.09

ESI-MS (positive mode):  $m/z$  calcd for  $\text{C}_{61}\text{H}_{64}\text{O}_7\text{N}_9\text{P}^+$  1066.47 Da, observed 1066.191 Da  $[\text{M}]^+$



### 2.3 Results and Discussion

For introduction of the bromine at the C8 position of deoxyguanosine, freshly recrystallized NBS was used; crude NBS resulted in lower yields for the reaction. In the third step of the scheme, which involved a Mitsunobu reaction to protect the carbonyl moiety, DIAD was preferentially used in place of DEAD. Again, DIAD resulted in better yields for the reaction. The final protection on the dG is a DMTr protection of the free primary amine. The DMTr group is believed to facilitate the successive Buchwald-Hartwig coupling reaction. This is generally attributed to the increased solubility of the dG in the reaction as a result of the non-polar DMTr group.

After the Buchwald-Hartwig coupling, all successive products are extremely prone to degradation, as they are acid-, light-, temperature-, and pressure-sensitive. The reactions are wrapped in aluminum foil to prevent the products from undergoing photodecomposition. Also, if the synthesis is paused at any point, the product is stored at -20 °C to limit the rate of degradation. At the final stage of the synthesis, the phosphoramidite adduct is kept at -80 °C and wrapped in foil to prevent degradation.

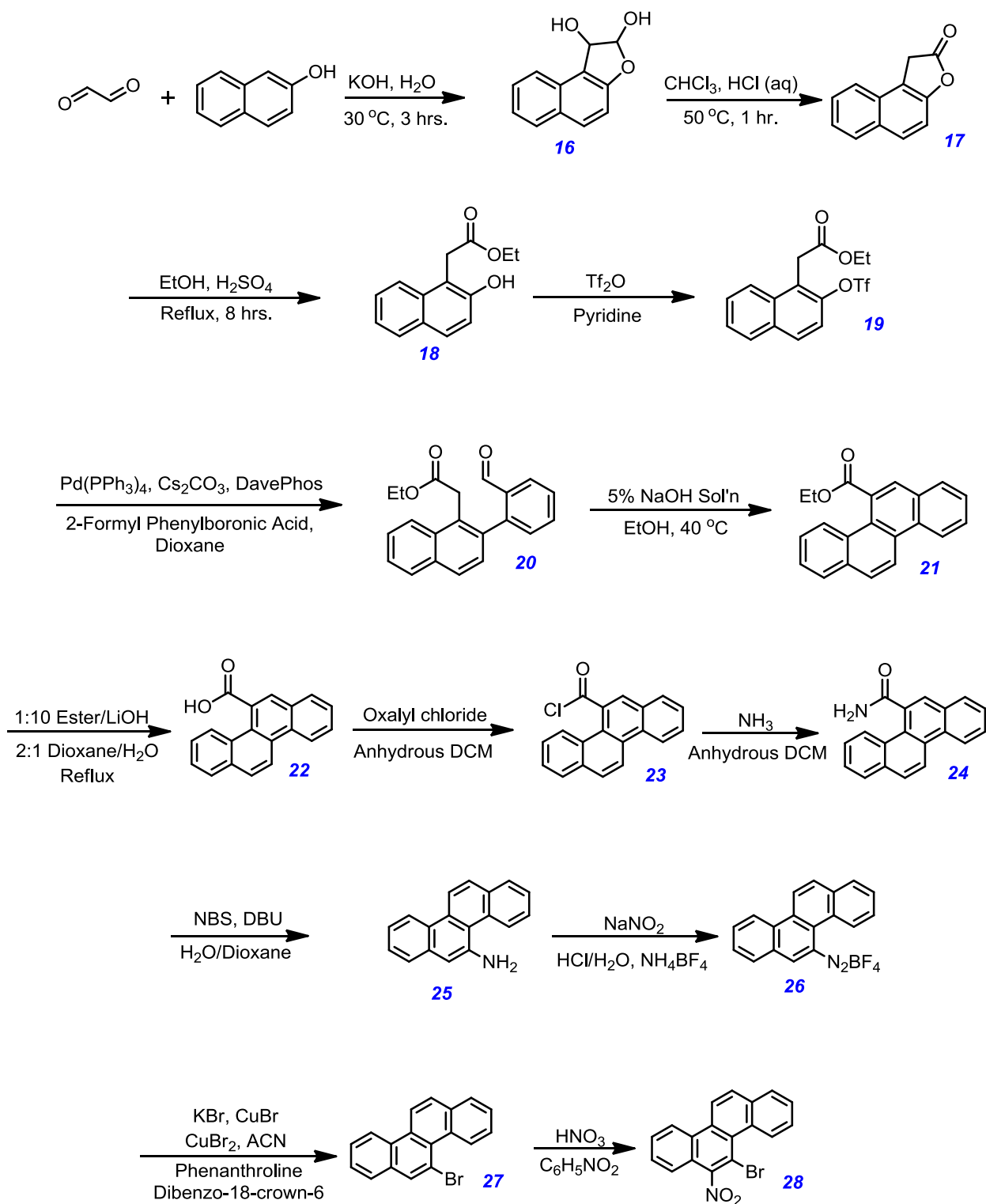
The Buchwald-Hartwig coupling products are purified *via* aluminum oxide column chromatography. This is done to prevent any degradation that the mildly acidic silica gel could potentially cause. After this however, silica gel is used since the most acid labile group present is the DMTr group. The DMTr group is then cleaved with an extremely dilute solution of HCl; the strength of the acid used is critical since the *N*-glycosidic bond is highly acid-sensitive. The deprotection of the TBDMS ether groups was carried out with 1M TBAF in THF, but this reaction could also be substituted with TEA•3HF. The final DMTr protection of the 5'OH group is a critical step. The reaction mixture must be very dry in order to succeed in the next step; as such, the starting material was thrice-co-evaporated with pyridine. Additionally, the total time of the reaction along with the equivalents of DMT-Cl used was vital. If a large excess of DMT-Cl is used, the time must be monitored very carefully to ensure that protection of the 3'-OH does not

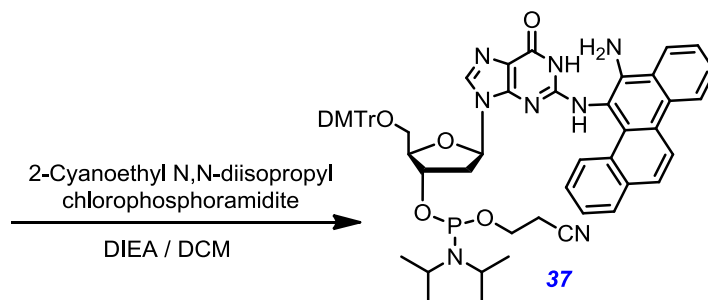
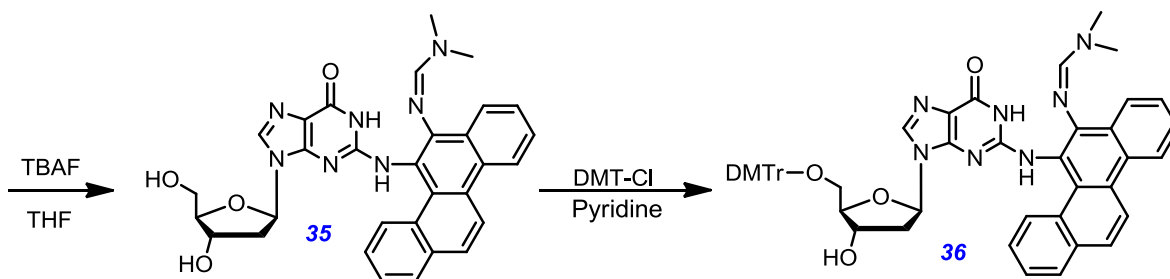
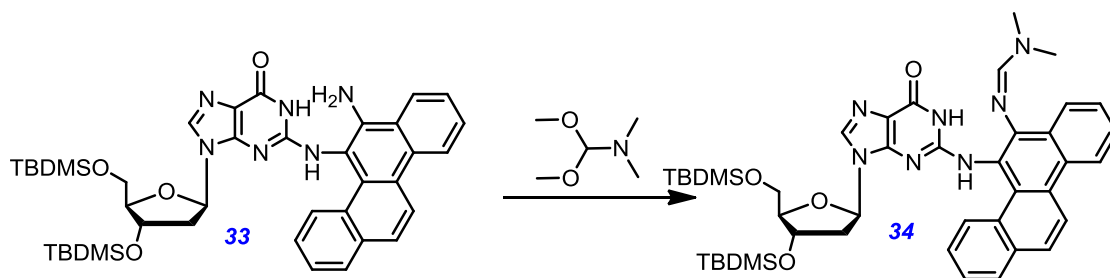
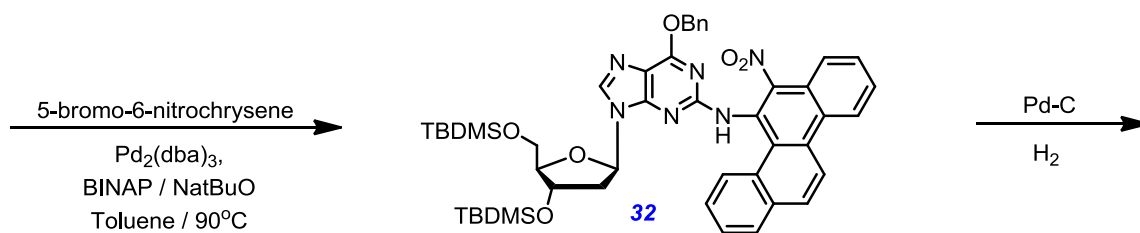
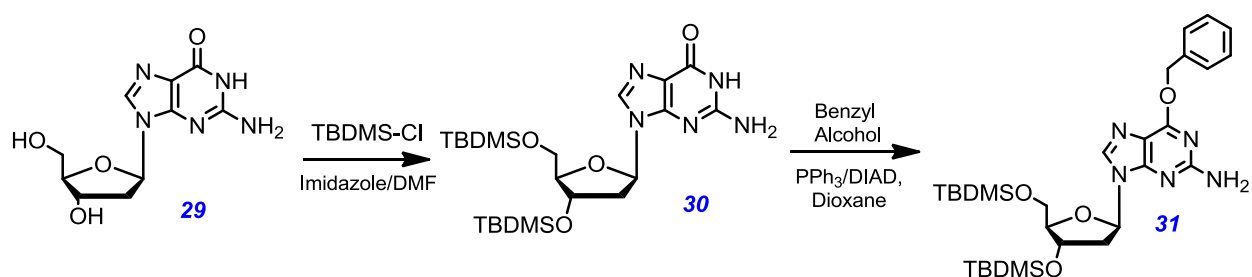
occur. A balance of 1.2 equivalents of DMT-Cl allowed the time component to be far less important, and given appropriate time, the reaction proceeded in good yield, without an excessive amount of product with both hydroxyl groups protected. The final step, phosphoramidite protection of the 3'-OH is also extremely sensitive. The starting material – which is one of the most stable products (relatively) within the scheme – was left to dry overnight under vacuum, to ensure no moisture would be present in the reaction. If this was not possible, the starting material was co-evaporated with methylene chloride multiple times and then left to dry under vacuum. The phosphoramidite reaction itself was performed in a glovebag with an argon atmosphere. The final two reactions were also purified with a basified silica gel column; this is to prevent the acidity of the silica gel from interfering with the products that were being separated. The synthesized phosphoramidite adduct is completely characterized (spectra show in the following section) and is ready for incorporation into an oligomer *via* solid-phase oligonucleotide synthesis.

## CHAPTER III

# SYNTHESIS OF THE $N^2$ PHOSPHORAMIDITE MONOMER OF $N^2$ - (6-AMINOCHRYSENE)-5'-O-(4,4'- DIMETHOXYTRITYL)-2'- DEOXYGUANOSINE

### 3.1 Original Synthetic Scheme for the 6-NC N<sup>2</sup>-dG Adduct





### 3.2 Materials and Methods

#### MATERIALS

Please refer to the materials section listed in the previous chapter.

#### PROCEDURES

**1,2-Dihydronaphtho[2,1-b]furan-1,2-diol (16)** – Freshly recrystallized 2-naphthol (2.00 g, 0.0139 mol) was added to a stirring Erlenmeyer flask of boiling deionized water (28 mL). The mixture was allowed to stir for 3-5 mins. To the stirring Erlenmeyer flask was added KOH (0.780 g, 0.0139 mol); the solution became homogenous and dark green. This solution was added dropwise over 1.5 h to a 500 mL round bottom flask equipped with a stirbar containing glyoxal (24 mL, 0.209 mol) at 40 °C. The reaction mixture was stirred for an additional 3 h. After this time, the reaction mixture was diluted with CHCl<sub>3</sub> (75 mL) and deionized water (75 mL). The layers were separated and the aqueous layer was extracted with CHCl<sub>3</sub> (2 x 75 mL). The organic layers were combined and washed with brine (1 x 50 mL). The organic layer was retained and dried over sodium sulfate. The solvent was removed *via* rotary evaporation. The crude product was purified by silica gel flash column chromatography with a step gradient of methanol (0-10%) in methylene chloride as the mobile phase. The product was isolated as a yellow-orange oil (2.30 g, 85% yield).

<sup>1</sup>H-NMR (400 MHz, DMSO-d<sub>6</sub>) δ ppm 5.25 (d, 1H, C<sub>12</sub>-H), 5.73 (d, 1H, C<sub>13</sub>-H), 5.86 (d, 1H, O<sub>15</sub>-H), 7.18 (d, 1H, C<sub>8</sub>-H), 7.35 (t, 1H, C<sub>2</sub>-H), 7.43 (d, 1H, O<sub>14</sub>-H), 7.53 (t, 1H, C<sub>1</sub>-H), 7.89 (m, 3H, C<sub>3</sub>-H, C<sub>6</sub>-H, C<sub>7</sub>-H)

<sup>13</sup>C-NMR (101 MHz, DMSO-d<sub>6</sub>) δ ppm 77.51 (C<sub>13</sub>), 109.52 (C<sub>12</sub>), 113.23 (C<sub>8</sub>), 120.34 (C<sub>10</sub>), 123.36 (C<sub>6</sub>), 123.68 (C<sub>2</sub>), 127.60 (C<sub>1</sub>), 129.28 (C<sub>3</sub>), 129.60 (C<sub>4</sub>), 13.44 (C<sub>5</sub>), 131.70 (C<sub>7</sub>), 157.55 (C<sub>9</sub>)

***Naphtho[2,1-b]furan-2(1H)-one (17)*** – In a 500 mL round bottom flask equipped with a stirbar was taken **16** (6.923 g, 0.03426 mol), CHCl<sub>3</sub> (145 mL), and 3N HCl (175 mL). The reaction mixture was stirred at 50 °C for 1 hr. After this time, the reaction mixture was diluted with CHCl<sub>3</sub> (100 mL) and deionized water (100 mL). The layers were separated and the aqueous layer extracted with CHCl<sub>3</sub> (2 x 100 mL). The organic layers were combined and washed with brine (1 x 50 mL). The organic layer was retained and dried over sodium sulfate. The solvent was removed *via* rotary evaporation. The crude product was purified by silica gel flash column chromatography with a step gradient of methanol (0-5%) in methylene chloride. The purified product was isolated as a light pink solid (5.211 g, 83% yield).

<sup>1</sup>H-NMR (400 MHz, DMSO-d<sub>6</sub>) δ ppm 4.18 (s, 2H, C<sub>13</sub>-2H), 7.47 (m, 2H, C<sub>1</sub>-H, C<sub>8</sub>-H), 7.59 (t, 1H, C<sub>2</sub>-H), 7.72 (d, 1H, C<sub>6</sub>-H), 7.95 (m, 2H, C<sub>3</sub>-H, C<sub>7</sub>-H)

<sup>13</sup>C-NMR (101 MHz, DMSO-d<sub>6</sub>) δ ppm 32.73 (C<sub>13</sub>), 112.02 (C<sub>8</sub>), 118.64 (C<sub>10</sub>), 124.18 (C<sub>6</sub>), 125.40 (C<sub>2</sub>), 128.05 (C<sub>1</sub>), 129.56 (C<sub>3</sub>), 129.64 (C<sub>5</sub>), 129.79 (C<sub>7</sub>), 130.72 (C<sub>4</sub>), 152.21 (C<sub>9</sub>), 175.59 (C<sub>12</sub>)

***Ethyl 2-(2-hydroxynaphthalen-1-yl)acetate (18)*** – In a 100 mL round bottom flask equipped with a stirbar was taken **17** (0.451 g, 0.00245 mol), ethanol (30 mL, 0.514 mol), and sulfuric acid (5.5 mL, 0.103 mol). The reaction was refluxed for 8 hh. After this time, the mixture was allowed to cool to room temperature and then neutralized with aqueous sodium bicarbonate. The resulting precipitate was filtered using a Büchner funnel and washed with cold deionized water to give **18** as a light blue crystalline solid (0.5246 g, 93% yield).

<sup>1</sup>H-NMR (400 MHz, DMSO-d<sub>6</sub>) δ ppm 1.18 (t, 3H, C<sub>16</sub>-3H), 4.05 (s, 2H, C<sub>11</sub>-2H), 4.09 (q, 2H, C<sub>15</sub>-H), 7.20 (d, 1H, C<sub>8</sub>-H), 7.31 (t, 1H, C<sub>1</sub>-H), 7.45 (t, 1H, C<sub>6</sub>-H), 7.76 (m, 3H, C<sub>2</sub>-H, C<sub>5</sub>-H, C<sub>7</sub>-H), 9.80 (C<sub>17</sub>-H)

<sup>13</sup>C-NMR (101 MHz, DMSO-d<sub>6</sub>) δ ppm 14.86 (C<sub>16</sub>), 31.03 (C<sub>11</sub>), 60.74 (C<sub>15</sub>), 113.14 (C<sub>10</sub>), 118.53 (C<sub>8</sub>), 123.02 (C<sub>5</sub>), 123.28 (C<sub>1</sub>), 127.01 (C<sub>6</sub>), 128.68 (C<sub>4</sub>), 128.97 (C<sub>2</sub>), 129.06 (C<sub>7</sub>), 134.25 (C<sub>3</sub>), 153.68 (C<sub>9</sub>), 172.07 (C<sub>12</sub>)

***Ethyl 2-(2-(((trifluoromethyl)sulfonyl)oxy)naphthalen-1-yl)acetate (19)*** – In a 25 mL round bottom flask equipped with a stirbar was taken **18** (0.2868 g, 1.246 mmol). The flask was placed under an N<sub>2</sub> atmosphere and then cooled to 0 °C in an ice bath; it was dissolved dry pyridine (2 mL). To the stirring mixture at 0 °C was slowly added triflic anhydride (0.233 mL, 1.385 mmol) dropwise. After stirring at 0 °C for 5 mins, the ice bath was removed and the flask was allowed to warm to room temperature. The reaction mixture was allowed to stir for 25 h at room temperature. After this time, the solvent was removed *via* rotary evaporation. The crude product was purified by silica gel flash column chromatography with a step gradient of ethyl acetate (0-20%) in hexanes as the mobile phase. The pure product was isolated as a light yellow oil (0.449 g, 99% yield).

<sup>1</sup>H-NMR (400 MHz, DMSO-d<sub>6</sub>) δ ppm 1.16 (t, 3H, C<sub>23</sub>-3H), 4.10 (q, 2H, C<sub>24</sub>-2H), 4.28 (s, 2H, C<sub>12</sub>-2H), 7.55 (d, C<sub>6</sub>-2H), 7.69 (m, 2H, C<sub>3</sub>-H, C<sub>7</sub>-H), 8.10 (m, 3H, C<sub>1</sub>-H, C<sub>2</sub>-H, C<sub>8</sub>-H)

<sup>13</sup>C-NMR (101 MHz, DMSO-d<sub>6</sub>) δ ppm 14.53 (C<sub>23</sub>), 32.10 (C<sub>24</sub>), 61.50 (C<sub>12</sub>), 117.17 (C<sub>15</sub>), 119.66 (C<sub>8</sub>), 120.34 (C<sub>15</sub>), 124.00 (C<sub>10</sub>), 125.63 (C<sub>6</sub>), 127.84 (C<sub>2</sub>), 128.62 (C<sub>1</sub>), 129.34 (C<sub>3</sub>), 131.20 (C<sub>7</sub>), 132.93 (C<sub>5</sub>), 133.14 (C<sub>4</sub>), 146.02 (C<sub>9</sub>), 169.96 (C<sub>11</sub>)

<sup>19</sup>F-NMR (376 MHz, DMSO-d<sub>6</sub>) δ ppm -73.93 (s, 3F, C<sub>15</sub>-3F)

***Ethyl 2-(2-(2-formylphenyl)naphthalen-1-yl)acetate (20)*** – In a 25 mL round bottom flask equipped with a stirbar was taken **19** (181 mg, 0.5 mmol) and dry dioxane (3 mL); flask was kept under an argon atmosphere. The flask was purged for 1 hr. with argon gas at room temperature. After this time, 2-



formyl phenylboronic acid (90 mg, 0.6 mmol), DavePhos (23 mg, 6 mol %), and tetrakis(triphenylphosphine)palladium(0) (46 mg, 8 mol %) was added to the flask and heated for an additional hour at 90 °C. After this time, cesium carbonate (489 mg, 1.5 mmol) was added to the flask and the flask was heated at 100 °C for 90 mins. The reaction was stopped at this time and the flask was allowed to cool to room temperature. The solvent was evaporated and the crude product was purified via silica gel flask column chromatography with ethyl acetate (0-20%) in hexanes as the mobile phase. A combination of **20** and **21** were obtained. The product **21** is sparingly soluble in hexanes, and the majority of it was obtained by filtering the combined fractions obtained after column chromatography; isolated as a white powder. The filtrate was collected; the solvent removed *via* rotary evaporation and the resulting green-brown viscous solid (~83.1 mg, ~55% yield) was used in the following reaction to generate **21**.

<sup>1</sup>H-NMR (400 MHz, CDCl<sub>3</sub>) δ ppm 1.14 (t, 3H, C<sub>24</sub>-3H), 3.93 (s, 2H, C<sub>17</sub>-2H), 4.07 (q, 2H, C<sub>23</sub>-2H), 7.39 (d, 1H, C<sub>8</sub>-H), 7.44 (d, 1H, C<sub>6</sub>-H), 7.57-7.70 (m, 4H, C<sub>1</sub>-H, C<sub>2</sub>-H, C<sub>13</sub>-H, C<sub>14</sub>-H), 7.87 (d, 1H, C<sub>12</sub>-H), 7.96 (d, 1H, C<sub>3</sub>-H), 8.06 (d, 1H, C<sub>15</sub>-H), 8.11 (dd, 1H, C<sub>7</sub>-H), 9.79 (s, 1H, C<sub>21</sub>-H)

**Ethyl chrysene-5-carboxylate (21)** – In a 250 mL round bottom flask equipped with a stirbar was taken the mixture of **20** and **21** (512 mg, 1.609 mmol) in ethyl alcohol (20 mL). The flask was heated to 40 °C. To the stirring solution was added 5% KOH in water (5 mL). The reaction was monitored by thin layer chromatography (TLC) (95:5 CH<sub>2</sub>Cl<sub>2</sub>/MeOH, v/v). After 12 hrs., the reaction mixture was filtered through a Büchner funnel. The desired compound precipitated out of the reaction mixture and was isolated as a white solid (329 mg, 68 % yield).

<sup>1</sup>H-NMR (400 MHz, DMSO-d<sub>6</sub>) δ ppm 1.32 (t, 3H, C<sub>23</sub>-3H), 4.48 (q, 2H, C<sub>22</sub>-2H), 7.68-7.73 (m, 2H, C<sub>3</sub>-H, C<sub>17</sub>-H), 7.76-7.80 (t, 1H, C<sub>16</sub>-H), 7.85-7.89 (t, 1H, C<sub>2</sub>-H), 8.15-8.29 (m, 4H, C<sub>4</sub>-H, C<sub>13</sub>-H, C<sub>15</sub>-H, C<sub>18</sub>-H), 8.33 (s, 1H, C<sub>7</sub>-H), 8.96 (d, 1H, C<sub>14</sub>-H), 9.00 (d, 1H, C<sub>1</sub>-H)

<sup>13</sup>C-NMR (101 MHz, DMSO-d<sub>6</sub>) δ ppm 14.26 (C<sub>23</sub>), 62.09 (C<sub>22</sub>), 121.11 (C<sub>14</sub>), 123.42 (C<sub>1</sub>), 125.50 (C<sub>8</sub>), 125.90 (C<sub>3</sub>), 126.69 (C<sub>17</sub>), 127.08 (C<sub>16</sub>), 127.29 (C<sub>13</sub>), 128.51 (C<sub>2</sub>), 128.61 (C<sub>15</sub>), 128.75 (C<sub>18</sub>), 129.42 (C<sub>4</sub>), 129.54 (C<sub>11</sub>), 129.96 (C<sub>7</sub>), 130.82 (C<sub>9</sub>), 131.55 (C<sub>5</sub>), 132.28 (C<sub>10</sub>), 132.38 (C<sub>12</sub>), 133.07 (C<sub>6</sub>), 172.21 (C<sub>19</sub>).

***Chrysene-5-carboxylic acid (22)*** – In a 25 mL round bottom flask equipped with a stirbar was taken **21** (100 mg, 0.333 mmol) dissolved in dioxane (10 mL). To it was added a solution of LiOH (100 mg, 3.330 mmol) in deionized water (5 mL). The reaction mixture was refluxed and stirred vigorously for 3 days. Once the reaction was complete, the flask was allowed to cool to room temperature. The reaction mixture was diluted with DI water (25 mL) and methylene chloride. Any excess starting material was removed via extraction of the solution with methylene chloride (1 x 25ml). The organic layer was retained and washed with DI H<sub>2</sub>O (3 x 50 mL). The aqueous layers were combined and acidified using 37% hydrochloric acid. The acidified aqueous layer was diluted with diethyl ether (75 mL) and washed with DI water (1 x 75 mL). The aqueous layer was retained and extracted again with ether (3 x 50 mL). The organic layers were combined and washed with brine (1 x 75 mL). The organic layer was retained, dried over sodium sulfate, and the solvent removed via rotary evaporation to give the desired product as a white solid (91 mg, 100 % yield).

<sup>1</sup>H-NMR (400 MHz, DMSO-d<sub>6</sub>) 7.65-7.70 (m, 2H, C<sub>2</sub>-H, C<sub>11</sub>-H), 7.75 (t, 1H, C<sub>3</sub>-H), 7.83 (t, 1H, C<sub>12</sub>-H), 8.13 (d, 1H, C<sub>1</sub>-H), 8.19 (d, 2H, C<sub>4</sub>-H, C<sub>10</sub>-H), 8.27 (s, 1H, C<sub>8</sub>-H), 8.48 (d, 1H, C<sub>17</sub>-H), 8.94 (d, 1H, C<sub>13</sub>-H), 8.96 (d, 1H, C<sub>16</sub>-H), 13.54 (br. s, 1H, -COOH)

<sup>13</sup>C-NMR (101 MHz, DMSO-d<sub>6</sub>) 121.37 (C<sub>16</sub>), 123.52 (C<sub>13</sub>), 124.18 (C<sub>11</sub>), 126.07 (C<sub>2</sub>), 126.17 (C<sub>3</sub>), 126.67 (C<sub>17</sub>), 127.42 (C<sub>12</sub>), 128.21 (C<sub>4</sub>), 128.42 (C<sub>1</sub>), 128.49 (C<sub>15</sub>), 128.50 (C<sub>10</sub>), 128.80 (C<sub>7</sub>), 129.01 (C<sub>5</sub>), 129.02 (C<sub>6</sub>), 130.25 (C<sub>8</sub>), 130.36 (C<sub>9</sub>), 130.44 (C<sub>18</sub>), 132.45 (C<sub>14</sub>), 172.56 (C<sub>19</sub>)

***Chrysene-5-carbonyl chloride (23)*** – In a 25 mL round bottom flask equipped with a stirbar was taken **22** (52 mg, 0.19 mmol). The flask was placed under an argon atmosphere. The compound was dissolved in anhydrous methylene chloride (15 mL); reaction mixture was cloudy white. Oxalyl chloride (0.1 mL, 0.382 mmol) was added to the flask; reaction mixture turned cloudy yellow. The reaction mixture was allowed to stir for 2 hrs. at room temperature. Upon completion, the reaction mixture became clear. At this point, the solvent was removed *via* rotary evaporation to give the pure product as a dark yellow solid (100% yield is assumed based on yield for the following reaction – the compound was not isolated)

***Chrysene-5-carboxamide (24)*** – In a 25 mL round bottom flask equipped with a stirbar was taken **23** (55.5 mg, 0.191 mmol). The flask was placed under an argon atmosphere, and the compound dissolved in anhydrous methylene chloride (5 mL). NH<sub>3</sub> was bubbled into the flask, and as the reaction progressed, the mixture became increasingly cloudy from its initial clear yellow color. Upon completion of the reaction, the reaction mixture was a cloudy white. After 2 h, the reaction was stopped, and the solvent removed *via* rotary evaporation to give the pure product as a white solid (52 mg, 100 % yield).

<sup>1</sup>H-NMR (400 MHz, DMSO-d<sub>6</sub>) 6.99-7.25 (br. s (rotomeric effect), 2H, N<sub>20</sub>-2H), 7.67-7.70 (m, 2H, C<sub>2</sub>-H, C<sub>11</sub>-H), 7.76 (t, 1H, C<sub>3</sub>-H), 7.84 (t, 1H, C<sub>12</sub>-H), 8.14 (m, 1H, C<sub>1</sub>-H), 8.20 (m, 2H, C<sub>4</sub>-H, C<sub>10</sub>-H), 8.28 (s, 1H, C<sub>8</sub>-H), 8.47 (d, 1H, C<sub>17</sub>-H), 8.94 (d, 1H, C<sub>13</sub>-H), 8.97 (d, 1H, C<sub>16</sub>-H)

<sup>13</sup>C-NMR (101 MHz, DMSO-d<sub>6</sub>)

***2'-deoxyguanosine, anhydrous (26)*** – In a 250 mL round bottom flask equipped with a stirbar was taken 2'-deoxyguanosine monohydrate (10 g, 0.0374 mol). To it was added pyridine (150 mL). The stirring mixture was refluxed for 5 h. After this time, the solvent was removed *via* rotary evaporation and the resulting dry dG was stored under N<sub>2</sub>.

**3',5'-O-bis(tert-butyldimethylsilyl)-2'-deoxyguanosine (27)** – In a 250 mL round bottom flask equipped with a stirbar was taken **26** (15.003 g, 56.140 mmol) and imidazole (18.265 g, 268.295 mmol). The flask was placed under an N<sub>2</sub> atmosphere. To the flask was added dry DMF (135 mL). The reaction mixture was left to stir at room temperature for 5-10 mins until the solution was homogenous. At this point, *tert*-butyldimethylsilyl chloride (23.246 g, 154.274 mmol); within 5 mins, the solution became transparent. The mixture was left to stir at room temperature under an N<sub>2</sub> atmosphere for 8 h. After this time, the reaction was quenched with methanol and the solvent removed *via* rotary evaporation. The crude product was diluted with methylene chloride ( ) and deionized water ( ). The layers were separated and the aqueous layer was extracted with methylene chloride (2 x 100 mL). The organic layers were combined and washed with brine (1 x 75 mL). The organic layer was dried over Na<sub>2</sub>SO<sub>4</sub> and the solvent removed *via* rotary evaporation. The compound was purified by silica gel flash column chromatography with methanol (0-5%) in methylene chloride as the mobile phase. The pure product was isolated as a white solid (21.435 g, 77%).

<sup>1</sup>H-NMR (400 MHz, DMSO-d<sub>6</sub>) δ ppm 0.04 (s, 3H, C<sub>22</sub>-3H), 0.05 (s, 3H, C<sub>21</sub>-3H), 0.10 (s, 6H, C<sub>28</sub>-3H, C<sub>29</sub>-3H), 0.87 (s, 9H, C<sub>24</sub>-3H, C<sub>25</sub>-3H, C<sub>26</sub>-3H), 0.89 (s, 9H, C<sub>31</sub>-3H, C<sub>32</sub>-3H, C<sub>33</sub>-3H), 2.20-2.26 (ddd, 1H, C<sub>13</sub>-H), 2.62-2.67 (ddd, 1H, C<sub>13</sub>-H'), 3.62-3.72 (qd, 2H, C<sub>18</sub>-2H), 3.80 (m, 1H, C<sub>12</sub>-H), 4.48 (m, 1H, C<sub>16</sub>-H), 6.09-6.12 (t, 1H, C<sub>14</sub>-H), 6.49 (br. s, 2H, N<sub>10</sub>-2H), 7.87 (s, 1H, C<sub>7</sub>-H), 10.63 (s, 1H, N<sub>1</sub>-H)

<sup>13</sup>C-NMR (101 MHz, DMSO-d<sub>6</sub>) δ ppm -5.53 (C<sub>29</sub>), -5.48 (C<sub>28</sub>), -4.97 (C<sub>22</sub>), -4.79 (C<sub>21</sub>), 17.70 (C<sub>30</sub>), 17.95 (C<sub>23</sub>), 25.67 (C<sub>31</sub>, C<sub>32</sub>, C<sub>33</sub>), 25.76 (C<sub>24</sub>, C<sub>25</sub>, C<sub>26</sub>), 62.74 (C<sub>13</sub>), 72.16 (C<sub>18</sub>), 82.10 (C<sub>12</sub>), 86.98 (C<sub>14</sub>), 116.63 (C<sub>16</sub>), 121.32 (C<sub>5</sub>), 134.86 (C<sub>7</sub>), 150.97 (C<sub>4</sub>), 153.72 (C<sub>2</sub>), 156.65 (C<sub>6</sub>)

**O<sup>6</sup>-benzyl-3',5'-O-bis(tert-butyldimethylsilyl)-2'-deoxyguanosine (28)** – In a 500 mL flask equipped with a stirbar was taken **27** (15.584 g, 31.434 mmol) and triphenylphosphine (14.403 g, 54.915 mmol). The

flask was placed under an N<sub>2</sub> atmosphere and to it was added dry dioxane (200 mL). To the stirring reaction mixture at room temperature, benzyl alcohol (5.702 mL, 55.104 mmol) was added. Diisopropyl azodicarboxylate (10.992 mL, 55.827 mmol) was added dropwise to the stirring mixture, which turned to a transparent yellow within 15 mins. The reaction was allowed to continue stirring at room temperature for 8 h under the N<sub>2</sub> atmosphere. After this time, the solvent was evaporated. The crude compound was purified by silica gel flash column chromatography with a step gradient of ethyl acetate (0-30%) in hexanes as the mobile phase. The product was isolated as a white solid (8.56 g, 46 % yield).

<sup>1</sup>H-NMR (400 MHz, CDCl<sub>3</sub>) δ ppm 0.07 (s, 3H, C<sub>34</sub>-3H), 0.08 (s, 3H, C<sub>33</sub>-3H), 0.10 (s, 6H, C<sub>35</sub>-3H, C<sub>36</sub>-3H), 0.91 (s, 9H, C<sub>38</sub>-3H, C<sub>39</sub>-3H, C<sub>40</sub>-3H), 0.92 (s, 9H, C<sub>30</sub>-3H, C<sub>31</sub>-3H, C<sub>32</sub>-3H), 2.35-2.40 (ddd, 1H, C<sub>13</sub>-H), 2.52-2.58 (ddd, 1H, C<sub>13</sub>-H'), 3.74-3.84 (qd, 2H, C<sub>18</sub>-2H), 3.96-3.99 (m, 1H, C<sub>12</sub>-H), 4.57-4.60 (m, 1H, C<sub>16</sub>-H), 5.01 (br. s, 2H, N<sub>10</sub>-2H), 5.54-5.61 (s, 2H, C<sub>20</sub>-2H), 6.33 (t, 1H, C<sub>14</sub>-H), 7.30-7.37 (m, 3H, C<sub>23</sub>-H, C<sub>24</sub>-H, C<sub>25</sub>-H), 7.48-7.51 (d, 2H, C<sub>22</sub>-H, C<sub>26</sub>-H), 7.93 (s, 1H, C<sub>7</sub>-H)

<sup>13</sup>C-NMR (101 MHz, CDCl<sub>3</sub>) δ ppm -5.24 (C<sub>36</sub>), -5.13 (C<sub>35</sub>), -4.55 (C<sub>34</sub>), -4.42 (C<sub>33</sub>), 18.25 (C<sub>37</sub>), 18.67 (C<sub>29</sub>), 26.00 (C<sub>38</sub>, C<sub>39</sub>, C<sub>40</sub>), 26.21 (C<sub>30</sub>, C<sub>31</sub>, C<sub>32</sub>), 41.27 (C<sub>13</sub>), 63.00 (C<sub>18</sub>), 68.54 (C<sub>20</sub>), 72.05 (C<sub>12</sub>), 84.10 (C<sub>14</sub>), 87.96 (C<sub>16</sub>), 116.07 (C<sub>5</sub>), 128.25 (C<sub>23</sub>, C<sub>25</sub>), 128.55 (C<sub>24</sub>), 128.61 (C<sub>22</sub>, C<sub>26</sub>), 136.52 (C<sub>21</sub>), 137.99 (C<sub>7</sub>), 154.50 (C<sub>4</sub>), 158.92 (C<sub>2</sub>), 161.21 (C<sub>6</sub>)

### 3.3 Results and Discussion

The N<sup>2</sup>-dG 6-nitrochrysene adduct is notably different from the C8-dG adduct due to the attachment point of the chrysene derivative to the guanine base. It attaches at the C<sub>5</sub> position of the aryl system as opposed to the C<sub>6</sub> position. It is this aspect of the adduct that makes the synthesis particularly challenging. Chrysene preferentially reacts at the 6 and 12 positions, making the process of putting a moiety at the 5 position difficult. After attempting various schemes which generally fell short of producing initial reactions with high yield, the scheme listed earlier was decided upon. High yields for the first few reactions are critical, because the scheme is approximately 20 steps long (depending on how the remainder of the scheme develops after Buchwald-Hartwig coupling). An inability to scale up the preliminary products would make the entire scheme tedious and in general, not viable for broad application. The other portion of the scheme, focused on development of the deoxyguanosine derivative for Buchwald-Hartwig coupling is completed.

In order to achieve putting an aryl bromide at the C<sub>5</sub> position of chrysene, attempts were made to simply put any functionality at the C<sub>5</sub> position that could later be altered to a bromide. It is impossible to use chrysene as a starting material, since the C<sub>5</sub> position cannot compete with the C<sub>6</sub> and C<sub>12</sub> positions in terms of reactivity. To work around this, a naphthol derivative was employed as a base for eventually building the polyaromatic system.<sup>[27]</sup> In this scheme,  $\beta$ -naphthol was used in conjunction with glyoxal to produce a diol, **16**. From this, the diol was oxidized to a lactone, which was successively broken to form an ethyl ester. At this point, the hydroxyl group at the beta position could easily be transformed to a triflate.<sup>[28]</sup> These four reactions worked in excellent yield and served as a solid foundation for the rest of the scheme since they are extremely easy to scale-up.

The purpose of creating the triflate is to perform a microwave Suzuki coupling that would ultimately create the backbone for the chrysene aromatic ring system.<sup>[29,30]</sup> This reaction was originally meant to

encompass not only the coupling to form the three ring system, but to also go further and cyclize to form the fourth ring which would then undergo condensation to form the chrysene ethyl ester, **21** (Figure 13). This one-pot reaction has previously been attempted for a phenanthrene system with limited success.<sup>[29]</sup> The group achieved their best coupling and cyclization yield with ethyl esters, which is why ethanol was chosen to break the lactone.

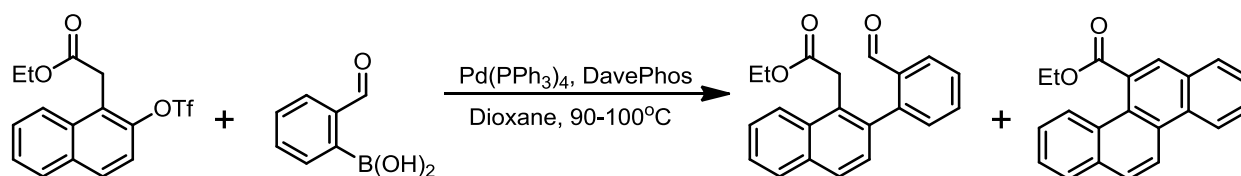


Figure 13: General Outline of the Suzuki coupling with Major Products

From this, a series of reactions were completed to standardize the reaction (Table 1). Originally, upon attempting the microwave reaction using the conditions outlined, no reaction was observed. In the beginning,  $\text{Pd(PPh}_3)_2\text{Cl}_2$  was used as the metal catalyst, with three equivalents of base to push the final cyclization and condensation. Proceeding to increase the temperature (*Entry 2*), the reaction appeared to have started to proceed. Attempts were made to increase the reaction time, in lieu of increasing the temperature, but it appeared as though the high temperatures facilitated the initiation of the reaction within a short period of time (*Entries 3 and 4*). Since difficulties with coupling reactions usually stem from the palladium catalyst, a switch was made to  $\text{Pd(PPh}_3)_4$ , a more reactive palladium catalyst. This produced notably higher yields upon increases in temperature and time. However, it should be noted that over time, a mixture of products was observed; the coupling product and the condensed product after cyclization. Due to the high degree of similarity between these two products' polarities, it is extremely difficult to separate them *via* column chromatography; as such, yields are given as approximate ranges for subsequent entries. Now that the reaction was starting, a higher catalyst loading was used to push it to proceeding further. Although this did work to some extent, it was found that heating at high temperature

for a long time would cause degradation of the desired product (**21**). In fact, **21** would undergo a form a decarboxylation and upon purification of the reaction mixture, pure chrysene was obtained.

	Triflate	Boronic Acid	Pd(PPh <sub>3</sub> ) <sub>2</sub> Cl <sub>2</sub>	Pd(PPh <sub>3</sub> ) <sub>4</sub>	Cs <sub>2</sub> CO <sub>3</sub>	Temperature (°C)	Microwave	Time	Yield
1	1	1.2	0.04	-	3	100	Yes	10 min	0%
2	1	1.2	0.04	-	3	130	Yes	10 min	<5%
3	1	1.2	0.04	-	3	120	Yes	20 min	0%
4	1	1.2	0.04	-	3	150	Yes	10 min	<10%
5	1	1.2	-	0.04	3	150	Yes	10 min	10%
6	1	1.2	-	0.04	3	150	Yes	30 min + 10 min	10-15%*
7	1	1.2	-	0.08	3	150	Yes	30 min	10-15%*
8	1	1.2	-	0.1	3	90, 1hr.; 100, 1hr.	No	2 hrs.	~45%
9	1	1.2	-	0.1	3**	90, 1hr.; 100, 1hr.	No	2 hrs.	~55%
10	1	1.2	-	0.08	3**	90, 1hr.; 100, 1hr.	No	2 hrs.	~55%
11	1	1.2	-	0.08	3**	90, 1hr.; 100, 1.5hr.	No	2.5 hrs.	60-65%
12	1	1.2	-	0.08	3**	90, 1hr.; 100, 2hr.	No	3 hrs.	50-55%
13	1	1.2	-	0.08	1.5**	90, 1hr.; 100, 1.5hr.	No	2.5 hrs.	55-65%

\*Estimated yield; mixture of products measured

\*\*Modified protocol used; base added before increase in temperature 1 hour into the reaction

Table 1: Standardization of the Suzuki Coupling Reaction in the N<sup>2</sup>-dG Scheme

After observing this, the coupling was switched from a microwave to a batch reaction, which could sustain heat at lower temperatures for a longer length of time. At the time, it was thought that reaction might proceed at a lower temperature with the new palladium catalyst; catalyst loading was also increased to better facilitate this. Entry 8 details the reaction conditions for the first batch reaction, which produced considerably higher yields. The Buchwald-Hartwig coupling procedure is similar to this, with the exception of the time of addition of the base. The delay in adding the base is thought to allow for better formation of the intermediate complex, which ultimately increase yield. Applying this thought process to the Suzuki coupling (*Entries 9-13*), it was hoped that the same overall yield increase would occur. As expected, the yield increased an additional 10%. After seeing these promising results, the catalyst loading was dropped slightly to see if there would be a drastic impact on the reaction yield, and the ideal catalyst loading was determined to be 8 mol %. At this time, the duration of the reaction was the final thing that was focused on, and 1.5 h after addition of the base was determined to give the maximum yield. Since all



of these conditions were still producing a mixture of products, and an additional reaction (simple addition of base with heat to promote cyclization and condensation) had to be done anyway on the portion of product that did not cyclize and condense, the equivalents of base were also cut down to 1.5 equivalents.<sup>[31]</sup> This did not seem to affect the overall outcome of the reaction. It should be noted, that with all of the coupling reactions presented in these syntheses, the yield did drop slightly (~5%) when the reaction was scaled up significantly.

After standardization of the coupling reaction and subsequent cyclization/condensation, a series of reactions were performed to produce an amide. This was accomplished through a hydrolysis of the ethyl ester, formation of an acyl chloride, and finally bubbling of ammonia to produce the amide. These all worked in excellent yield. It should be noted that the hydrolysis reaction is best done with LiOH as the base.<sup>[32]</sup> Initially, the reaction was attempted with both KOH and NaOH (since they were stronger bases), but the reaction did not proceed as readily with KOH and took a significantly longer time to proceed with NaOH. In the end, LiOH worked best; this is attributed to the lithium ion being able to better coordinate with the oxygens in the ester since lithium is a far smaller ion. Additionally, the formation of the acyl chloride was originally attempted with SOCl<sub>2</sub> as a reagent<sup>[33]</sup>, but upon encountering a difficult work-up, the reagent was changed to oxalyl chloride.<sup>[34]</sup> Finally, the bubbling of ammonia<sup>[35]</sup> was decided upon, to avoid the use of more dangerous reagents such as NaNH<sub>2</sub>.<sup>[36]</sup>

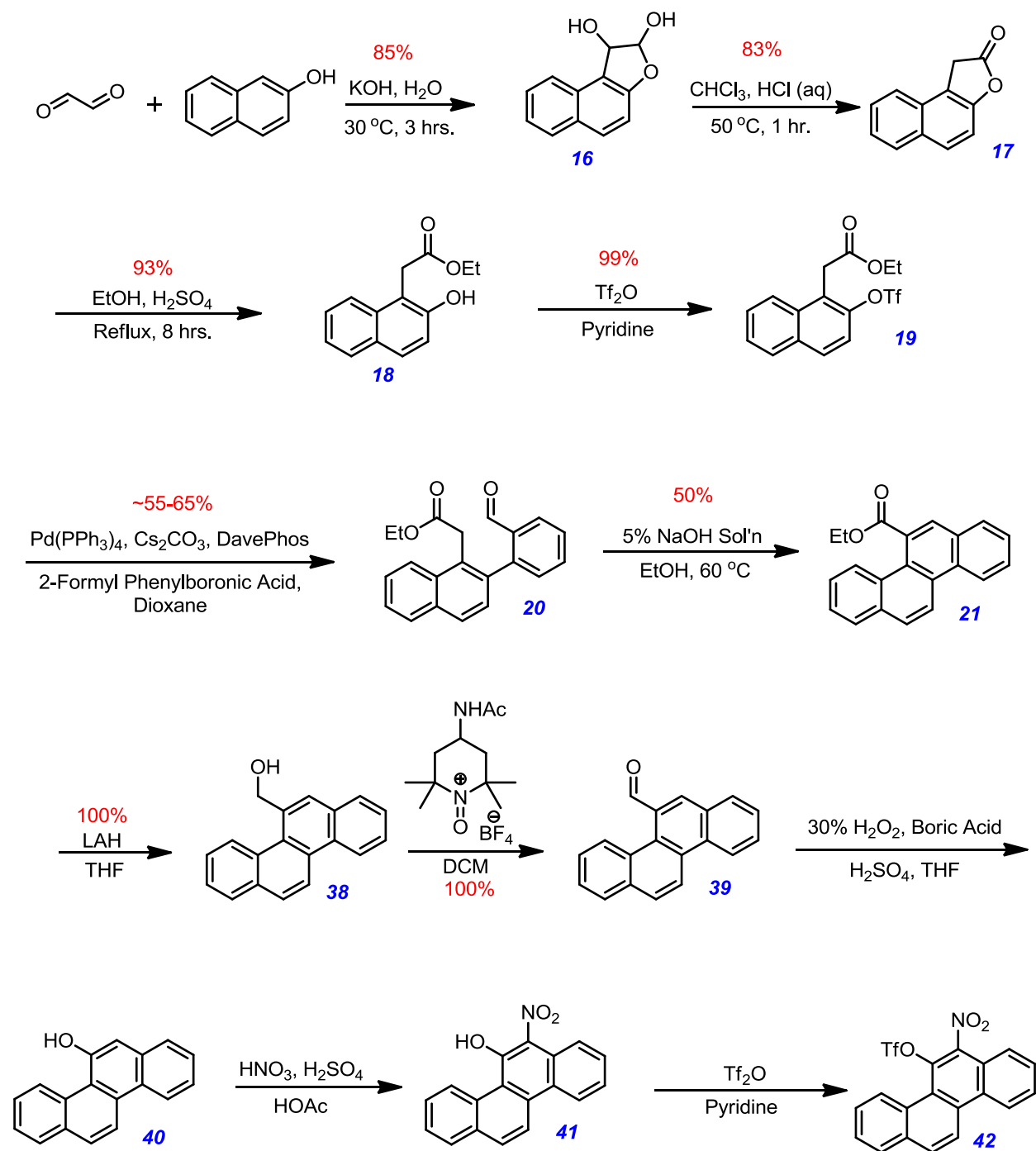
Following production of the amide, the rest of the synthesis involved a Hoffman rearrangement and degradation to produce an aryl amine, which could then undergo Sandmeyer bromination. Ultimately, this would put a bromine in the desired C5 position on chrysene. Then, the final reaction reprises the nitration reaction which was already done in the prior C8-dG scheme.

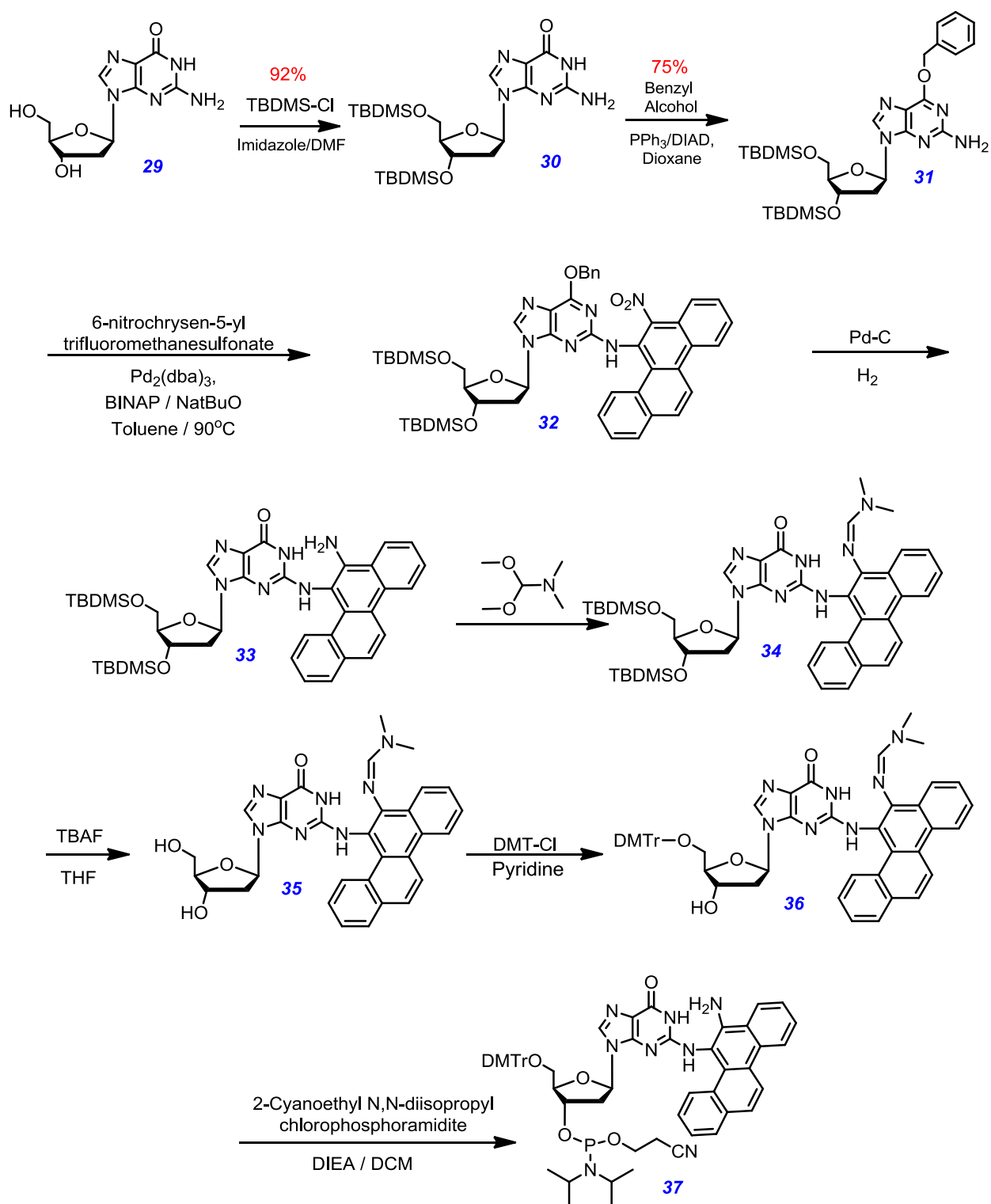
The Hoffman reaction proved to be difficult. After standardizing the reaction, it was clear that a multitude of not only the product, but byproducts and starting materials remained in the reaction

mixture.<sup>[37]</sup> Although the product was not isolated, characteristic peaks of the product were present in the NMR of the crude reaction mixture. Workup of the mixture through extractions eliminated the acid formed, but the byproducts proved to be extremely difficult to separate out of the mixture. Silica gel column chromatography resulted in the product (and other byproducts) adhering to the solid phase. This was not entirely unsurprising due to the nitroreduction reaction that produced 6-aminochrysene in the previous scheme. It was clear that a portion of the 6-AC did remain on the column. This was not a problem in the prior scheme where the reaction proceeded well, so the majority of the compound came off of the plug with a more polar solvent (such as methanol). However, the Hoffman reaction required a proper separation, so the compounds cannot simply be forced off of the column. In an attempt to reduce the attraction of the compound to the stationary phase, the next attempt at purification used basified silica gel (using triethylamine). This did not yield better results. To eliminate acidity altogether, neutral aluminum oxide was used as the stationary phase, and a proper separation was still not achieved.

As detailed in the above paragraph, the Hoffman reaction posed many difficulties, and it was not clear the two-step Sandmeyer bromination<sup>[38]</sup> would work efficiently and in good yield as well. Further research was done to see if these reactions could be circumvented or replaced altogether with higher yielding reactions. An altered scheme is presented in the following sections.

### 3.4 Modified Synthetic Scheme for the 6-NC N<sup>2</sup>-dG Adduct





### 3.5 Materials and Methods

#### MATERIALS

Please refer to the listed materials within the previous chapter.

#### PROCEDURES

**Chrysen-5-ylmethanol (38)** - In an oven-dried 50 mL round bottom flask equipped with a stirbar was taken lithium aluminum hydride (20 mg, 0.499 mmol). The flask was immediately placed under an argon atmosphere. To it was added anhydrous THF (3 mL) and the flask was allowed to stir in an ice bath for 5-10 mins. During this time, **21** (100 mg, 0.333 mmol) was dissolved in anhydrous THF and added dropwise to the flask containing LAH. The reaction was allowed to stir under argon at 0 °C for 2.5 h. At this time, the flask was taken out of the ice bath. The white precipitate was filtered off and washed with DCM. The filtrate was diluted with methylene chloride (50 mL) and deionized water (50 mL). The aqueous layer was extracted with methylene chloride (30 mL). The combined organic layers were washed with brine (50 mL). The organic layer was then dried over sodium sulfate, and the solvent removed *via* rotary evaporation to afford the pure compound as a white solid (86 mg, 100% yield).

<sup>1</sup>H-NMR (400 MHz, CDCl<sub>3</sub>) δ ppm 2.11 (br. s., -OH), 5.45 (s, 2H, -CH<sub>2</sub>), 7.63-7.73 (m, 4H, CR-4H), 7.97-8.03 (m, 3H, CR-3H), 8.16 (s, 1H, CR-H), 8.75 (dd, 2H, CR-2H), 8.95 (d, 1H, CR-H)

<sup>13</sup>C-NMR (101 MHz, CDCl<sub>3</sub>) δ ppm 66.84, 121.51, 123.14, 126.09, 126.22, 126.93, 127.78, 128.18, 128.46, 129.82, 130.34, 130.47, 131.32, 133.15, 135.45.

**Chrysene-5-carbaldehyde (39)** – To a 500 mL round bottom flask equipped with a stirbar was taken **#** (532 mg, 2.060 mmol) in methylene chloride (400 mL); the amount of solvent was maximized to increase the speed of the reaction. To the stirring mixture was added 4-(acetylamino)-2,2,6,6-tetramethyl-1-oxo-piperidinium tetrafluoroborate (Bobbitt's Salt, 618 mg, 2.060 mmol). Upon addition of Bobbitt's salt, the

mixture immediately turned a bright yellow. Following this, silica gel (532 mg, 1 wt. eq. to alcohol) was added to the mixture. The solution was allowed to stir for 10 h. The reaction was monitored by TLC (neat methylene chloride) and upon completion, the reaction mixture turned clear and translucent. When the reaction was complete, the solution was filtered through a silica gel plug with neat methylene chloride to afford the product as a white solid (522 mg, 95% yield).

<sup>1</sup>H-NMR (400 MHz, CDCl<sub>3</sub>) δ ppm 7.74-7.91 (m, 3H, CR-3H), 8.12-8.21 (m, 4H, CR-4H), 8.50 (s, 1H, CR-H), 8.81 (dd, 2H, CR-2H), 10.68 (s, 1H, -CHO)

### 3.6 Results and Discussion

Initially, the scheme called for 5-bromo-6-nitrochrysene as a coupling substrate for the Buchwald-Hartwig coupling. Due to difficulties encountered in that scheme, the reactant was altered to have a triflate moiety in place of the bromide. The use of a triflate for a Buchwald-Hartwig coupling between a PAH and a DNA nucleoside is very uncommon.<sup>[39]</sup> An amino group with an aryl bromide has been almost exclusively used in most syntheses of this type. However, there have been many precedents in general for joining aryl triflates and amino groups *via* Buchwald-Hartwig couplings.<sup>[40]</sup> Based on this, the new scheme was conceived to circumvent both the Hoffman degradation and Sandmeyer bromination reactions.

Starting from the ethyl 5-chrysene carboxylate, a lithium aluminum hydride reduction was performed to produce the corresponding alcohol.<sup>[41]</sup> This reaction worked in excellent yield, without any need for column chromatography purification. Following this, the product was oxidized to the corresponding aldehyde. Oxidation was accomplished with Bobbitt's salt, an oxoammonium salt which is known to be particularly environmentally friendly.<sup>[42]</sup> It avoids the use of toxic metal catalysts such as PCC and PDC (both chromium-containing reagents), which can contaminate water supplies, interfere with plant physiological processes such as photosynthesis, and cause soil erosion.<sup>[43]</sup> Taking an experimental viewpoint, the PCC/PDC approach also involves a monotonous reaction work-up. From a synthetic standpoint, the reaction is excellent because it is a colorimetric process and upon completion, can be purified with a simple silica gel plug. The reaction initially is golden-yellow in color, which progressively turns lighter. Once complete, the reaction becomes clear and translucent.

The subsequent reaction, taking an aromatic aldehyde to an alcohol moiety directly off of the aryl ring with loss of one carbon, is far more complex.<sup>[44]</sup> Standardization of this reaction is currently underway. Initial attempts to conduct the reaction at room temperature yielded very slow formation of a product (not

isolated, due to the small amount generated). Another attempt at the reaction, in refluxing conditions to produce more product at a faster rate, resulted in a complex mixture of products. Currently, I am attempting to identify the compounds resulted from this reaction. Additional studies will be conducted at a slightly elevated temperature to reduce the amount of byproducts.

The successive steps in the production of the 5-trifluoromethanesulfonate-6-nitrochrysene are expected to proceed readily and in good yield. The nitration reaction will be adapted from the C8 chrysene scheme detailed in the previous chapter and the triflate formation will be performed in the same manner as provided earlier in this scheme.

Following this, the Buchwald-Hartwig coupling reaction is expected to work well owing to the presence of the nitro group on the aryl reactant. Since the aryl halide/triflate is meant to be “nucleophilic” in nature while the organometallic compound is generally “electrophilic” in nature, the presence of electron-withdrawing groups on the aryl halide/triflate should enhance the efficiency of the coupling reaction. This effect is mainly attributed to the oxidative portion of the catalytic cycle, which proceeds faster when the palladium catalyst adds into electron-deficient aryl systems.

The remaining series of de-protections and re-protections to form a DNA adduct suitable for solid-phase oligonucleotide synthesis should work well. The only problem that is anticipated is the concurrent reduction of the benzyl ether and nitro groups. This reaction typically only serves to deprotect the carbonyl by reducing the benzyl ether protecting group. However, it is expected to work for both groups. In the case that it does not work or does not work efficiently, hydrazine and potentially mild heat will be used. The second approach has been proven to work efficiently and in good yield in literature. A major problem though is the addition of heat. Assuming that the  $N^2$  adduct is as unstable to light, heat, and acid as the C8 adduct was, it would be preferred if the reaction could be accomplished without the addition of heat. In a broad outlook on the scheme with the unstable nature of the compounds in mind, it is also



recommended that the scheme not be halted at any point after the Buchwald-Hartwig coupling. Due to the sensitive nature of the components, if the scheme must be paused, it is highly recommended that the products be kept sealed, under argon, wrapped in aluminum foil (to prevent light exposure) within -20 °C (if only overnight) or preferably, -80 °C (if for a period of time exceeding 12 h).

## **CHAPTER IV**

# **CONCLUSION AND FUTURE WORK**

## ***Conclusion***

These syntheses were designed and carried out to enable biological studies aimed toward understanding the initiation phase of cancer. These studies of the carcinogens are critical, since 6-nitrochrysene, though not as prevalent in the atmosphere as some of the other carcinogens, has been proven to be one of the most potent carcinogens of the PAH family. This work entails the syntheses of two 6-nitrochrysene deoxyguanosine adducts using a total synthesis approach.

The first adduct, C8-dG, has been completed in its entirety. The Buchwald-Hartwig coupling reaction was successful in forming the C-N bond between 6-aminochrysene and protected 8-bromo-dG. The C8-CR-dG phosphoramidite monomer has been prepared, and solid-phase oligonucleotide synthesis of a 12-mer has been completed.

The second project detailed was the  $N^2$ -dG project. The protected dG precursor has already been prepared and an outline for the projected scheme up to the phosphoramidite monomer has been planned and outlined. Thus far in the projected scheme, there are three steps left before the chrysene derivative for coupling will be prepared. The coupling is expected to occur in good yield, and the subsequent steps are also expected to proceed readily.

### Future Work

The C8-CR-dG phosphoramidite has been used for oligonucleotide synthesis. (Figure 14):

12-mer Sequence: 5' - GTG CXT GTT TGT - 3'

X: the C8-dG chrysene adduct, pictured on right

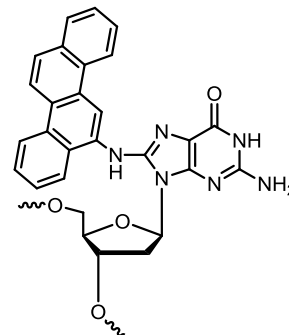


Figure 14: Final Oligomer for the C8-dG Adduct Incorporation

The 12-mer is a sequence from the *p53* gene, a tumor suppressor gene. This gene contains a mutational hotspot in the codon 273, where the adduct is located - the “X” in Figure 14. Mutations in these sequences have been detected in human cancers. So the adducted oligonucleotide will be a valuable substrate for biological and structural studies. The oligonucleotide will be incorporated into a vector which can be utilized in studies of both prokaryotic and eukaryotic cells. In these studies, the mutagenicity of the adduct will be determined. In addition, the roles played by various TLS polymerases will be investigated.

In the  $N^2$ -CR-dG adduct work, the reaction to produce 5-hydroxychrysene will soon be standardized. The remaining two steps are expected to proceed readily as they have been completed before in prior schemes using reasonable facsimiles of the starting materials in the  $N^2$ -CR-dG scheme. Also, research is being done to ascertain alternate routes of nitroreduction without the use of heat, in case the standard palladium-catalyzed hydrogenation does not also work to reduce the nitro group in a later reaction of the scheme. In a final attempt to overcome this problem, an additional step can be added to the scheme which will separately reduce the nitro group on the chrysene ring system. As the synthesis already contains 20

synthetic steps, this alternative will be only be used as a last resort. Aside from these two reactions, all other steps should result in good yield. Once the phosphoramidite monomer of the  $N^2$ -CR-dG adduct is prepared, it too will be used for solid-phase synthesis.

## References

- Pierce, B. A. *Genetics, A Conceptual Approach*, 4<sup>th</sup> ed.; W. H. Freeman and Company: New York, 2012.
- (a) Dizdaroglu, M. *Free Radical Biology & Medicine*, **1991**, *10*, 225-242. (b) Burney, S.; Caulfield, J. L.; Niles, J. C.; Wichnok, J. S.; Tannenbaum, S. R. *Mutation Research*, **1999**, *424*, 37-49. (c) Valko, M.; Izakovic, M.; Mazur, M.; Rhodes, C. J.; Telser, J. **2004**, *266*, 37-56. (d) Wiseman, H.; Halliwell, B. *Biochem. J.* **1996**, *313*, 17-29. (e) Marnett, L. J. *Carcinogenesis*, **2000**, *21*, 361-370.
- Bartek, Jiri; Lukas, Jiri (2001) "Mammalian G1- and S-phase checkpoints in response to DNA damage". *Current Opinion in Cell Biology* *13* (6): 738–747.
- Waters, L. S.; Minesinger, B. K.; Wiltout, M. E.; D'Souza, S.; Woodruff, R. V.; Walker, G. C. *Microbiol. Mol. Biol. Rev.* **2009**, *73*, 134-154.
- Microbiol Mol Biol Rev.* 2009 Mar; *73*(1): 134–154.
- Talaska, G.; Underwood, P.; Maier, A.; Lewtas, J.; Rothman, N.; Jaeger, M. *Environ. Health Perspect.* **1996**, *104*, 901-906.
- (a) Fromme, J. C.; Verdine, G. L. *DNA Repair and Replication*, **2004**, *69*, 1-41. (b) Krokan, H. E.; Bjørås, M. *Cold Spring Harv. Perspect. Biol.*, **2013**, *5*, 27-47.
- (a) Sancar, A.; Tang, M. *Photochemistry and Photobiology*, **1993**, *57*, 905-921. (b) Reardon, J. T.; Sancar, A. *Progress in Nucleic Acid Research and Molecular Biology*, **2005**, *79*, 183-235.
- (a) Prakash, S.; Johnson, R. E.; Prakash, L. *Annual Review of Biochemistry*, **2005**, *74*, 317-353. (b) Bienko, M.; Green, C. M.; Crosetto, N.; Rudolf, F.; Zapart, G.; Coull, B.; Kannouche, P.; Wilder, G.; Peter, M.; Lehmann, A. R.; Hofmann, K.; Dikic, I. *Science*, **2005**, *5755*, 1821-1824. (c) Masutani, C., Kusumoto, R., Iwai, S. and Hanaoka, F. *EMBO Journal*, **2000**, *19*, 3100–3109. (d) McCulloch, S. D.; Kunkel, T. A. *Cell Research*, **2008**, *18*, 148-161. (e) Kai, Mihoko, K.; Wang, T. S.-F. *Genes & Dev.* **2003**, *17*, 64-76.
- Purohit, V.; Basu, A. K. *Chem. Res. Toxicol.*, **2000**, *8*, 673-692.
- (a) Pitts, J. N.; Jr., van Cauwenberghe, K. A.; Grosjean, D.; Schmidt, J. P.; Fitz, D. R.; Belser, W. L.; Knudson, G. B.; Hynds, P. M. *Science*, **1978**, *202*, 515-519. (b) Jager, J. *Chromatogr.* **1978**, *152*, 573-578.
- Dimashki, M.; Harrad, S.; Harrison, R. M. *Atmospheric Environment*, **2000**, *15*, 2459-2469.
- (a) Phillips, R.; Daub, G.; Hunt, J. The Synthesis of Some New Azabenz[a]pyrenes and Monomethylazabenz[a]pyrenes, *J. Org Chem*, **1972**, *37*, 2030-2033. (b) Patnaik, P., A Comprehensive Guide to the Properties of Hazardous Chemical Substances. 2nd ed. 1999: John Wiley & Sons Publishers. (c) NTP 12th Report on Carcinogens. Rep Carcinog, **2011**. *12*: p. 5-6, 286-291. (d) Mumtaz, M.; George, J. Toxicological Profile for Polycyclic Aromatic Hydrocarbons. **1995**
- (a) Grantham, P.H.; Ba-Giao, N.; Mohan, L.C.; Benjamin, T.; Roller, P.P.; Weisburger, E.K. The Metabolism of 6-Aminochrysene in Rat, *European Journal of Cancer and Clinical Oncology*, **1976**, *12*: 227-235. (b) Hodgson, R.M.; Grover, P.L.; Sims, P. *European Journal of Cancer and Clinical Oncology*, **1983**, *19*: 1289 (c) Boyiri, T., Leszczynska, J., Desai, D., Amin, S., Nixon, D. W. and El-Bayoumy, K. (2002), Metabolism and DNA binding of the environmental pollutant 6-nitrochrysene in primary culture of human breast cells and in cultured MCF-10A, MCF-7 and MDA-MB-435s cell lines. *Int. J. Cancer*, *100*: 395–400.
- Wood, A. W.; Levin, W.; Ryan, D.; Thomas, P. E.; Yagi, H.; Mah, H. D.; Thakker, D. R.; Jerina, D. M.; Conney, A. H. *Biochemical and Biophysical Research Communications*, **1977**, *3*, 847-854.
- (a) *The Bay Region Theory of Polycyclic Aromatic Hydrocarbon Carcinogenesis*. Lehr, R. E.; Kumar, S.; Levin, W.; Wood, A. W.; Chang, R. L.; Conney, A. H.; Yagi, H.; Sayer, J. M.; Jerina, D. M. *Polycyclic Hydrocarbons and Carcinogenesis*, **1985**, 63-84. DOI: 10.1021/bk-1985-0283.ch004 (b) Balam Muñoz and Arnulfo Albores (2011). DNA Damage Caused by Polycyclic Aromatic Hydrocarbons: Mechanisms and Markers, Selected Topics in DNA Repair, Prof. Clark

- Chen (Ed.), ISBN: 978-953-307-606-5, InTech (c) Glatt, H.; Abu-Shqara, E.; Harvey, R. G.; Blum, J. *Mutation Research*, **1994**, 308, 135-141.
17. (a) Nordqvist, M.; Thakker, D. R.; Vyas, K. P.; Yahi, H.; Levin, W.; Ryan, D. E.; Thomas, P. E.; Conney, A. H.; Jerina, D. M. *Molecular Pharmacology*, **1980**, 19, 168-178. (b) Manning, B. W.; Campbell, W. L.; Franklin, W.; Delclos, K. B.; Cerniglia, C. E. *Applied and Environmental Microbiology*, **1988**, 1, 197-203. (c) Delclos, K. B.; Talaska, G.; Walker, R. P.; Brassinne, C.; Sculier, J. P. *Nitroarenes, Environmental Science Research*, **1990**, 40, 295-307. (d) Delclos, K. B.; El-Bayoumy, K.; Casciano, D. A.; Walker, R. P.; Kadlubar, F. F.; Hecht, S. S.; Shivapurkar, N.; Mandal, S.; Stoner, G. D. *Cancer Research*, **1989**, 49, 2909-2913. (e) Pothuluri, J. V.; Sutherland, J. B.; Freeman, J. P.; Cerniglia, C. E. *Applied and Environmental Microbiology*, **1998**, 8, 3106-3109.
  18. (a) Elmquist, C.E.; Stover, J.S.; Wang, Z.; Rizzo, C.J. Site-Specific Synthesis and Properties of Oligonucleotides Containing C8-Deoxyguanosine Adducts of the Dietary Mutagen IQ, *J. Am. Chem. Soc.* 2004, 126, 11189-11201. (b) Stover, J.S.; Rizzo, C.J. Synthesis of Oligonucleotides Containing the N2-Deoxyguanosine Adduct of the Dietary Carcinogen 2-Amino-3-methylimidazo[4,5-f]quinolone, *J. Am. Chem. Soc.* **2007**, 129, 1972-1979. (c) Thomson, P.F.; Lagisetty, P.; Balzarini, J.; De Clercq, E.; Lakshman, M.K. Palladium-Catalyzed Aryl Amination Reactions of 6-Bromo- and 6-Chloropurine Nucleosides, *Adv. Synth. Catal.* **2010**, 352: 1728-1735. (d) Takamura-Enya, T.; Kawanishi, M.; Yagi, T.; Hisamatsu, Y. Structural Identification of DNA Adducts Derived from 3-Nitrobenzothione, a Potent Carcinogen Present in the Atmosphere, *Chem. Asian J.* **2007**, 2, 1174-1185.
  19. *Strategic Applications of Named Reactions in Organic Synthesis*; Kurti, L., Czako B. Elsevier Academic Press: Burlington, MA, 2005
  20. (a) Birkholz, M.; Freixa, Z.; van Leeuwen, P. W. N. M. *Chem. Soc. Rev.*, **2009**, 4, 853-1200. (b) Hartwig, J. F. *Synlett*, **1997**, 4, 329-340. (c) Hartwig, J. F. *Angew. Chem. Int. Ed.* **1998**, 37, 2046-2067. (d) Wolfe, J. P.; Wagaw, S.; Marcoux, J-F.; Buchwald, S. L. *Acc. Chem. Res.* **1998**, 12, 805-818. (e) Hartwig, J. F. *Acc. Chem. Res.* **1998**, 12, 852-860.
  21. Singh, U, K.; Strieter, E. R.; Blackmond, D. G.; Buchwald, S. L.; *J. Am. Chem. Soc.* **2002**, 124, 14104.
  22. Shekar, S.; Ryberg, P.; Hartwig, J. F.; Matthew, J. S.; Blackmond, D. G.; Strieter, E. R.; Buchwald, S. L. *J. Am. Chem. Soc.* **2006**, 128, 3584-3591.
  23. Brown, T.; Brown Jr., T. *Nucleic Acids Book*, ATDBio Ltd: 2015 (accessed Mar 14, 2015).
  24. (a) Barawkar, D. A.; Linkletter, B.; Cruice, T. C. *Bioorganic & Medicinal Chemistry Letters*, **1998**, 12, 1517-1520. (b) Bergmann, F.; Bannwarth, W. *Tetrahedron Letters*, **1995**, 11, 1839-1842. (c) Lönnberg, H. *Bioconjugate Chem.*, **2009**, 20, 1065-1094.
  25. Venkatesan, H.; Greenberg, M. M. *J. Org. Chem.*, **1996**, 61, 525-529.
  26. (a) Saito, Y.; Koda, M.; Shinohara, Y.; Saito, I. *Tetrahedron Letters*, **2011**, 52, 491-49. (b) Saito, Y.; Suzuki, A.; Imai, K.; Nemoto, N.; Saito, I. *Tetrahedron Letters*, **2010**, 51, 260-2609.
  27. Kito, T.; Yoshinaga, K.; Yamaye, M.; Mizobe, H. *J. Org. Chem.* **1991**, 56, 3336-3339.
  28. (a) Frantz, D. E. Weaver, D. G.; Carey, J. P. Kress, M. H. Dolling, U. H. *Org. Lett.* **2002**, 26, 4717-4718. (b) Echavarren, A. M.; Stille, J. K. *J. Am. Chem. Soc.* **1987**, 109, 5478-5486.
  29. Kim, Y. H.; Lee, H.; Kim, Y. J.; Kim, B. T.; Heo, J. *J. Org. Chem.* **2008**, 73, 495-501.
  30. (a) Littke, A. F.; Dai, C.; Fu, G. C. *J. Am. Chem. Soc.*, **2000**, 122, 4020-4028. (b) Doucet, H. *J. Org. Chem.* **2008**, 2013-2030. (c) Espino, G.; Kurbangalieva, A.; Brown, J. M. *Chem. Comm.* **2007**, 1742-1744.
  31. Park, K.; Kim, B. T.; Heo, J. *Eur. J. Org. Chem.* **2014**, 164-170.
  32. Khurana, J. M.; Chauhan, S.; Bansal, G. *Monatshete für Chemie*, **2004**, 135, 83-87.
  33. Whie, E. H.; Aufdermarsh Jr., C. A. *J. Am. Chem. Soc.* **1961**, 77, 6011-6014.
  34. (a) Du, X.; Bian, Q.; Wang, H.; Yu, S.; Kou, J.; Wang, Z.; Li, Z.; Zhao, W. *Org. Biomol. Chem.* **2014**, 12, 5427. (b) Karthikeyan, J.; Haridharan, R.; Cheng, C. *Angew. Chem.* **2012**, 49, 12343-12347. (c) Pellegata, R.; Villa, I.; Palmisano, G.; Lesma, G. *Communications*, **1985**, 517-519.

35. Csomós, P.; Fodor, L.; Mándity, I.; Bermáth, G. *Tetrahedron*, **2007**, *63*, 4983-4989.
36. (a) Kuhn, L. P.; Corwin, A. H. *J. Am. Chem. Soc.* **1948**, *10*, 3370-3375. (b) Wallace, R. G.; Barker, J. M.; Wood, M. L. *Synthesis*, **1990**, 1143-1144.
37. Liguori, L.; Bjørsvik, H. *Org. Process Res. Dev.* **2011**, *15*, 997-1009.
38. Beletskaya, I.P.; Sigeev, A.S.; Peregudov, A.S.; Petrovskii, P.V. Catalytic Sandmeyer Bromination, *Journal of Synthetic Organic Chemistry*, **2007**, *16*, 2534-2538
39. (a) Gillet, L. C. J.; Schärer, O. D. *Org. Lett.* **2002**, *24*, 4205-4208. (b) De Riccardis, F.; Johnson, F. *Org. Lett.* **2000**, *3*, 293-295.
40. (a) Yang, B. H.; Buchwald, S. L. *J. Organometallic Chem.* **1999**, *576*, 125-146. (b) Wolfe, J. P.; Tomori, H.; Sadighi, J. P.; Yin, J.; Buchwald, S. L. *J. Org. Chem.* **2000**, *65*, 1158-1174.
41. Takatori, K.; Nishihara, M.; Nishiyama, Y.; Kajiware, M. *Tetrahedron*, **1998**, *54*, 15861-15869.
42. Qiu, J. C.; Pradhan, P. P.; Blanck, N. B.; Bobbitt, J. M.; Bailey, W. F. *Org. Lett.* **2012**, *1*, 350-353.
43. Bobbitt, J. M. *J. Org. Chem.* **1998**, *63*, 9367-9374.
44. Roy, A.; Reddy, K. R.; Mohanta, P. K.; Ila, H.; Junjappat, H. *Synthetic Communications*, **1999**, *21*, 3781-3791.



## **APPENDIX A**

### **NMR AND MASS SPECTRA FOR C8-CR-DG ADDUCT**

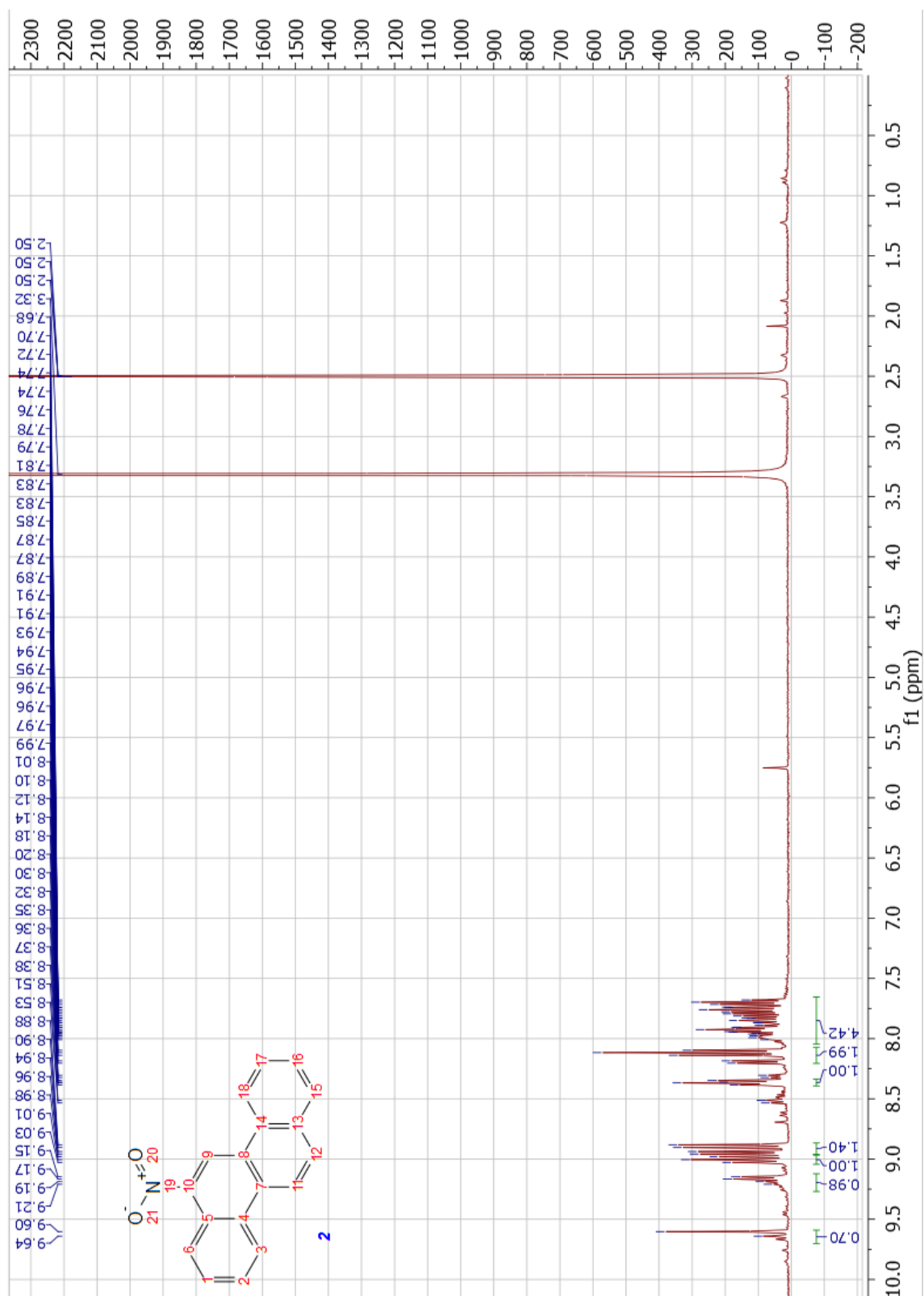


Figure 15:  $^1\text{H}$ -NMR of 6-Nitrochrysene

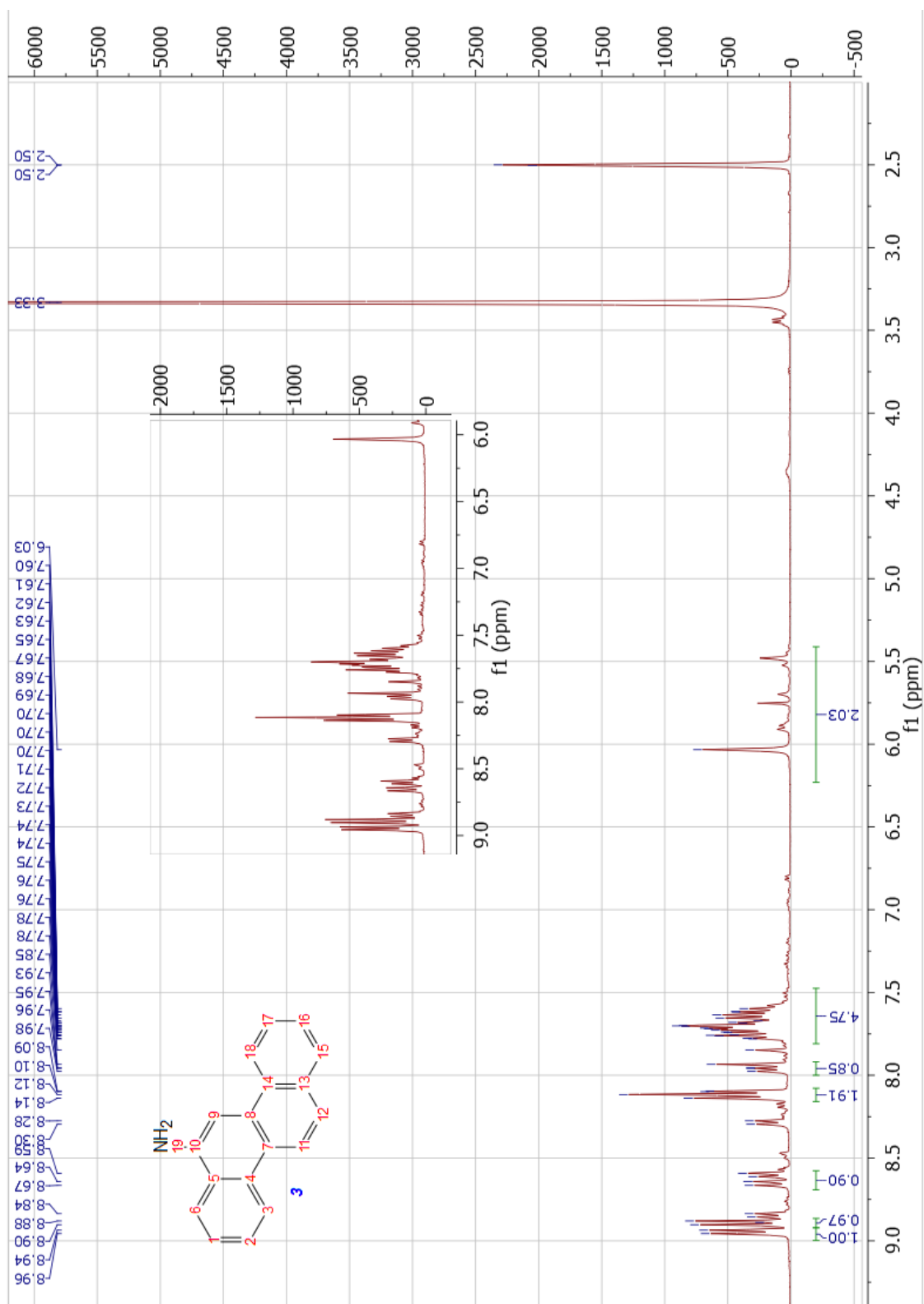


Figure 16:  $^1\text{H}$ -NMR of 6-Aminochrysene

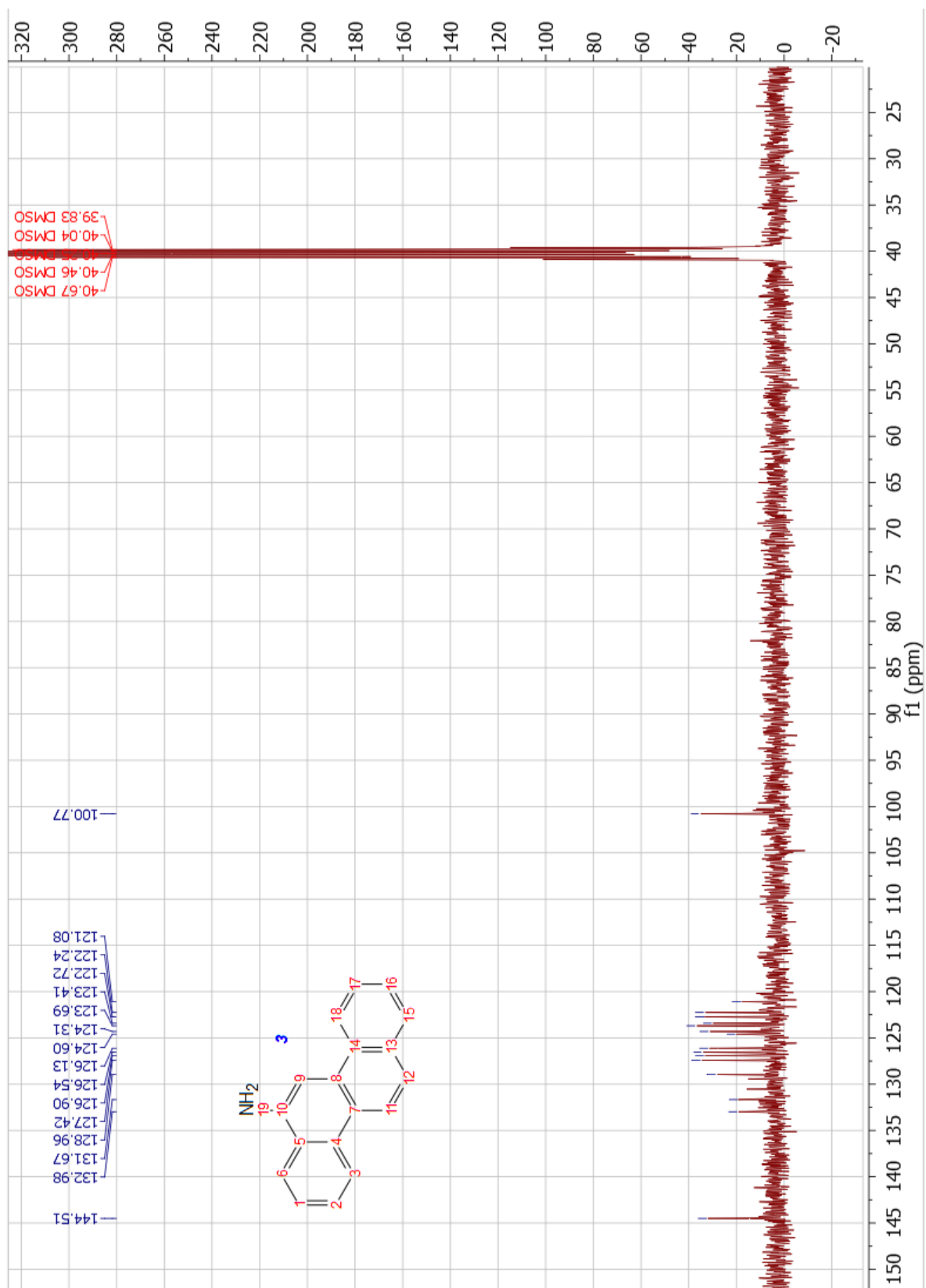


Figure 17:  $^{13}\text{C}$ -NMR of 6-Aminochrysene



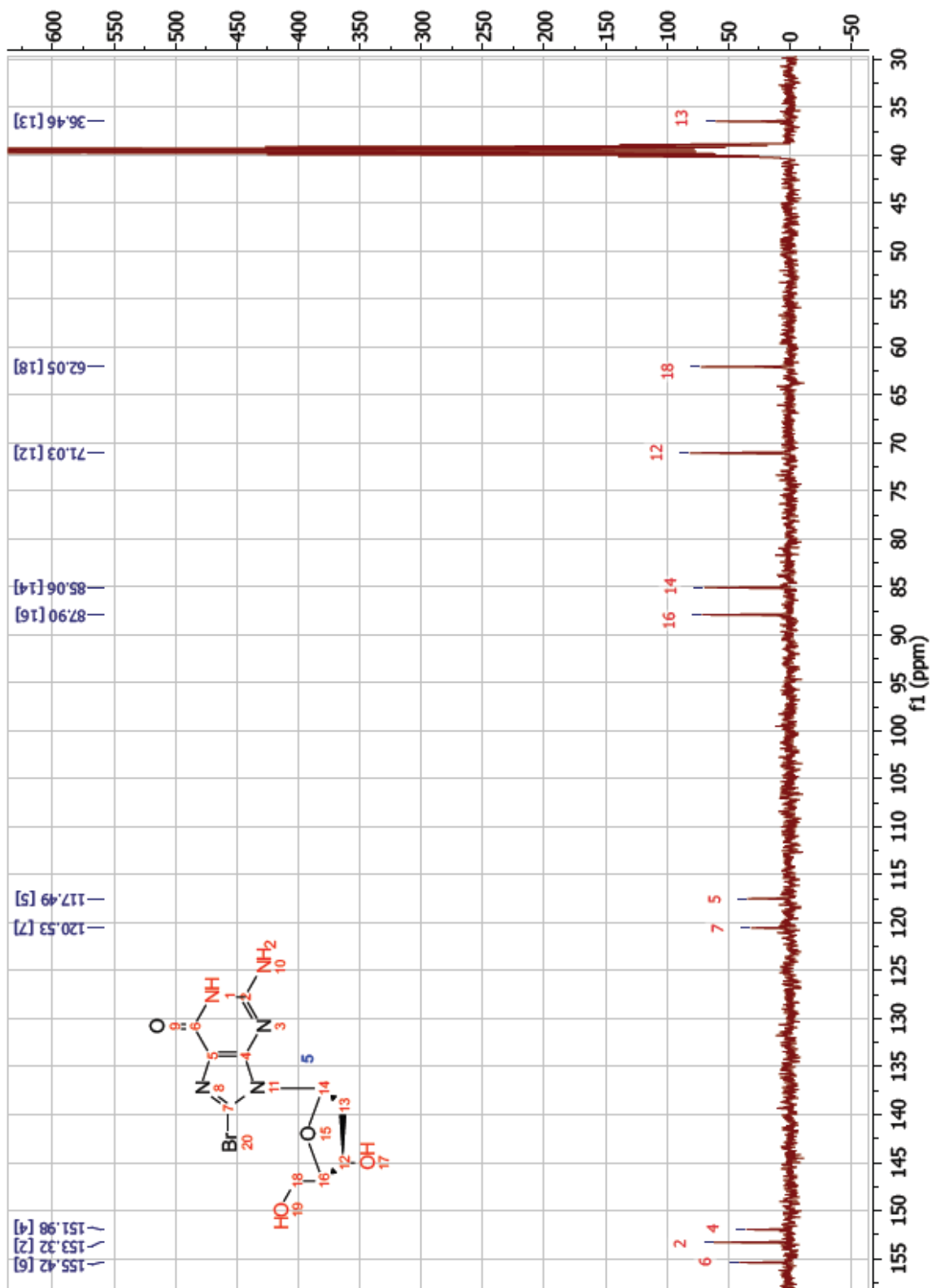


Figure 19:  $^{13}\text{C}$ -NMR of 8-Bromo-2'-deoxyguanosine

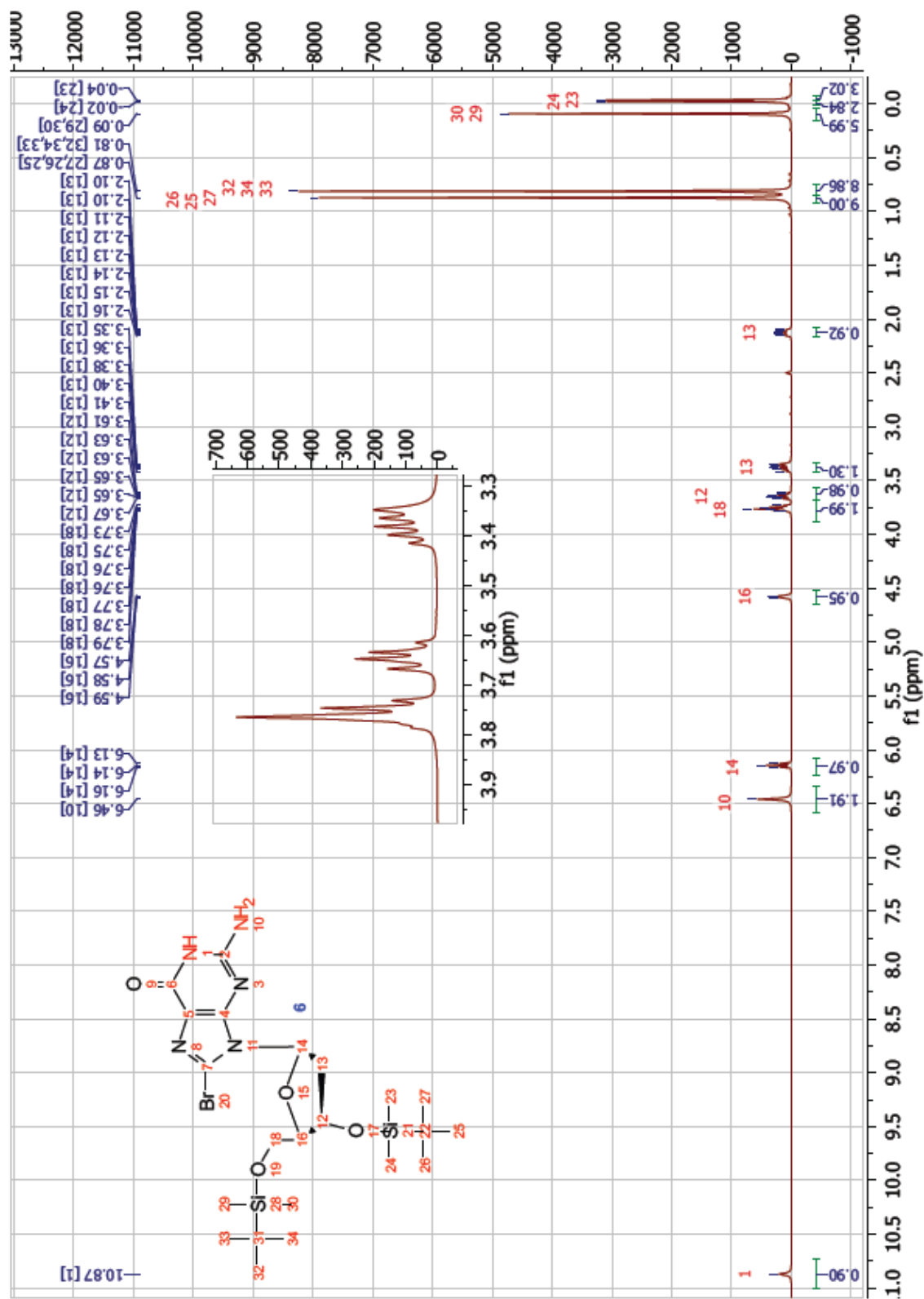


Figure 20:  $^1\text{H}$ -NMR of 8-Bromo-3',5'-O-bis(*tert*-butyldimethylsilyl)-2'-deoxyguanosine

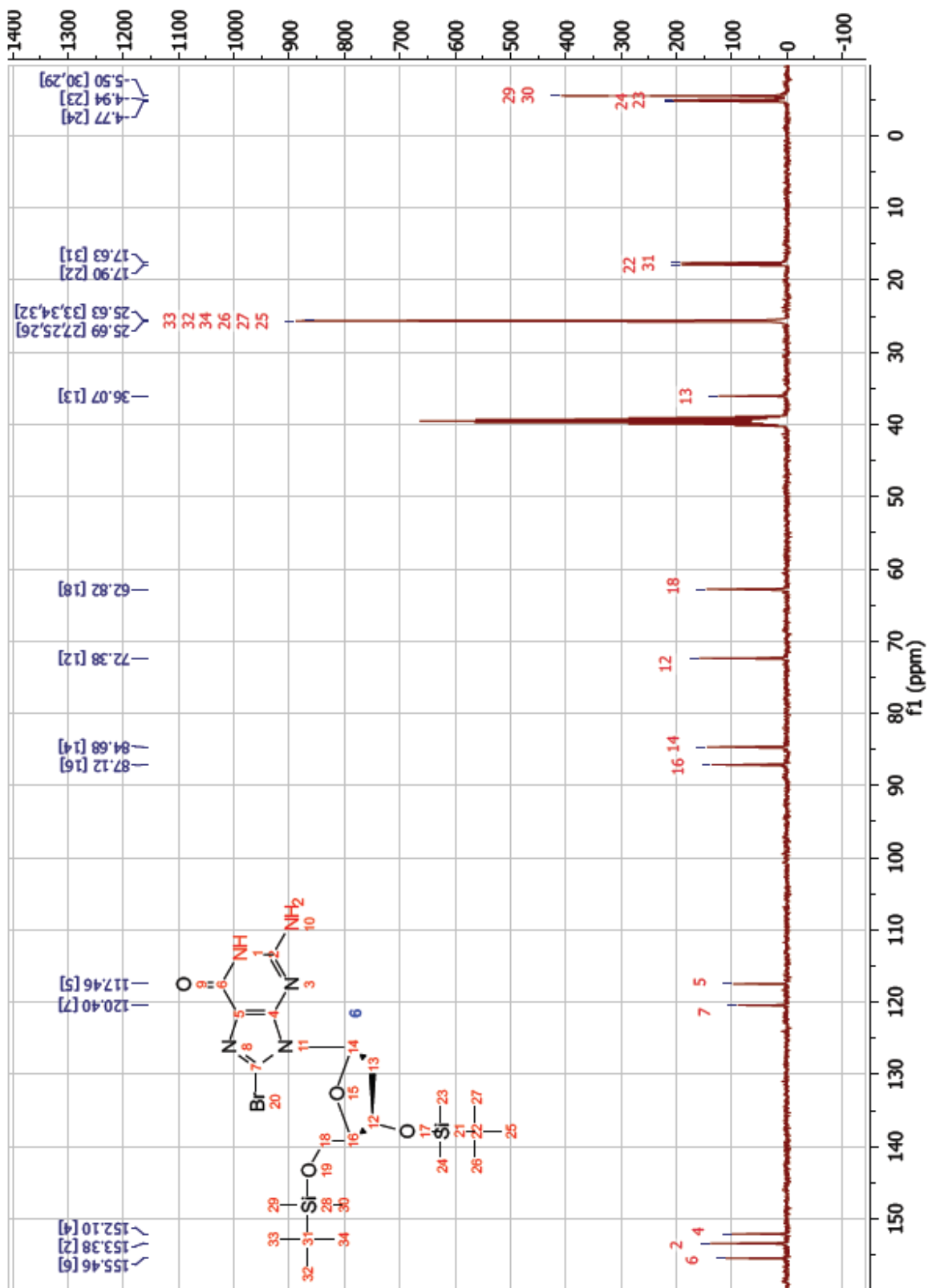


Figure 21: <sup>13</sup>C-NMR of 8-Bromo-3',5'-O-bis(*tert*-butyldimethylsilyl)-2'-deoxyguanosine



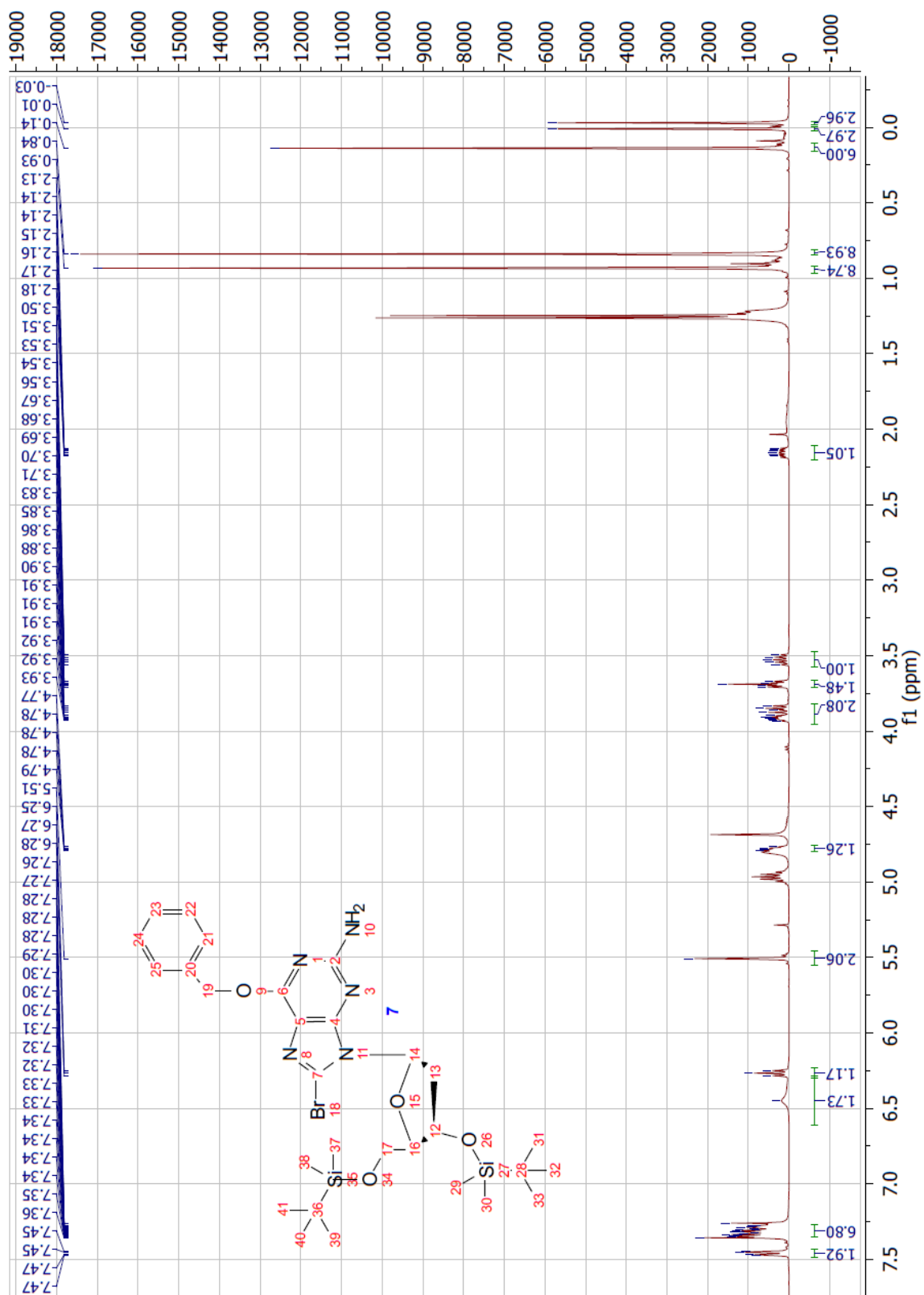


Figure 22:  $^1\text{H}$ -NMR of  $\text{O}^6$ -Benzyl-8-bromo-3',5'-O-bis(*tert*-butyldimethylsilyl)-2'-deoxyguanosine

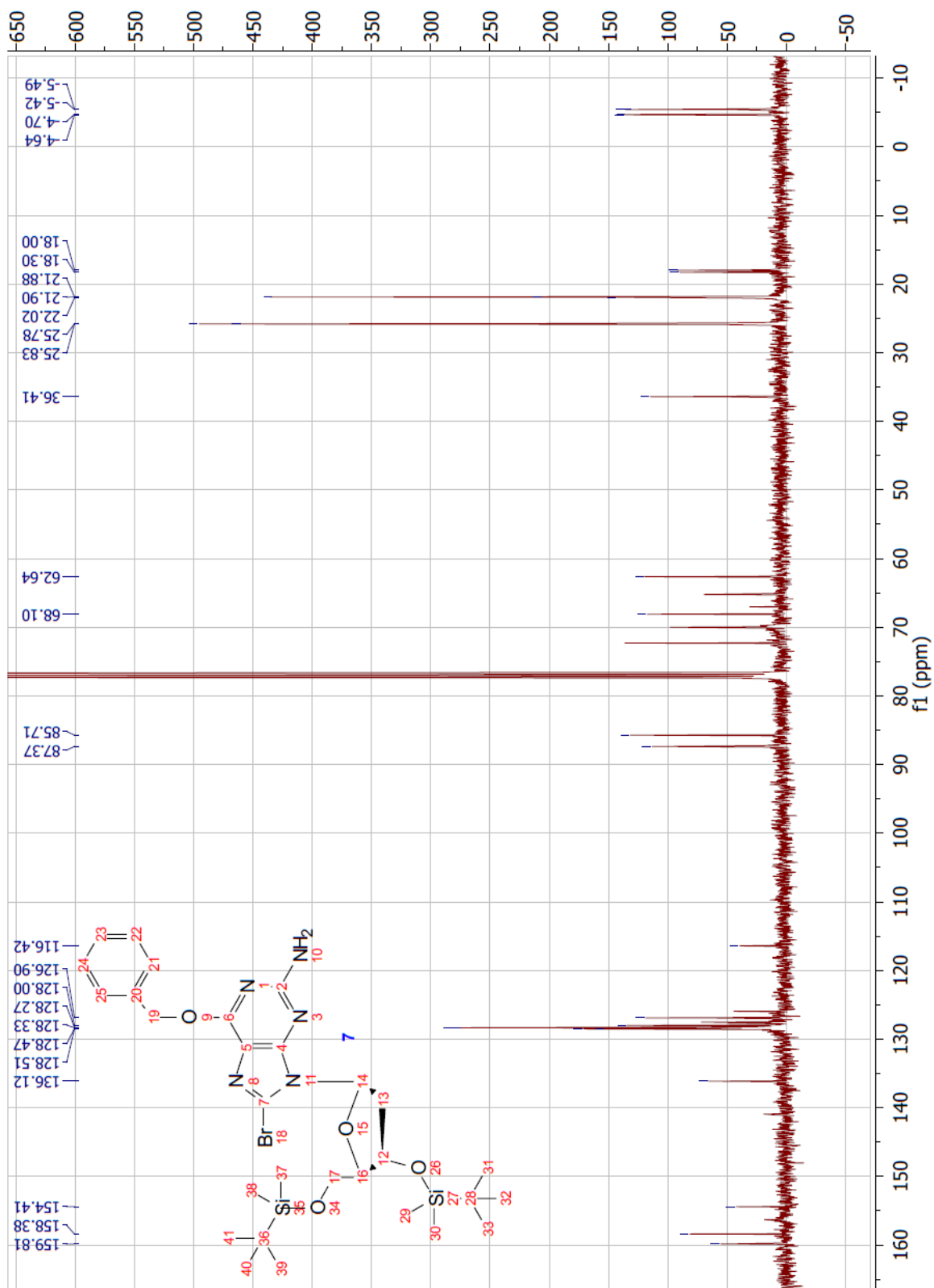


Figure 23: <sup>13</sup>C-NMR of O<sup>6</sup>-Benzyl-8-bromo-3',5'-O-bis(*tert*-butyldimethylsilyl)-2'-deoxyguanosine

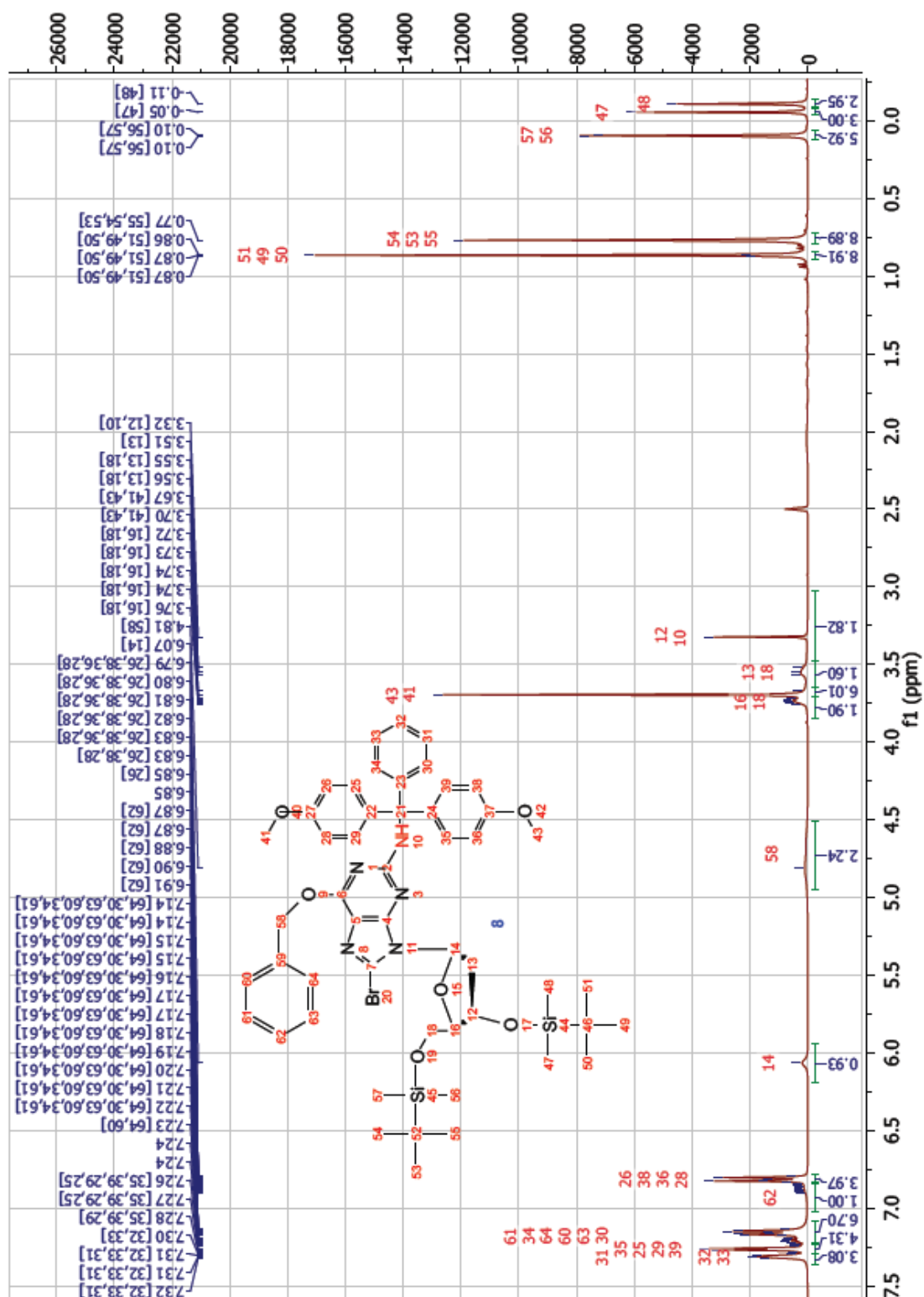


Figure 24:  $^1\text{H}$ -NMR of  $\text{O}^6$ -Benzyl-8-bromo-3',5'-O-bis(*tert*-butyl dimethylsilyl)- $\text{N}^2$ -dimethoxytrityl-2'-deoxyguanosine

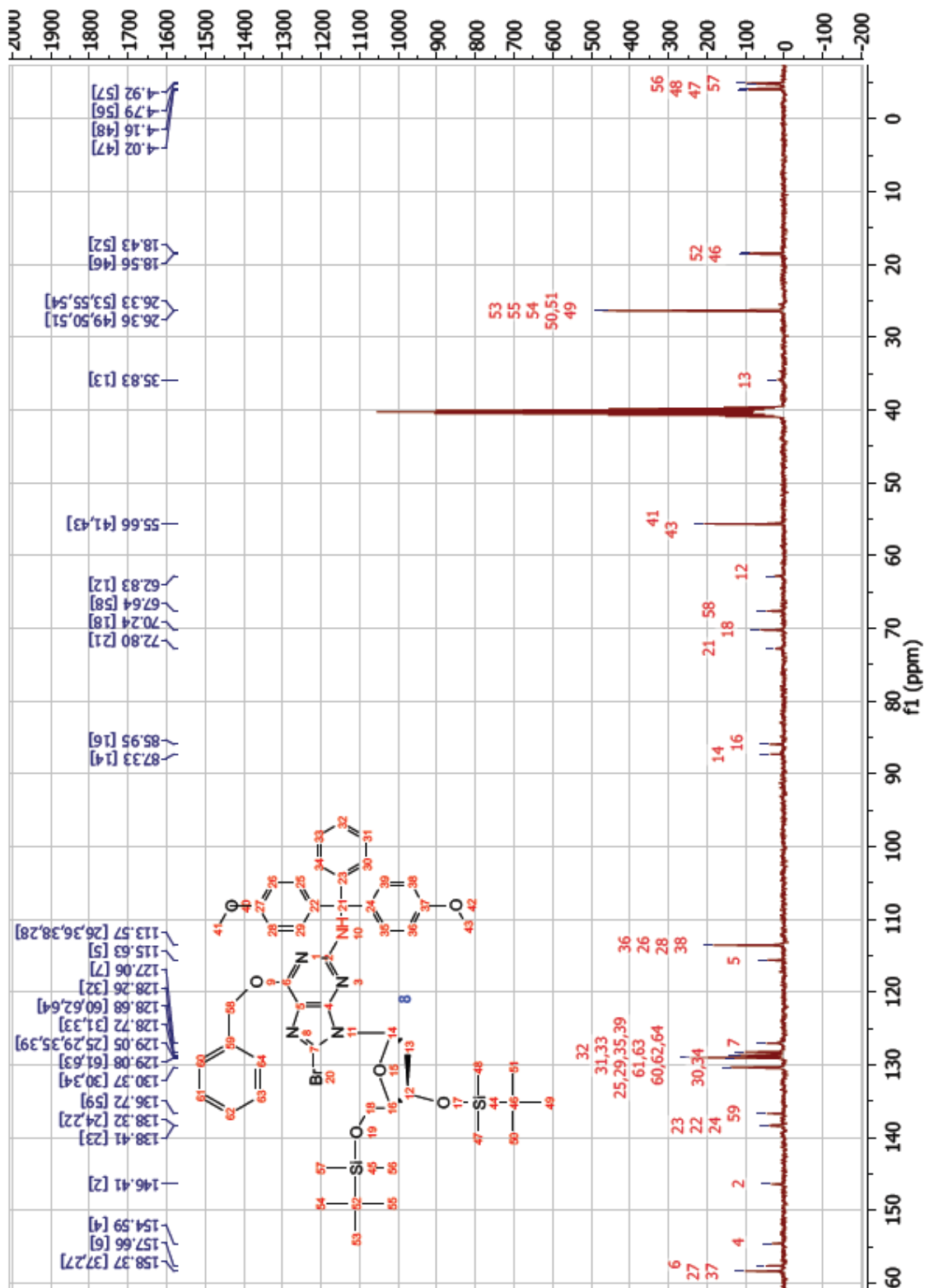


Figure 25:  $^{13}\text{C}$ -NMR of  $\text{O}^6$ -Benzyl-8-bromo-3',5'-O-bis(*tert*-butyldimethylsilyl)- $\text{N}^2$ -dimethoxytrityl-2'-deoxyguanosine



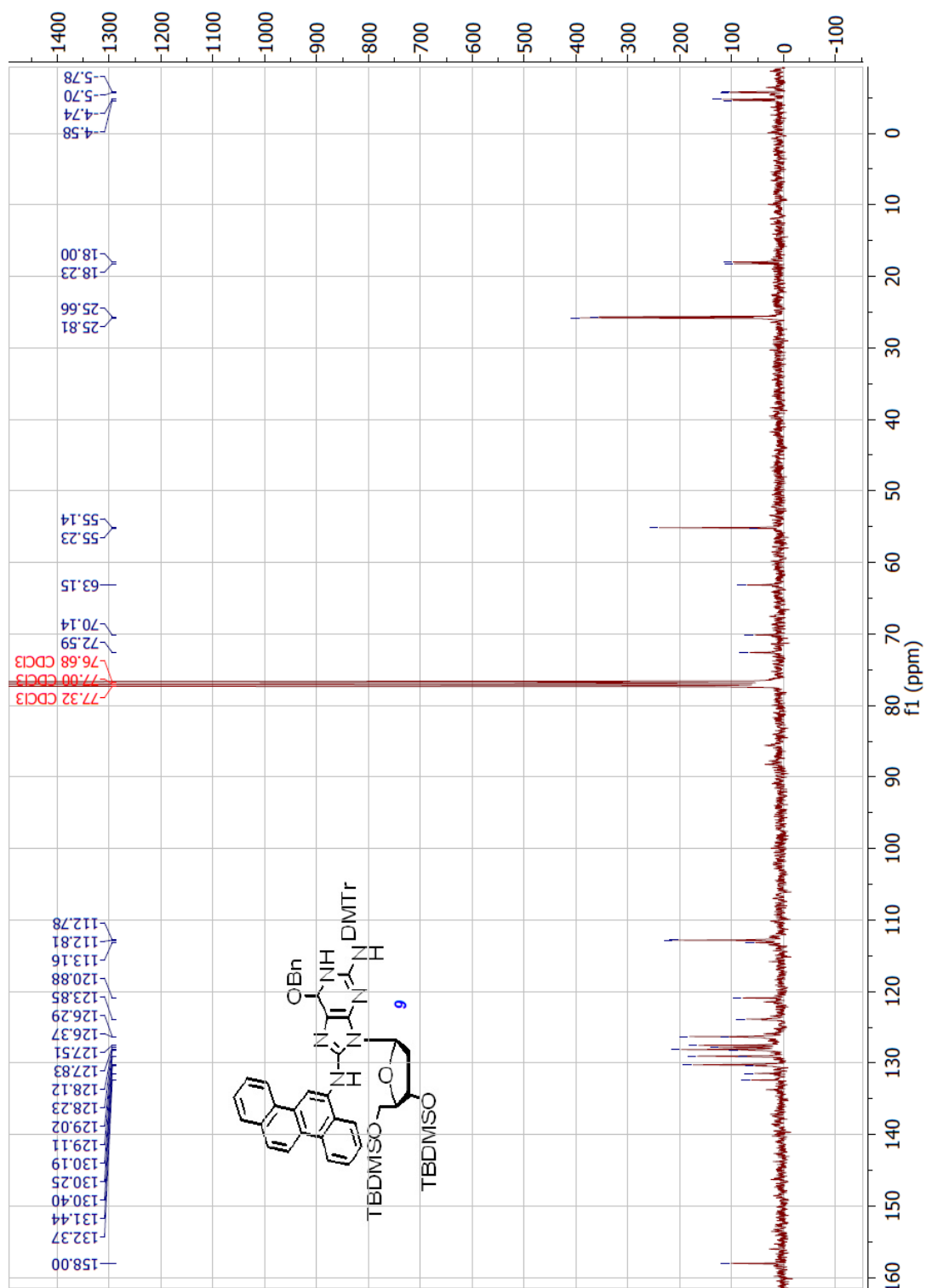


Figure 27:  $^{13}\text{C}$ -NMR of 8-(N-6-Aminochrysene)-O<sup>6</sup>-benzyl-3',5'-O-bis(*tert*-butyldimethylsilyl)-N<sup>2</sup>-dimethoxytrityl-2'-deoxyguanosine

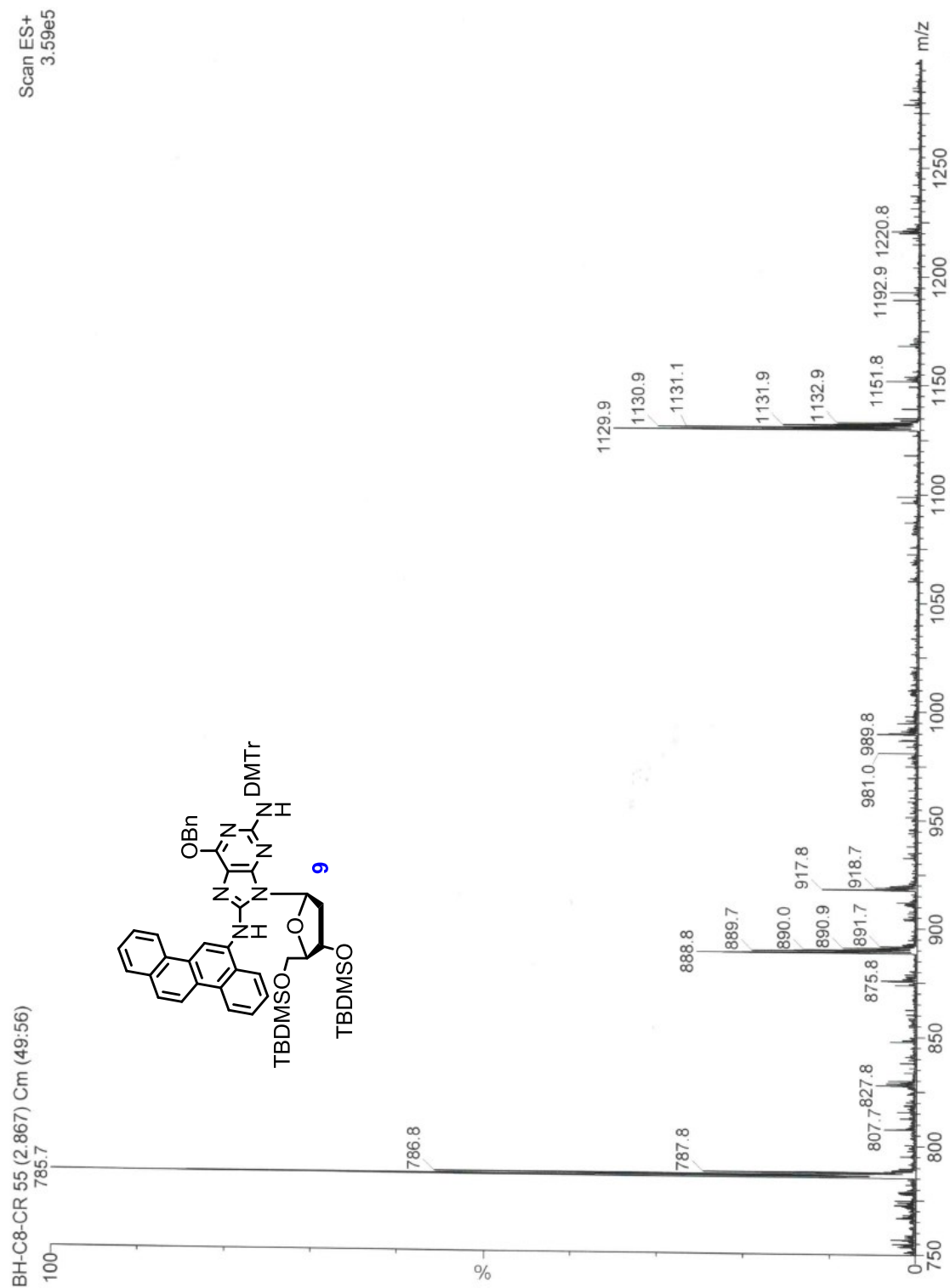
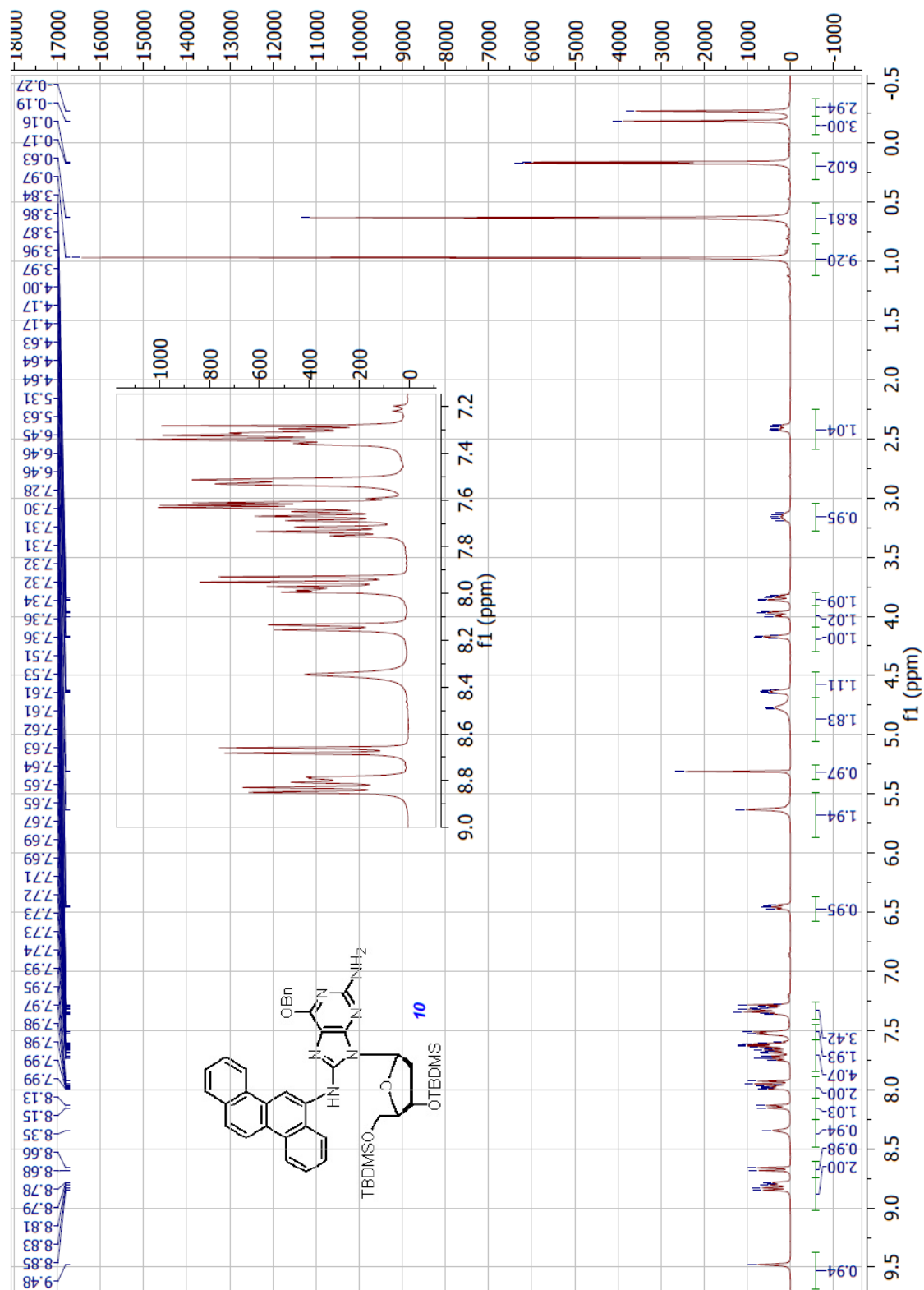
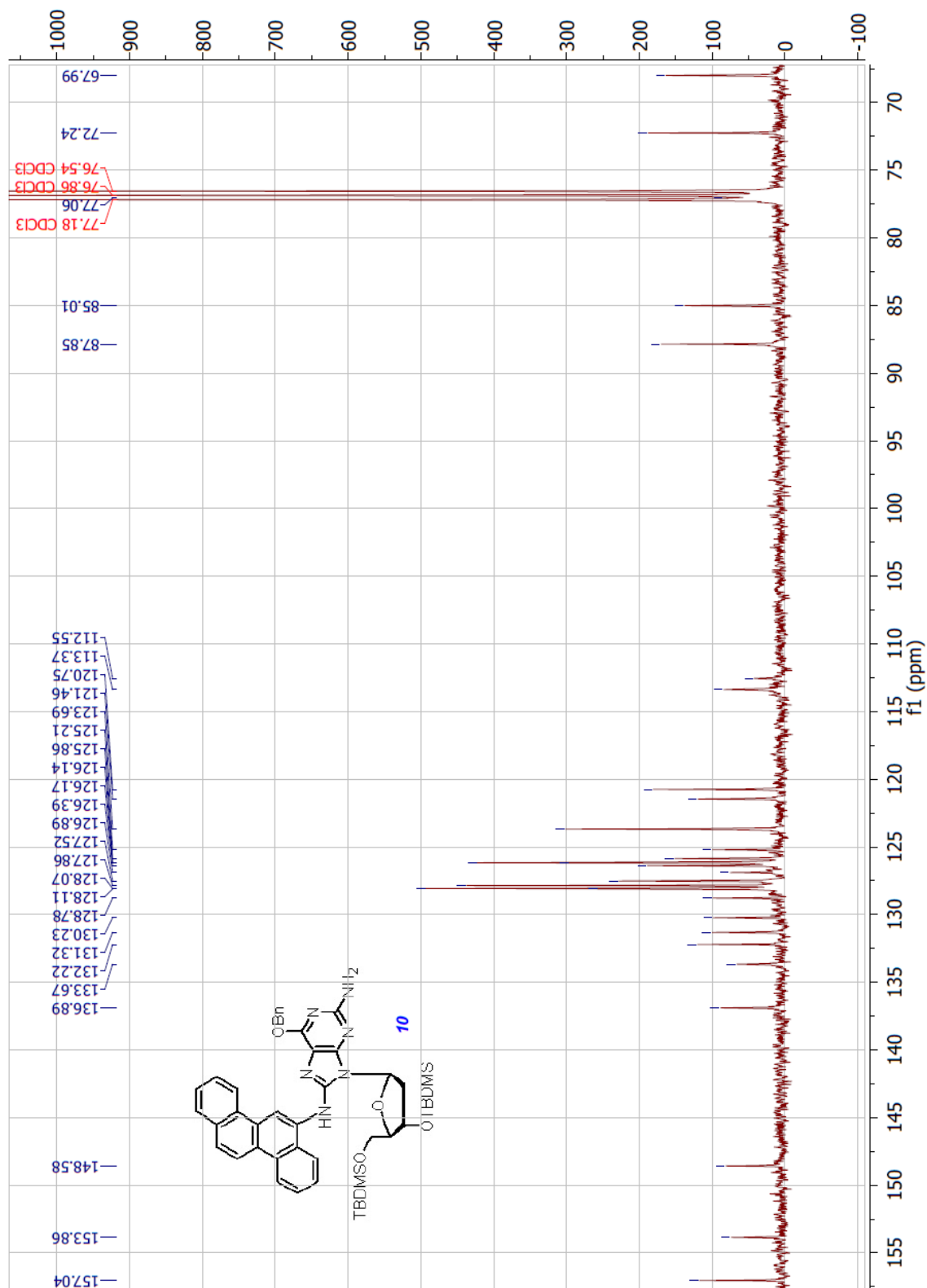


Figure 28: Mass Spectrum of 8-(*N*-6-Aminochrysene)-O<sup>6</sup>-benzyl-3',5'-O-bis(*tert*-butyldimethylsilyl)-*N*<sup>2</sup>-dimethoxytrityl-2'-deoxyguanosine







**Figure 30:  $^{13}\text{C}$ -NMR of 8-(N-6-aminochrysene)-O<sup>6</sup>-benzyl-3',5'-O-bis(*tert*-butyldimethylsilyl)-2'-deoxyguanosine**

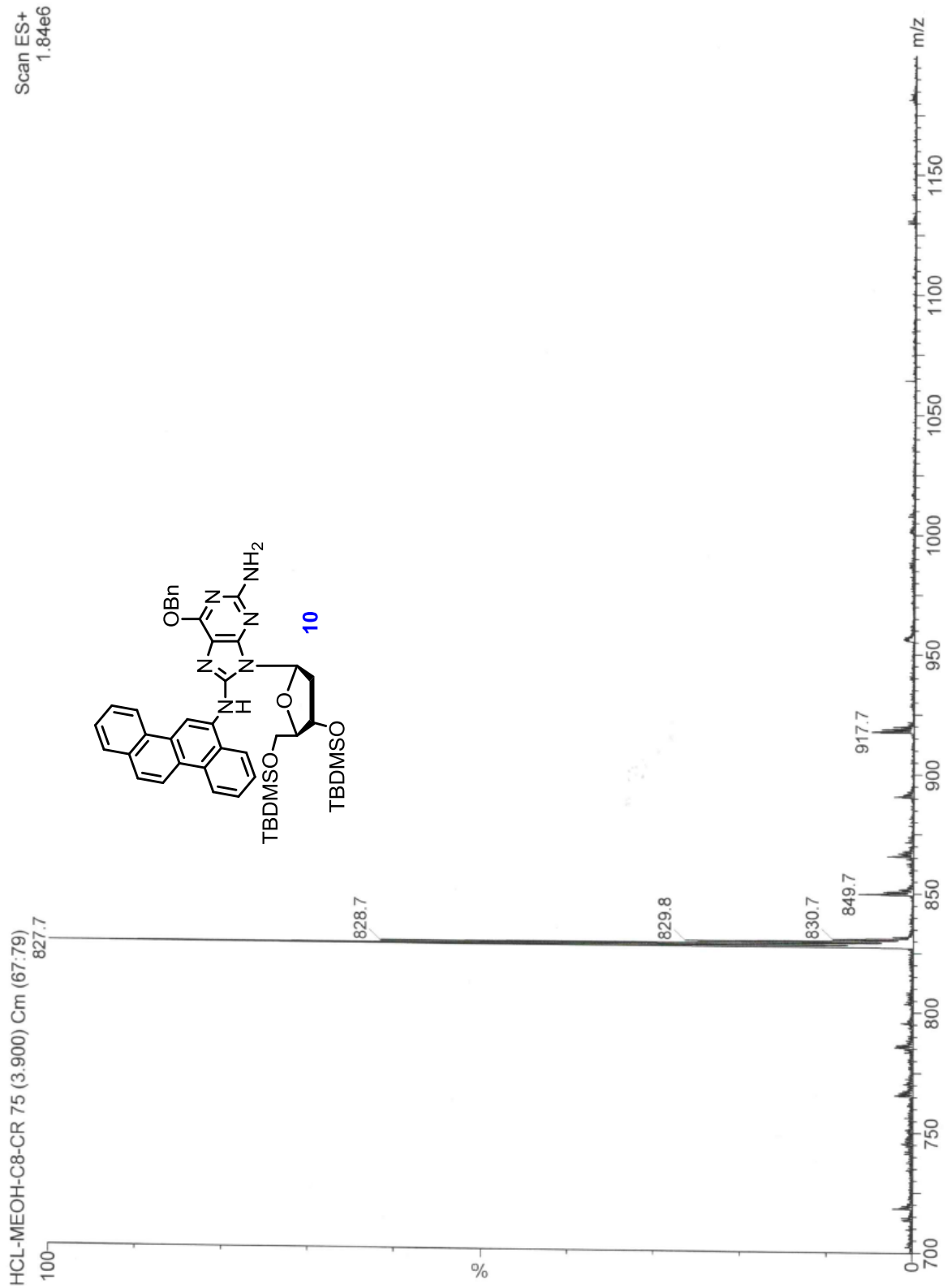


**Figure 31: Mass Spectrum of 8-(N-6-Aminochrysene)-O<sup>6</sup>-benzyl-3',5'-O-bis(*tert*-butyldimethylsilyl)-2'-deoxyguanosine**

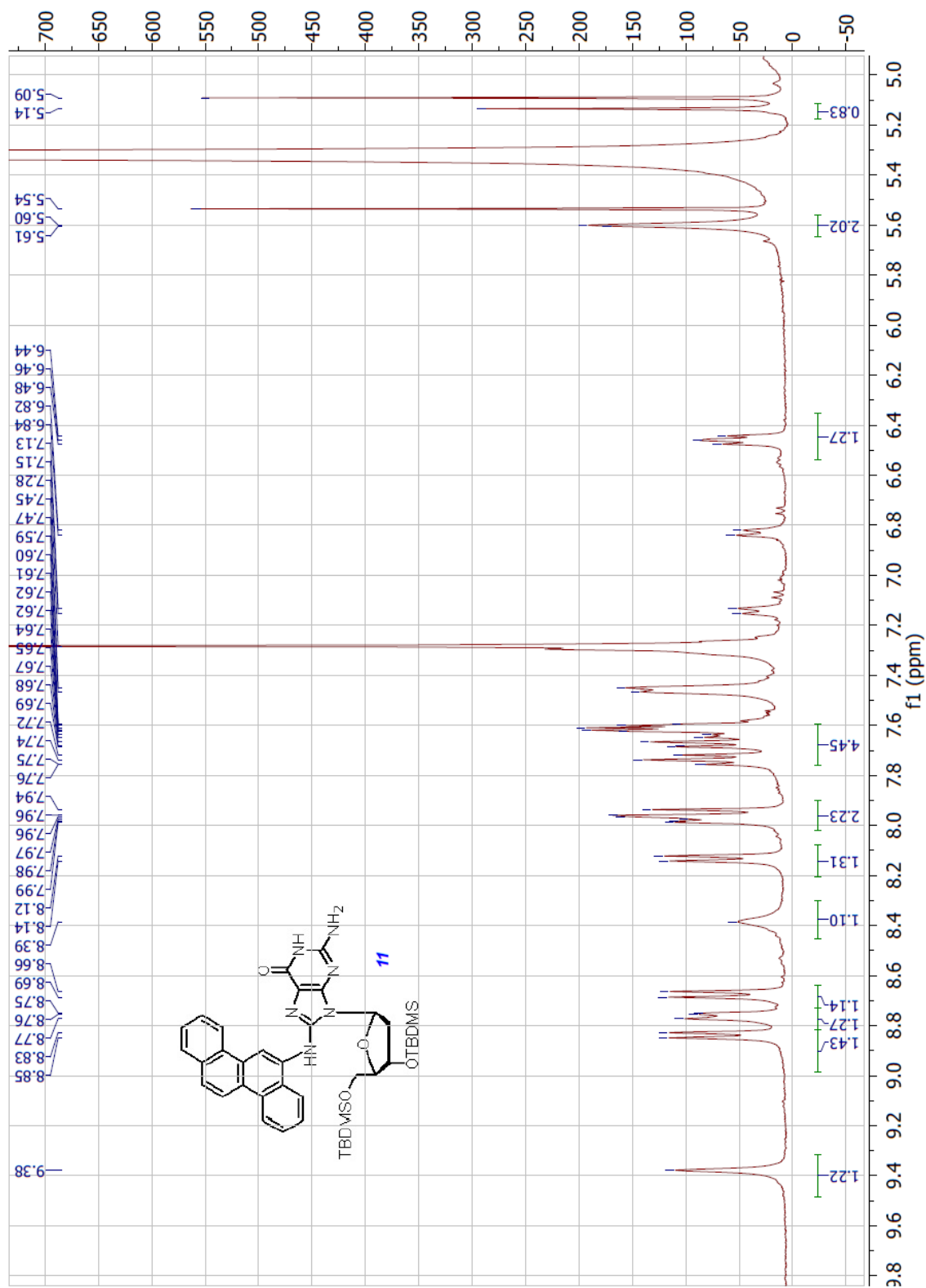


Figure 32: <sup>1</sup>H-NMR of 8-(N-6-Aminochrysene)-3',5'-O-bis(*tert*-butyldimethylsilyl)-2'-deoxyguanosine

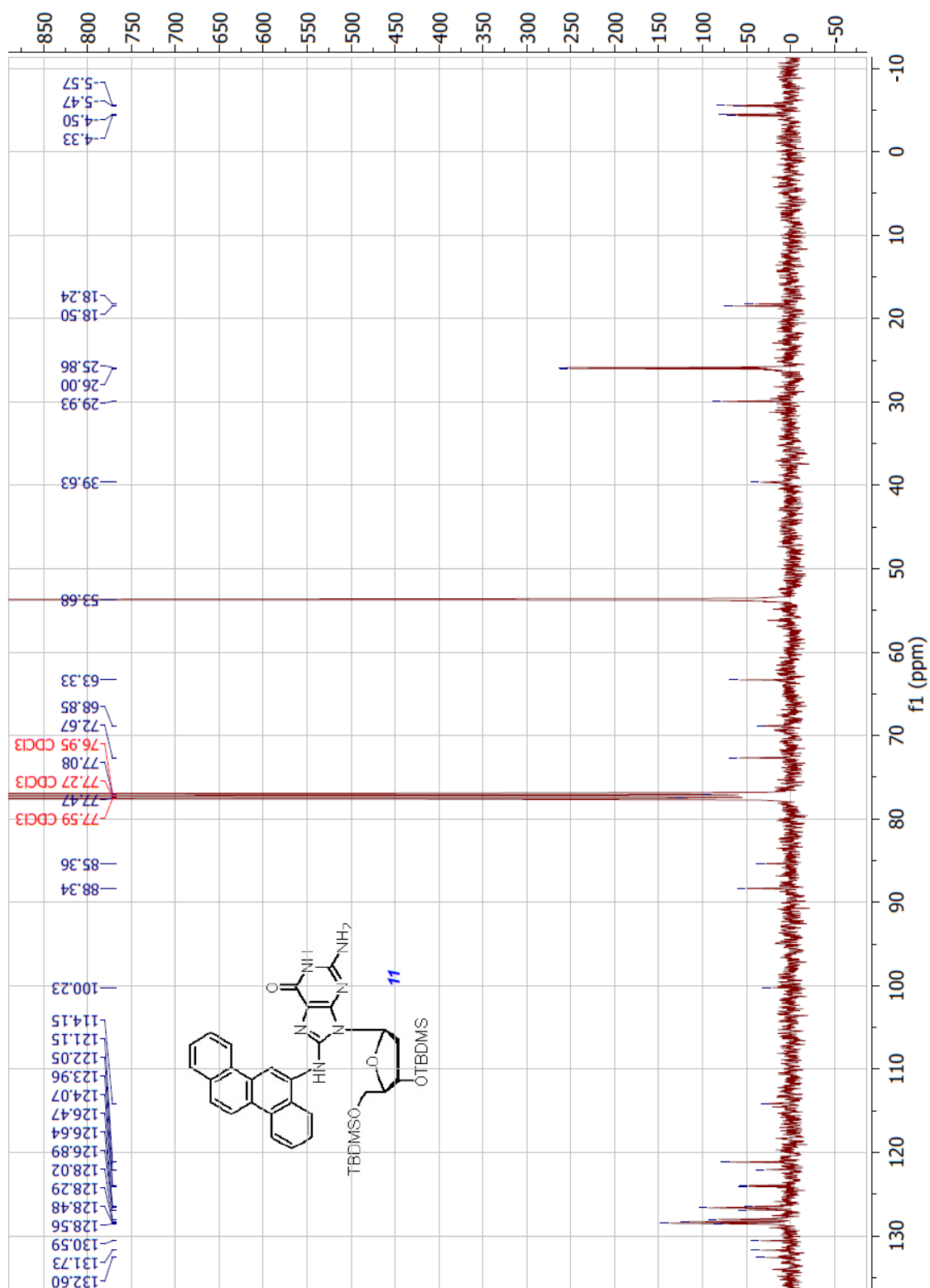
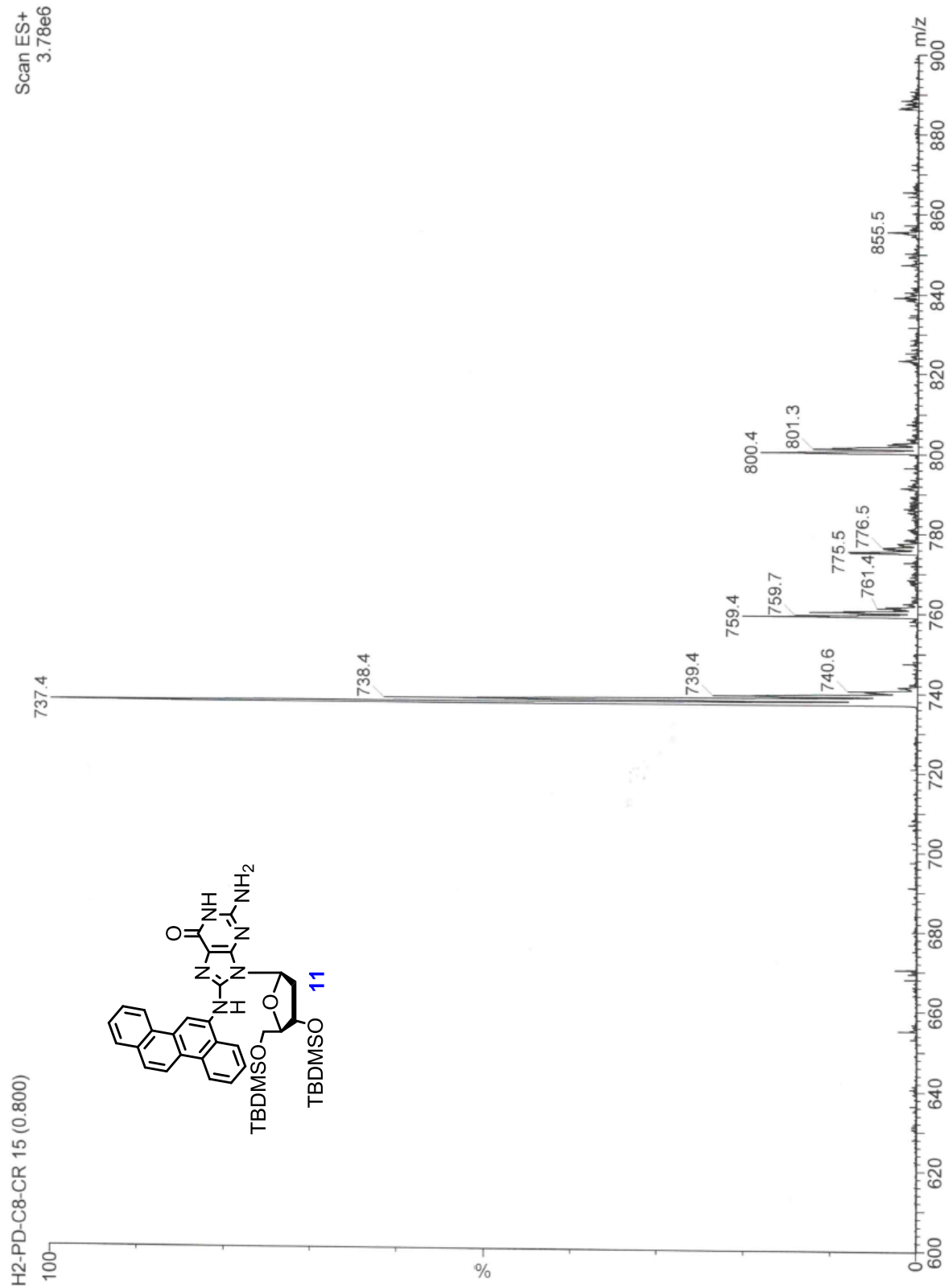
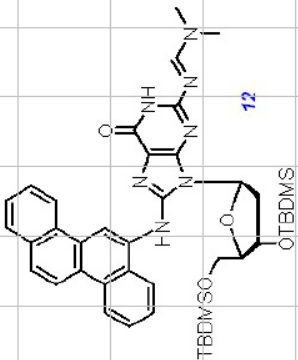


Figure 33: <sup>13</sup>C-NMR of 8-(N-6-Aminochrysene)-3',5'-O-bis(*tert*-butyldimethylsilyl)-2'-deoxyguanosine



**Figure 34: Mass Spectrum of 8-(N-6-Aminochrysen)-3',5'-O-bis(*tert*-butyldimethylsilyl)-2'-deoxyguanosine**



81

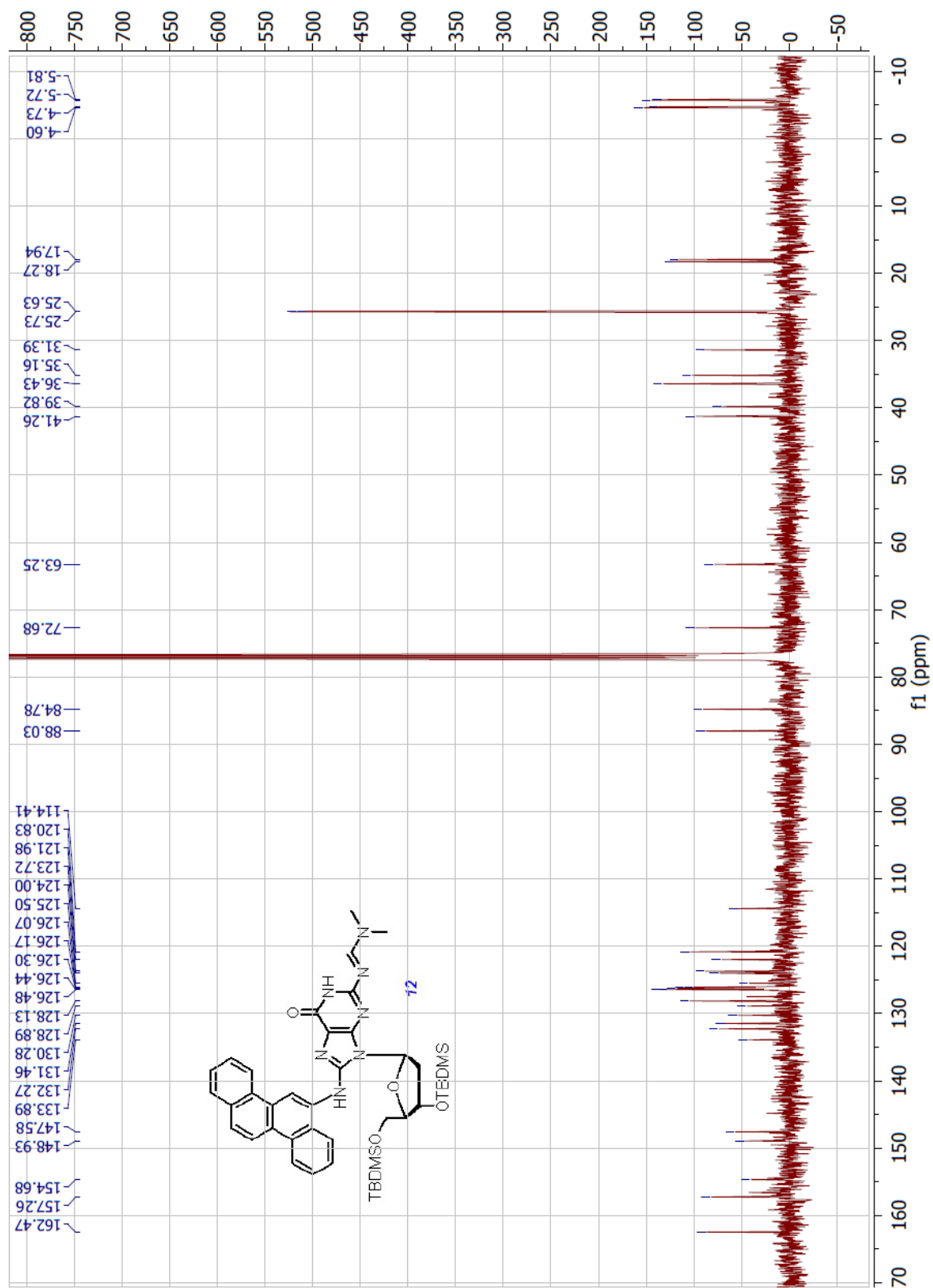


Figure 36:  $^{13}\text{C}$ -NMR of 8-(N-6-Aminochrysene)-3',5'-O-bis(*tert*-butyldimethylsilyl)- $\text{N}^2$ -DMF-2'-deoxyguanosine

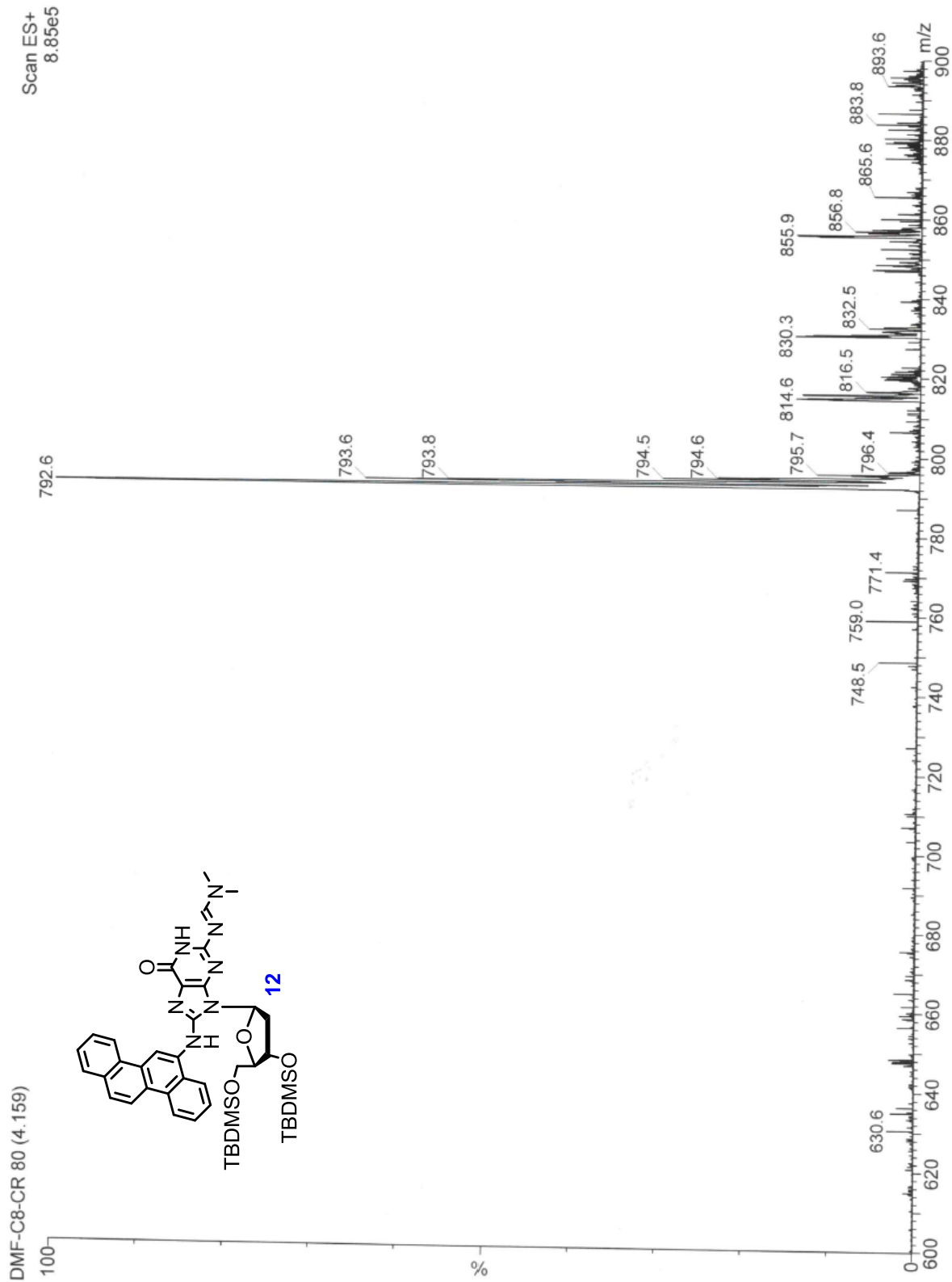


Figure 37: Mass Spectrum of 8-(N-6-Aminochrysene)-3',5'-O-bis(*tert*-butyldimethylsilyl)-N<sup>2</sup>-DMF-2'-deoxyguanosine



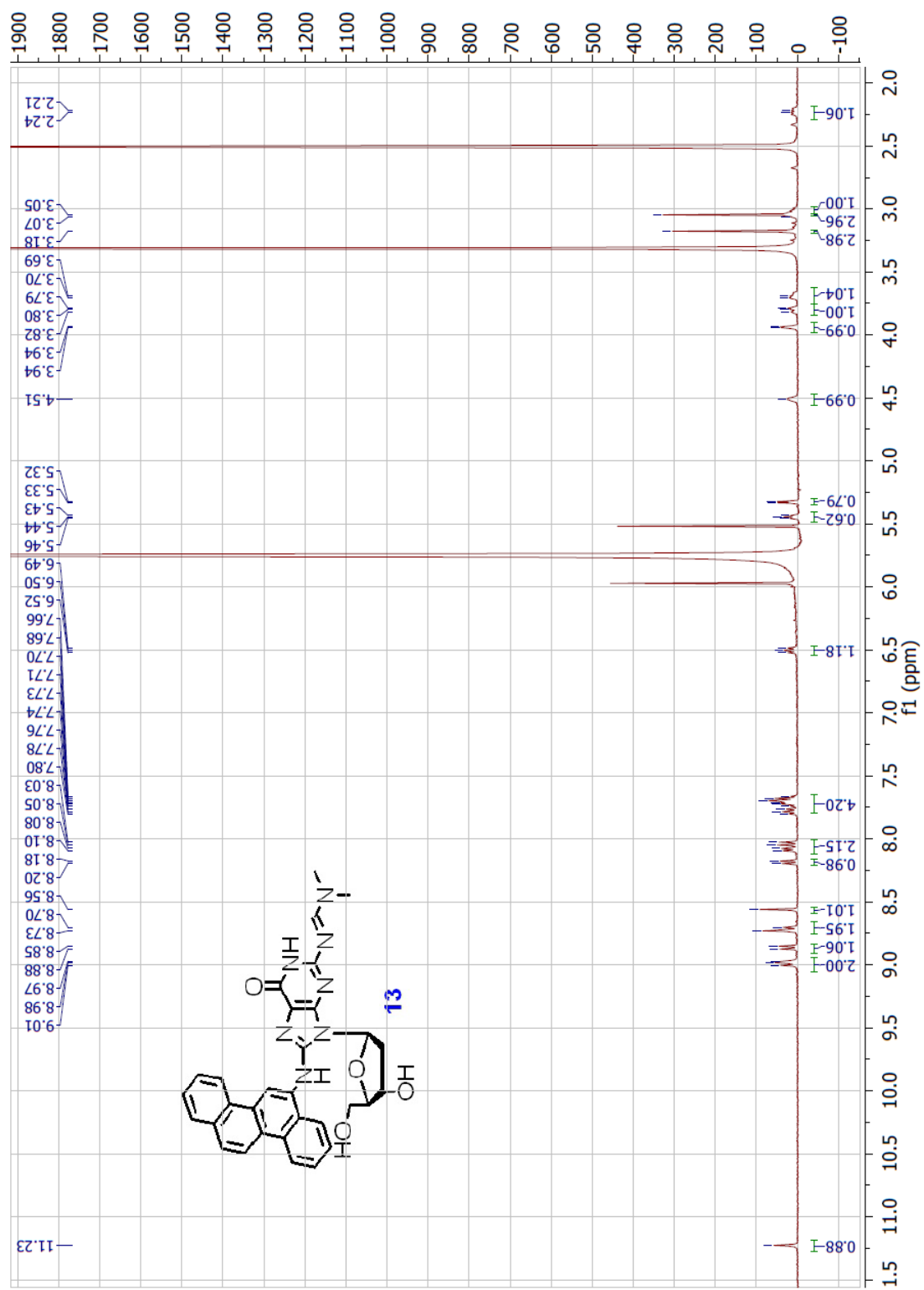


Figure 38: <sup>1</sup>H-NMR of 8-(N-6-Aminochrysene)-N<sup>2</sup>-DMF-2'-deoxyguanosine

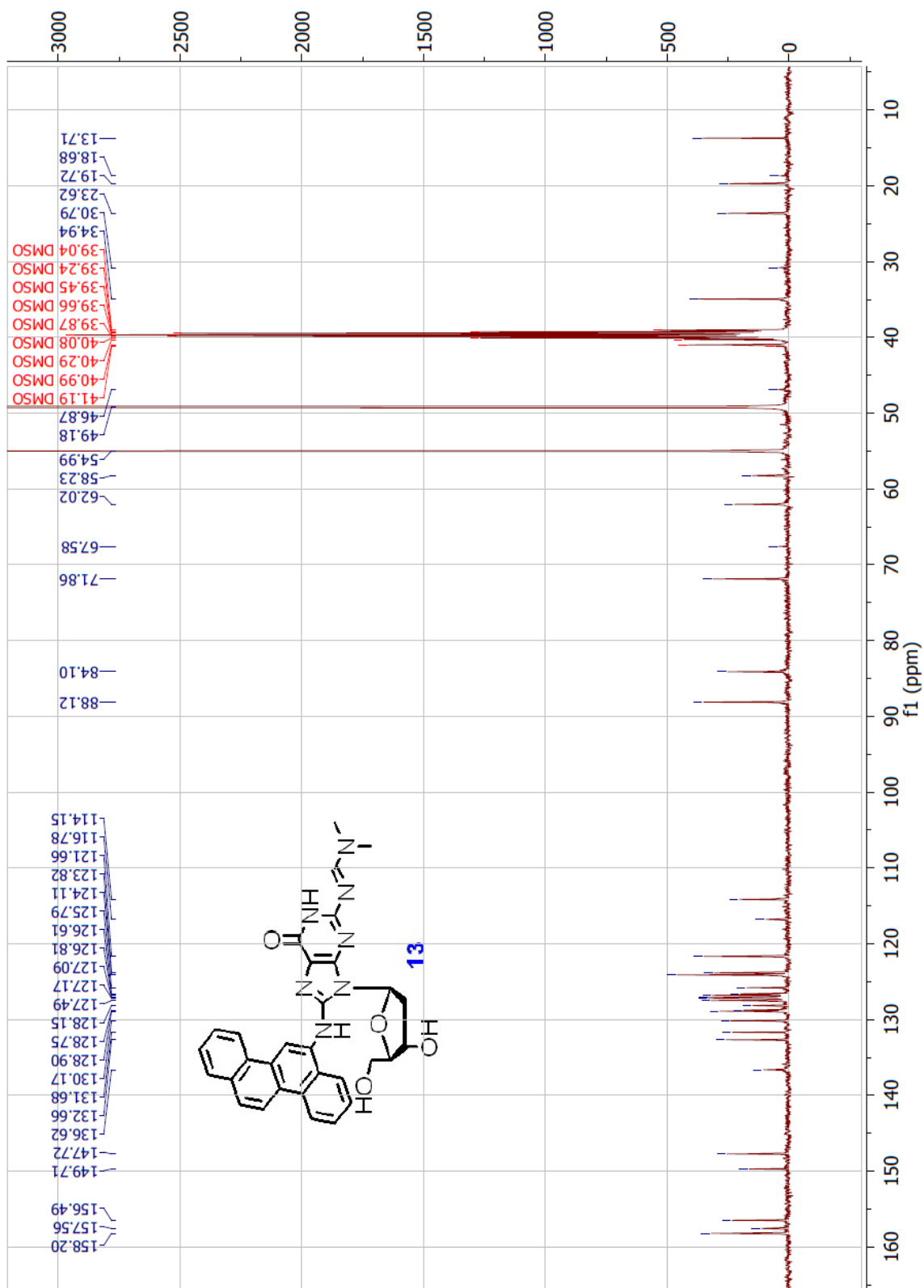


Figure 39:  $^{13}\text{C}$ -NMR of 8-(N-6-Aminochrysene)-N<sup>2</sup>-DMF-2'-deoxyguanosine

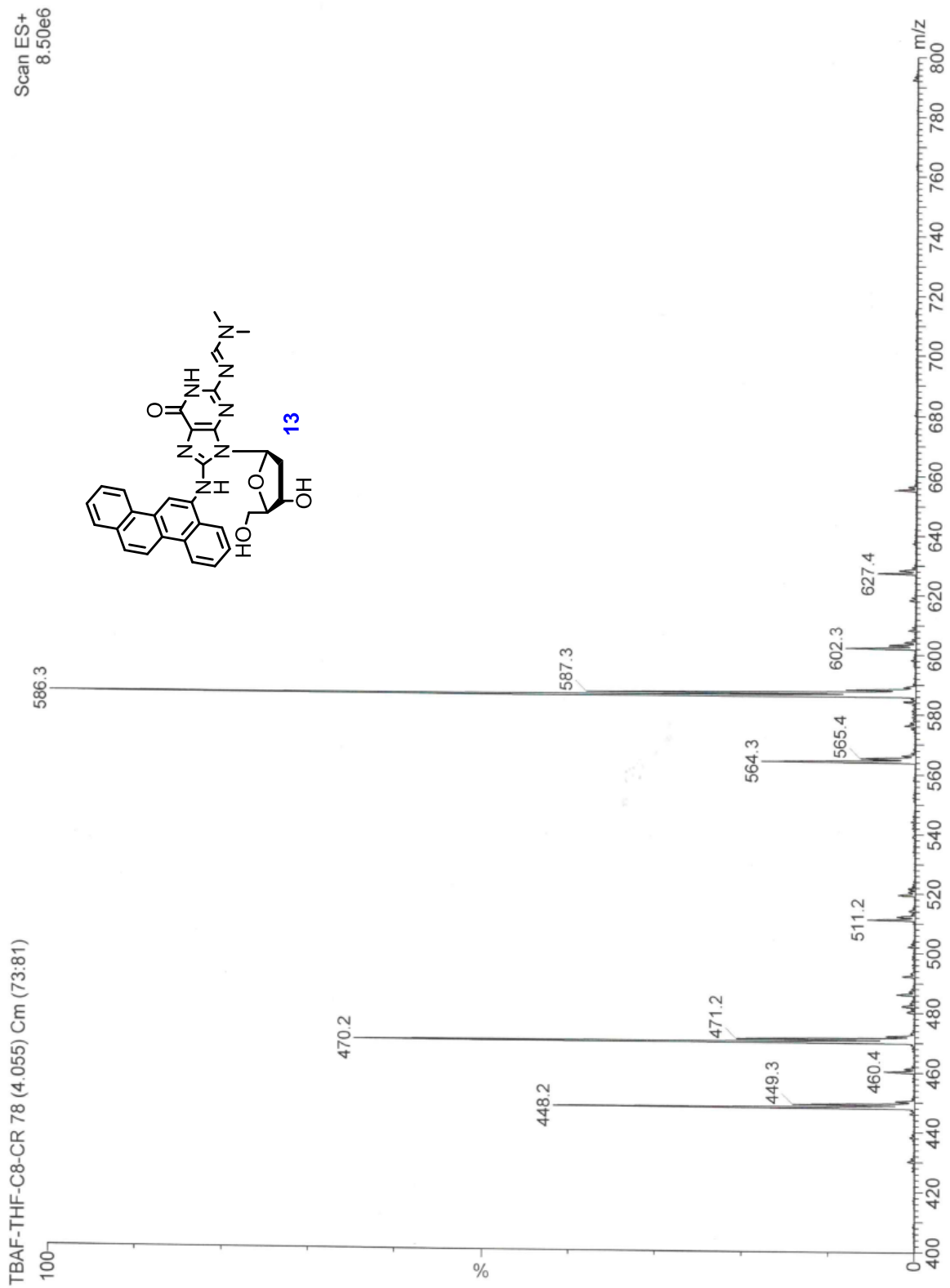
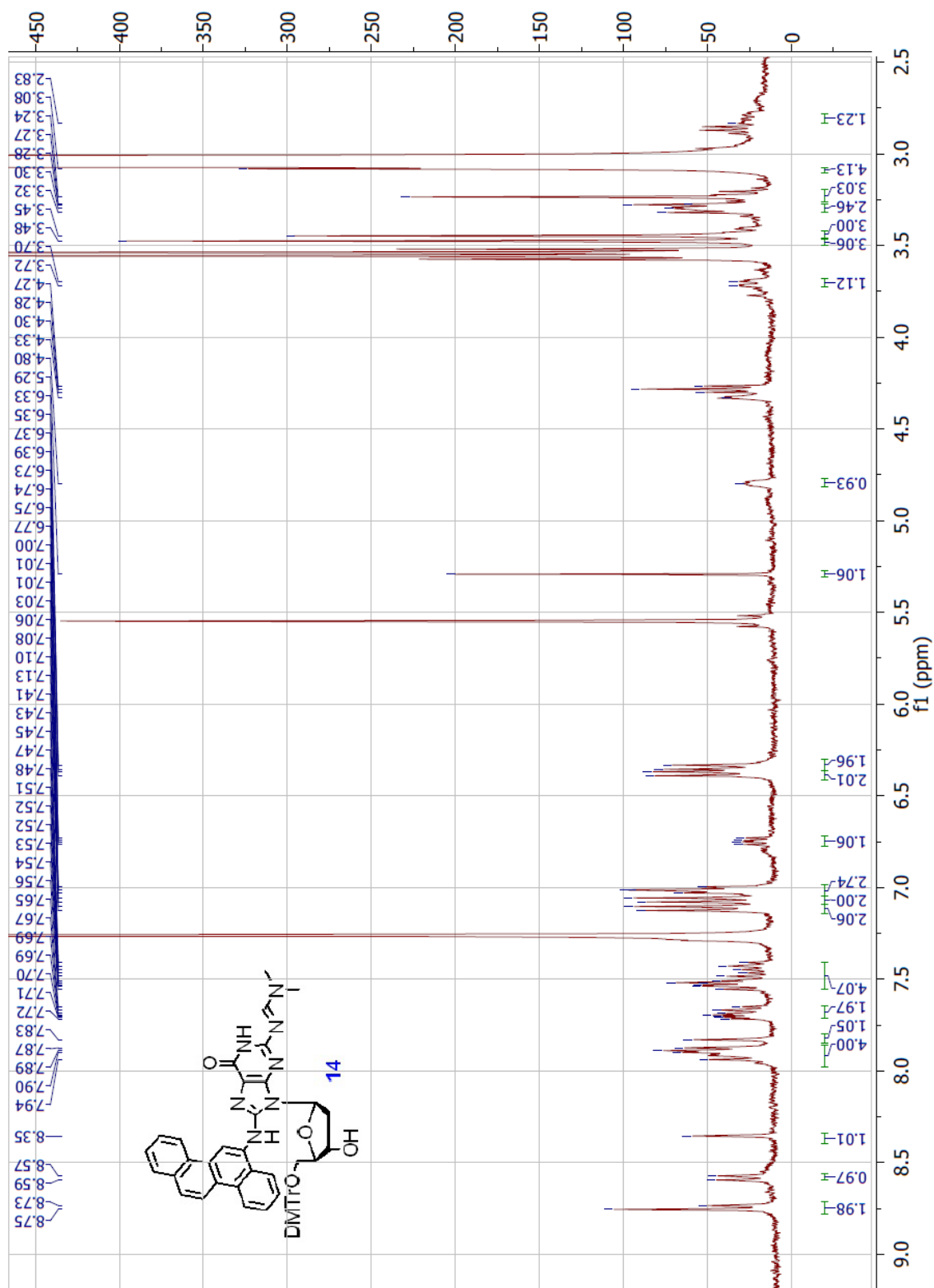


Figure 40: Mass Spectrum of 8-(N-6-Aminochrysene)-N<sup>2</sup>-DMF-2'-deoxyguanosine



**Figure 41: <sup>1</sup>H-NMR of 8-(N-6-Aminochrysene)-N<sup>2</sup>-DMF-5'-O-(4,4'-dimethoxytrityl)-2'-deoxyguanosine**

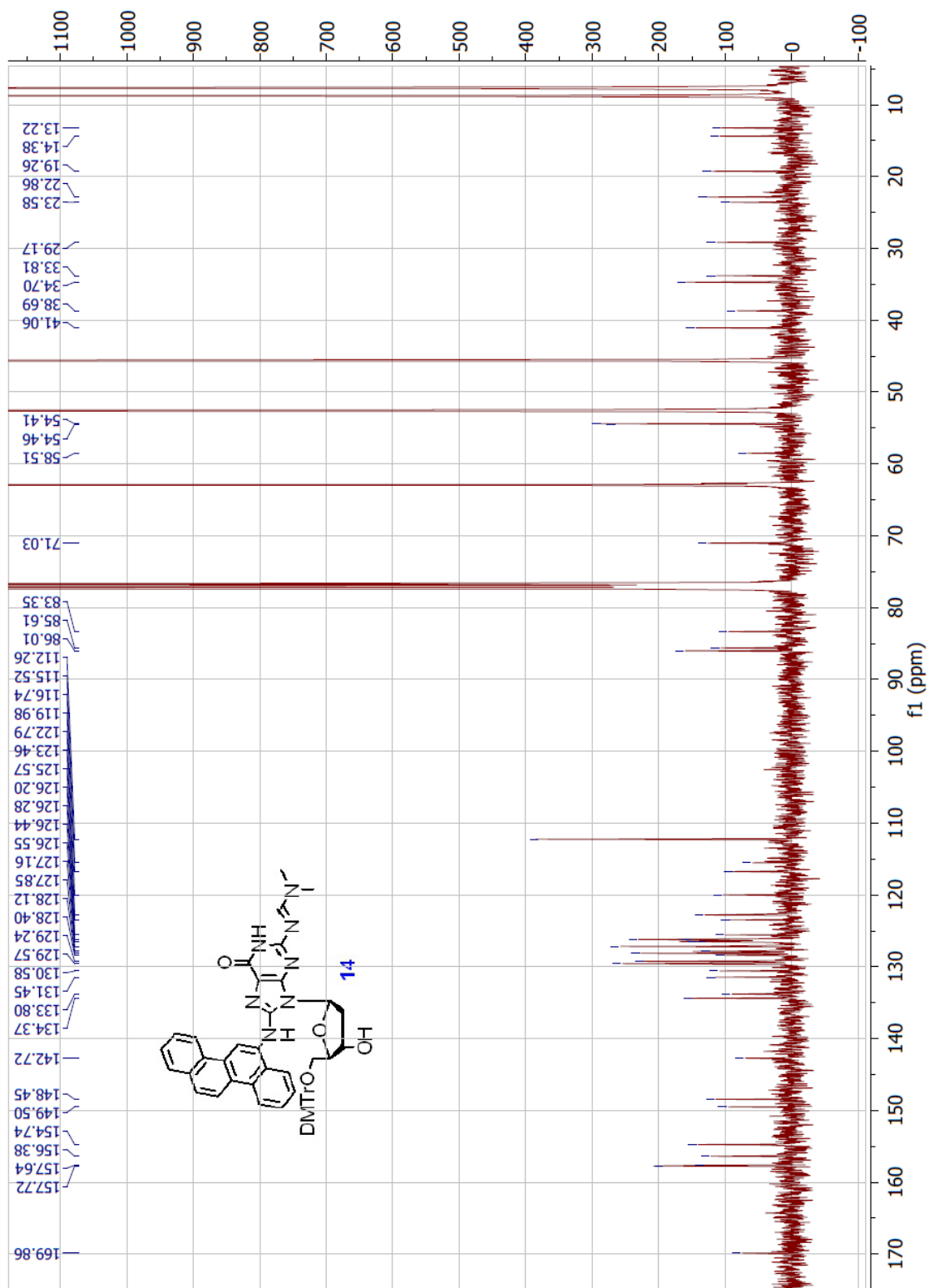
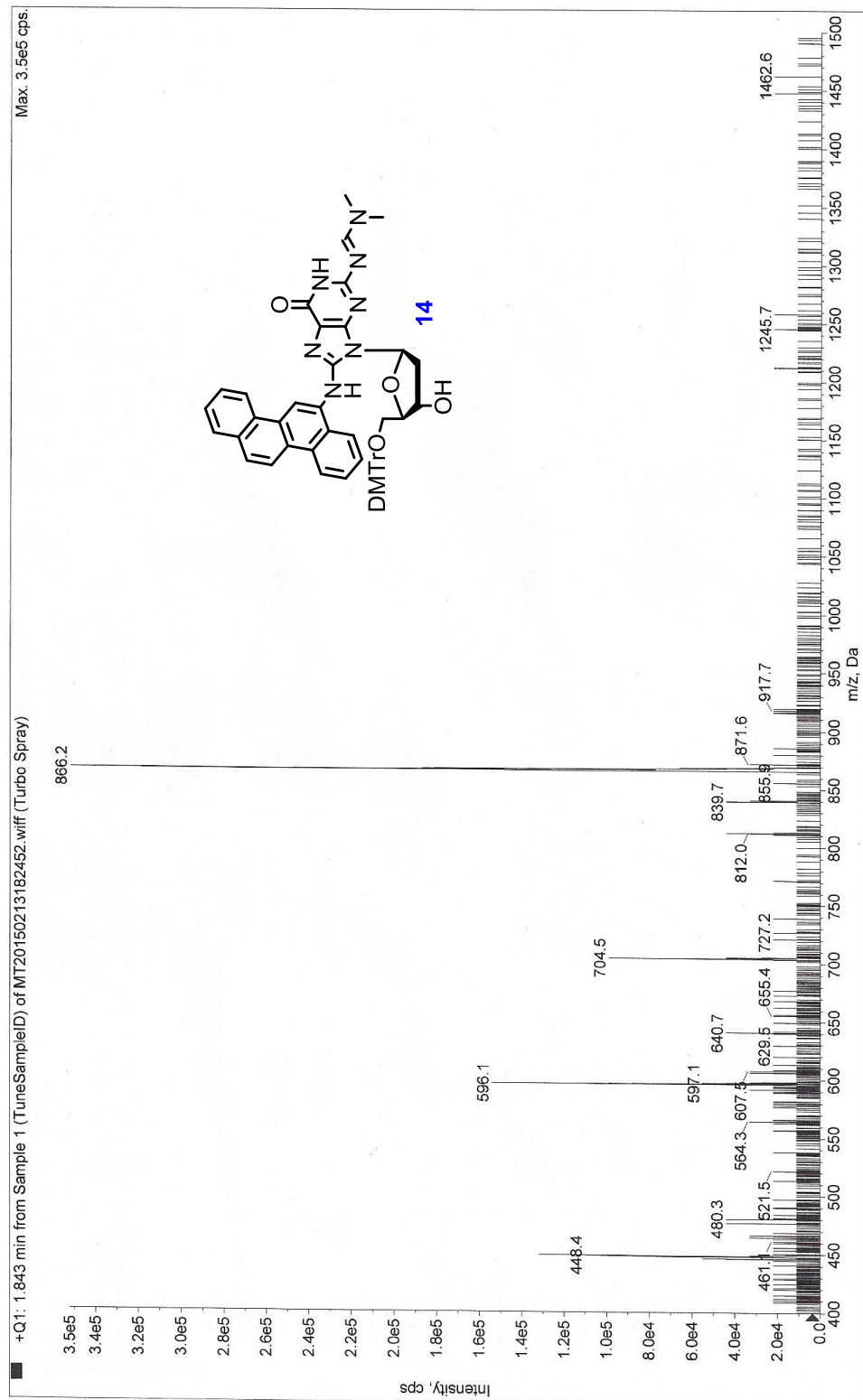
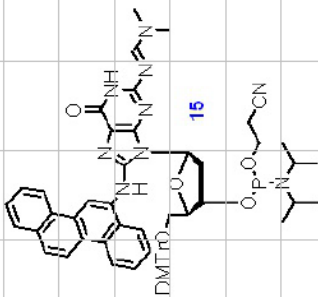


Figure 42:  $^{13}\text{C}$ -NMR of 8-(N-6-Aminochrysene)-N<sup>2</sup>-DMF-5'-O-(4,4'-dimethoxytrityl)-2'-deoxyguanosine



**Figure 43: Mass Spectrum of 8-(N-6-Aminochrysene)-N<sup>2</sup>-DMF-5'-O-(4,4'-dimethoxytrityl)-2'-deoxyguanosine**



90

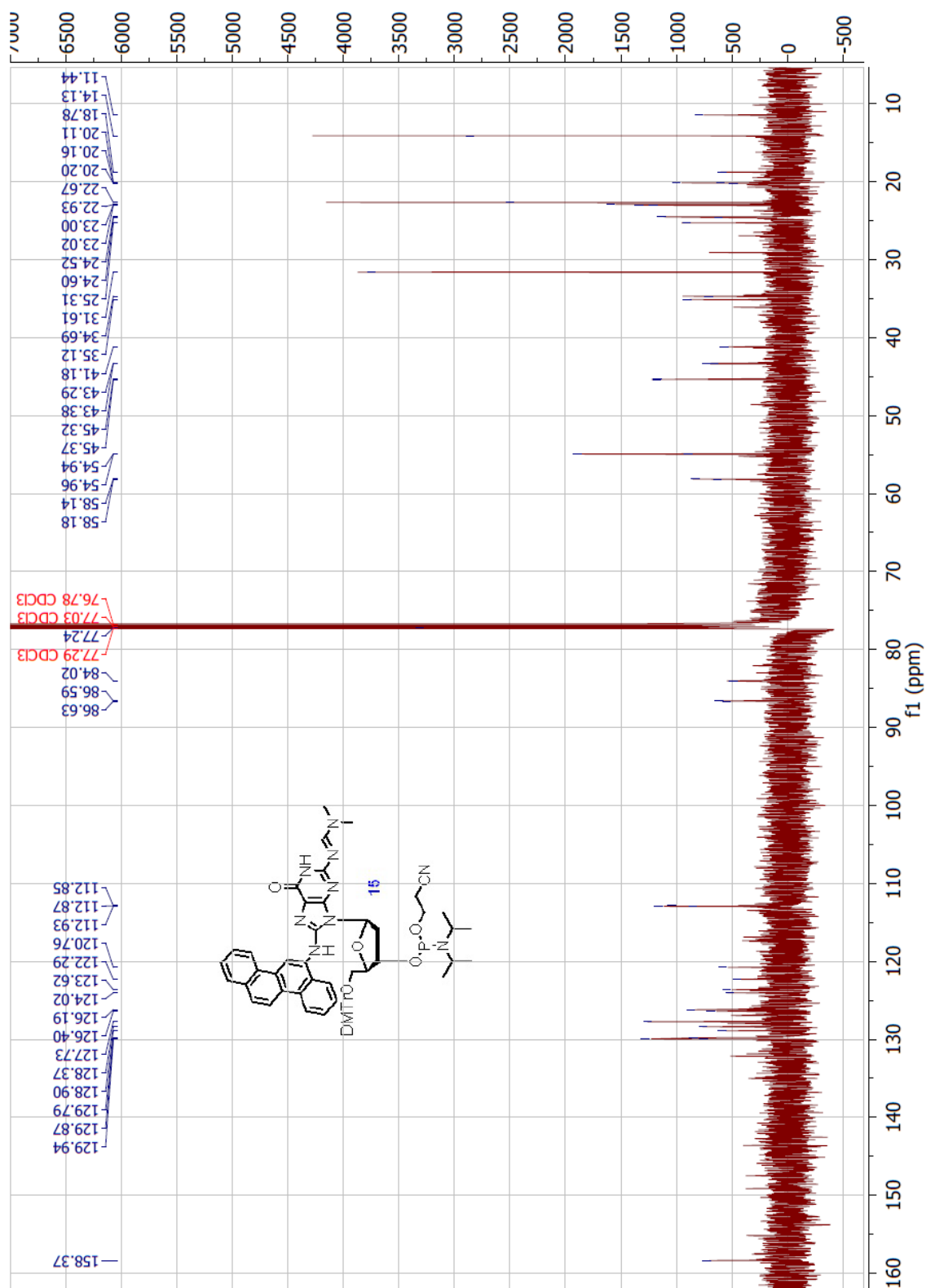


Figure 45: <sup>13</sup>C-NMR of 8-(N-6-Aminochrysene)-N<sup>2</sup>'-DMF-5'-O-(4,4'-dimethoxytrityl)-3'-cyanoethyl-2'-deoxyguanosine phosphoramidite



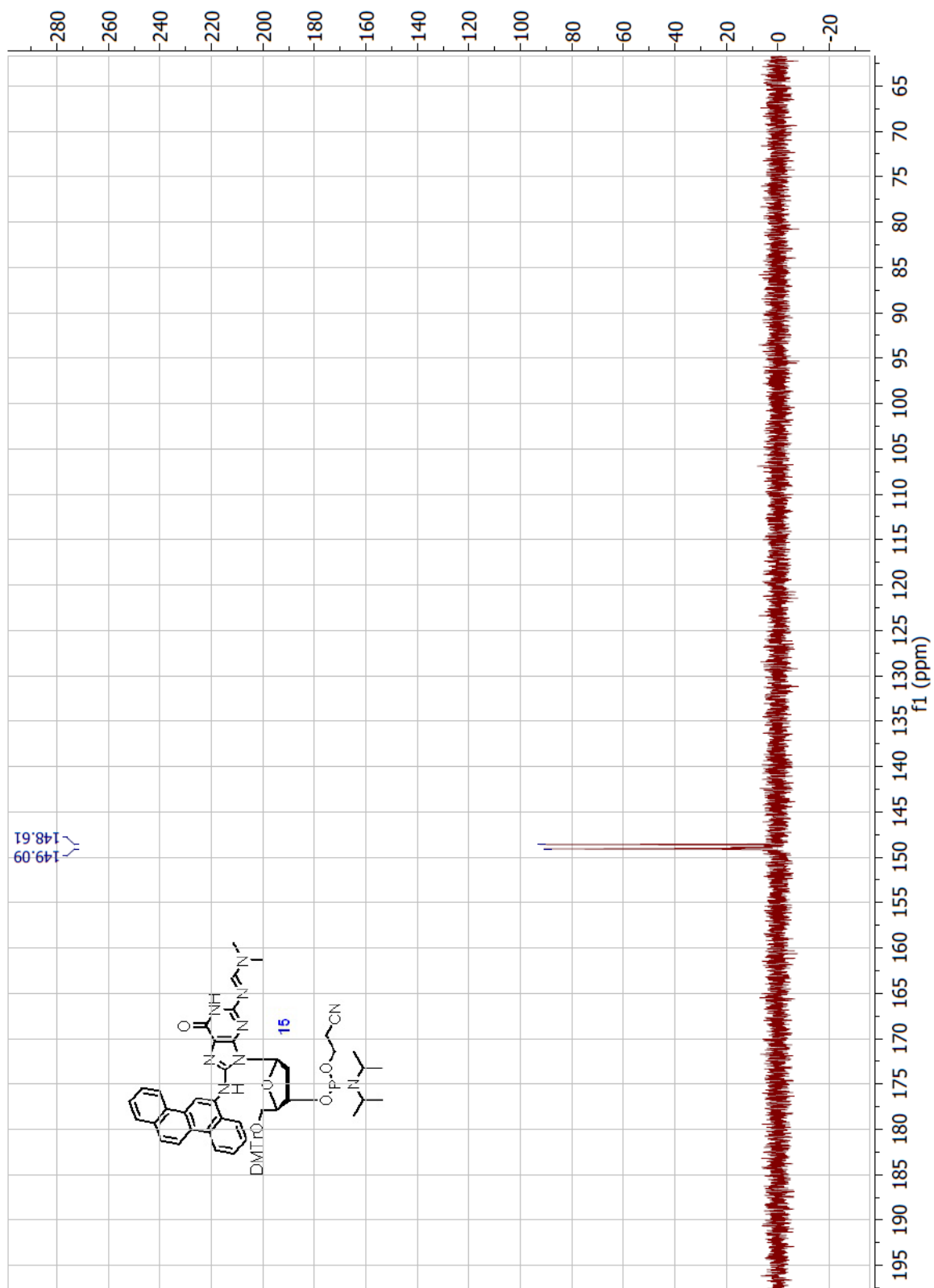


Figure 46:  $^{31}\text{P}$ -NMR of 8-(N-6-Aminochrysene)- $N^2$ -DMF-5'-O-(4,4'-dimethoxytrityl)-3'-cyanoethyl-2'-deoxyguanosine phosphoramidite

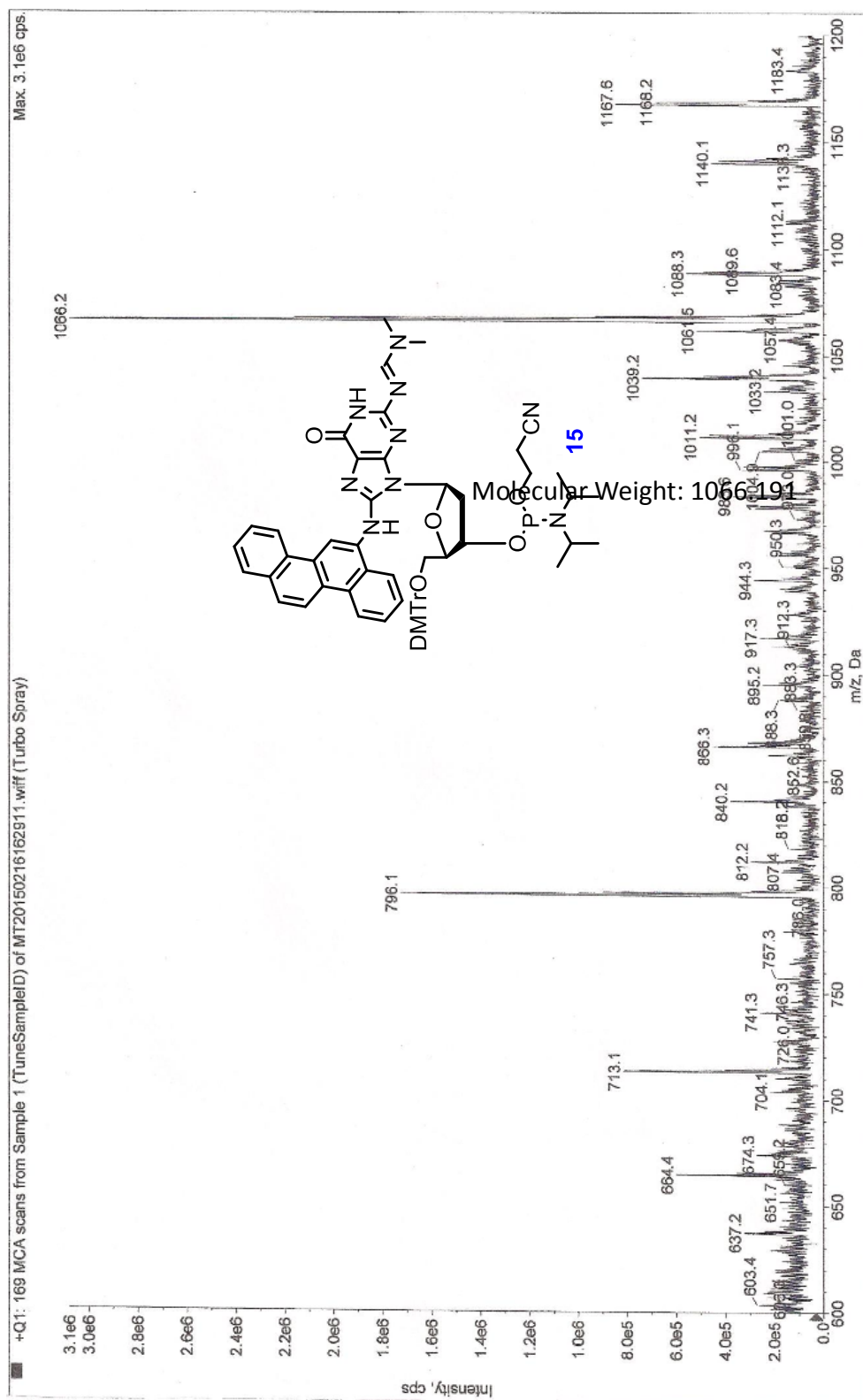


Figure 47: Mass Spectrum of 8-(N-6-Aminochrysene)-N<sup>2</sup>-DMF-5'-O-(4,4'-dimethoxytrityl)-3'-cyanoethyl-2'-deoxyguanosine phosphoramidite

## **APPENDIX B**

### **NMR AND MASS SPECTRA FOR $N^2$ -CR-DG ADDUCT**

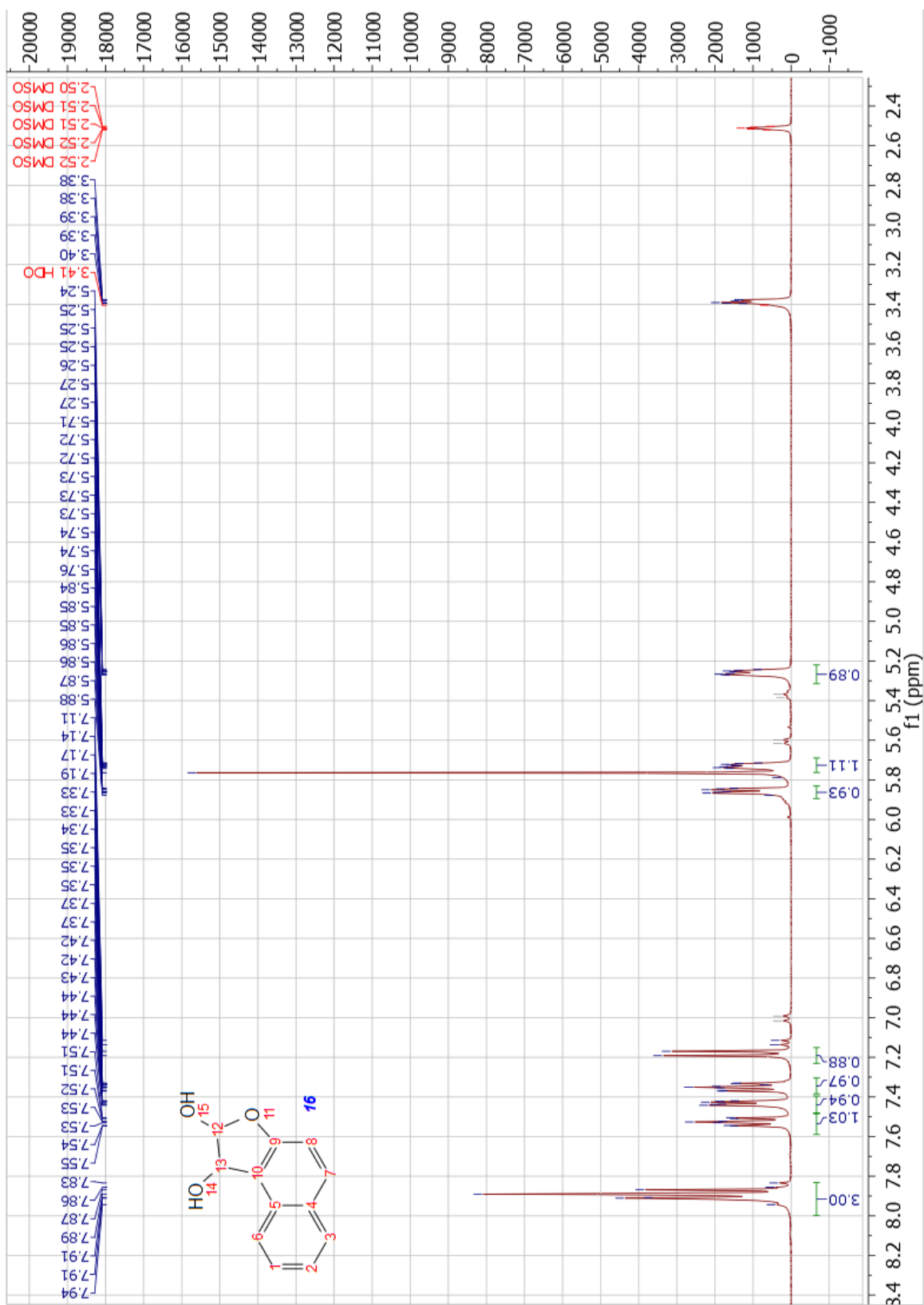


Figure 48:  $^1\text{H}$ -NMR of 1,2-Dihydronaphtho[2,1-b]furan-1,2-diol

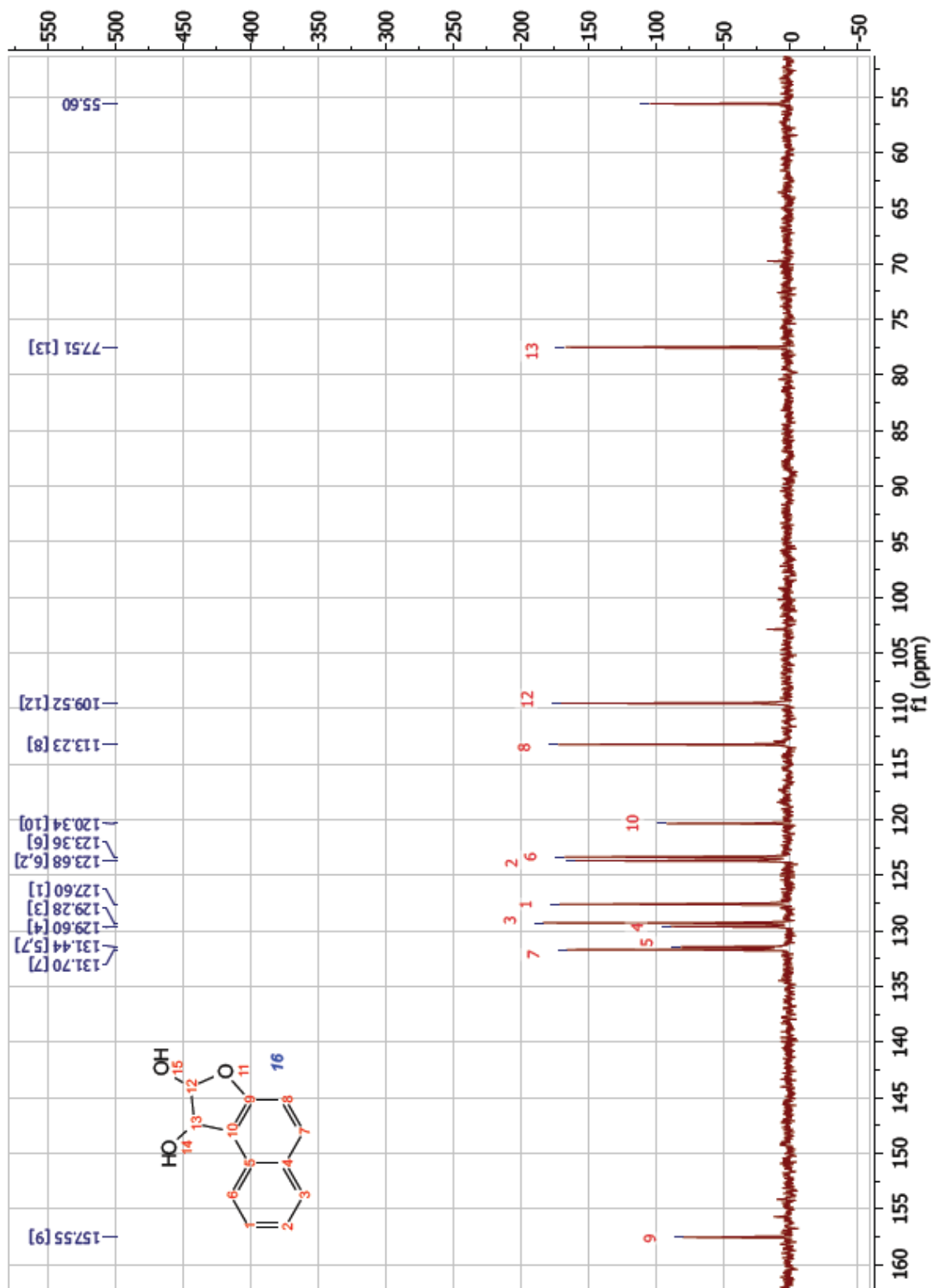


Figure 49: <sup>13</sup>C-NMR of 1,2-Dihydronaphtho[2,1-b]furan-1,2-diol

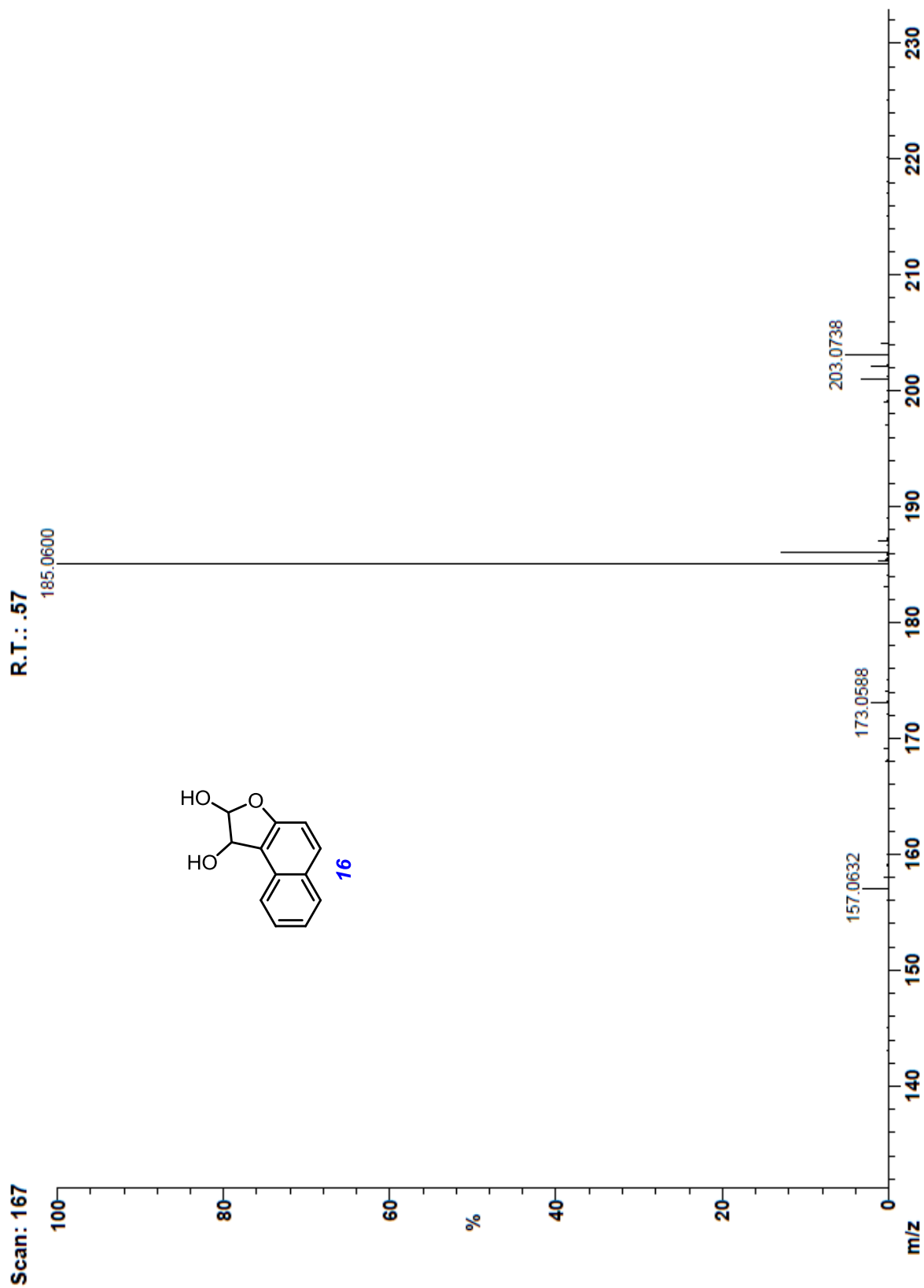
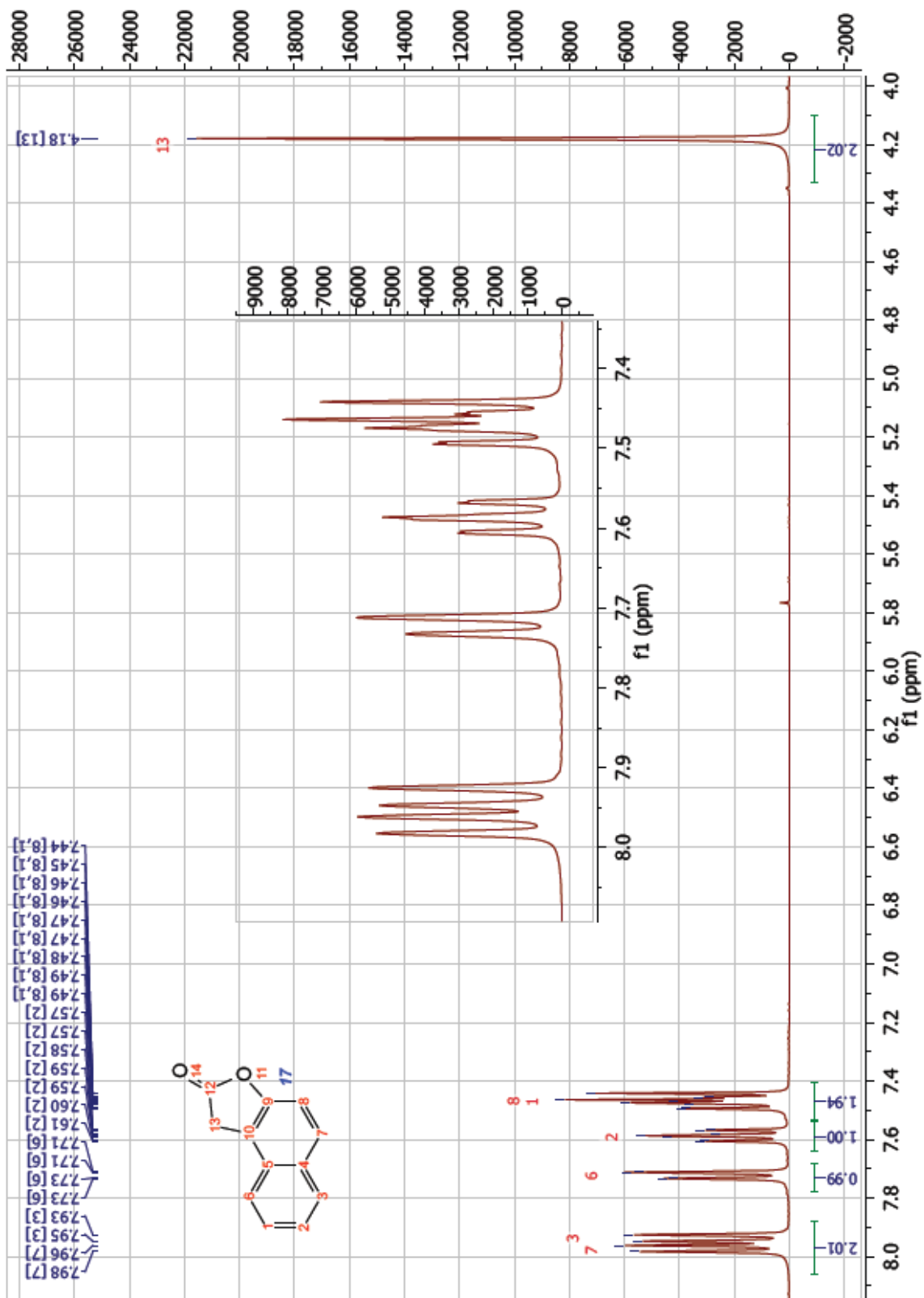


Figure 50: Mass Spectrum of 1,2-Dihydronaphtho[2,1-b]furan-1,2-diol



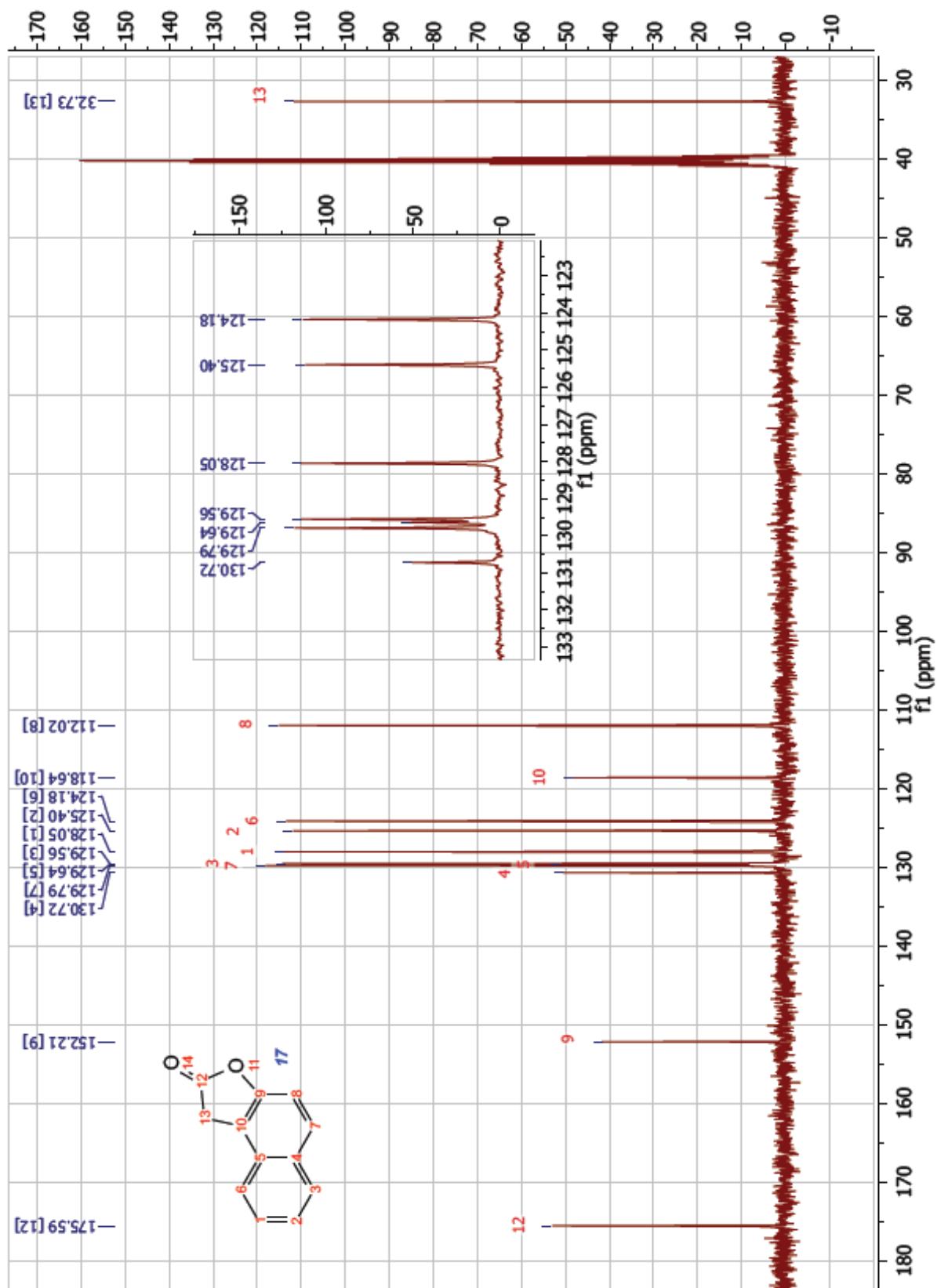


Figure 52:  $^{13}\text{C}$ -NMR of Naphtho[2,1-b]furan-2(1H)-one



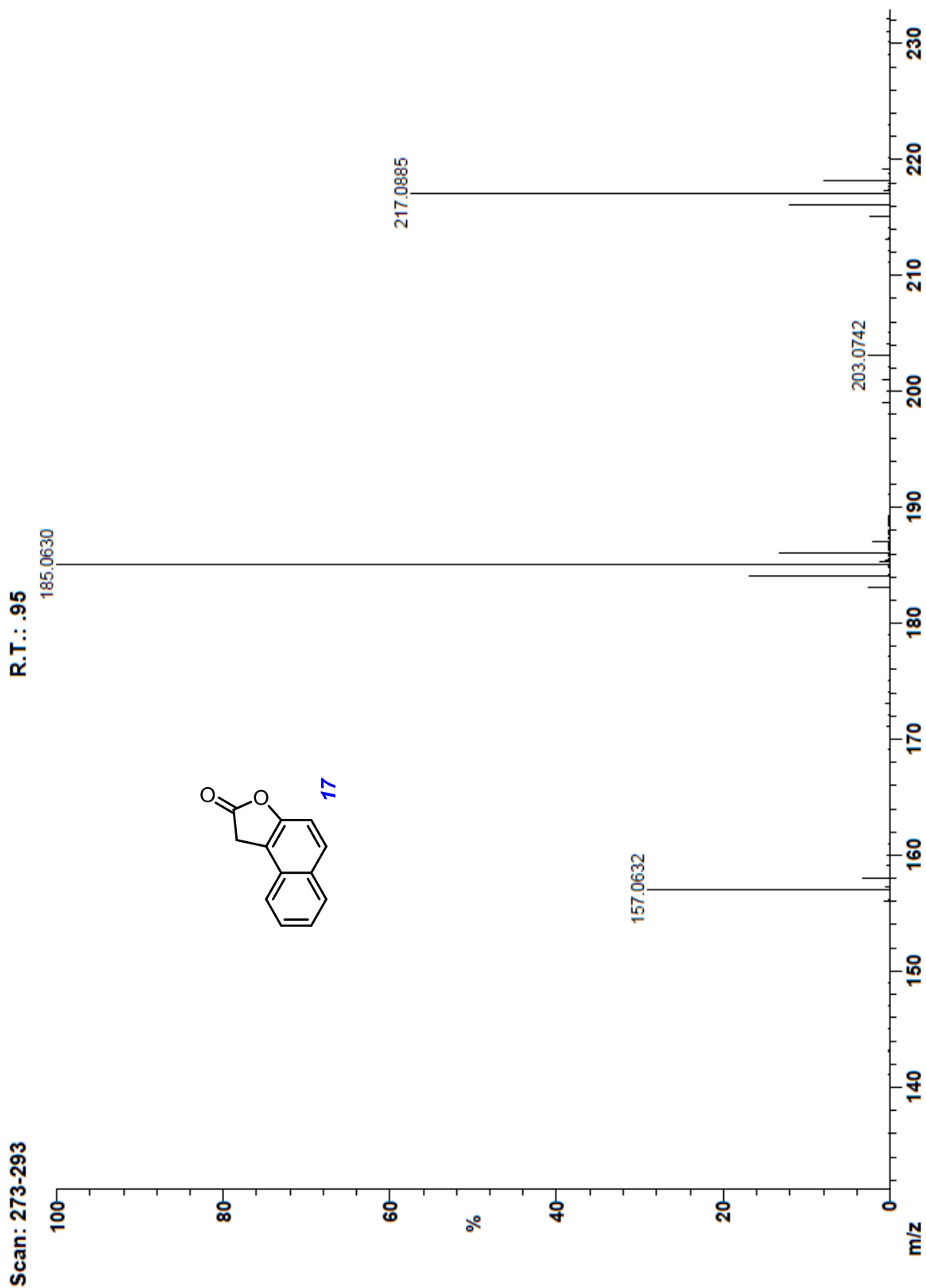


Figure 53: Mass Spectrum of Naphtho[2,1-b]furan-2(1H)-one

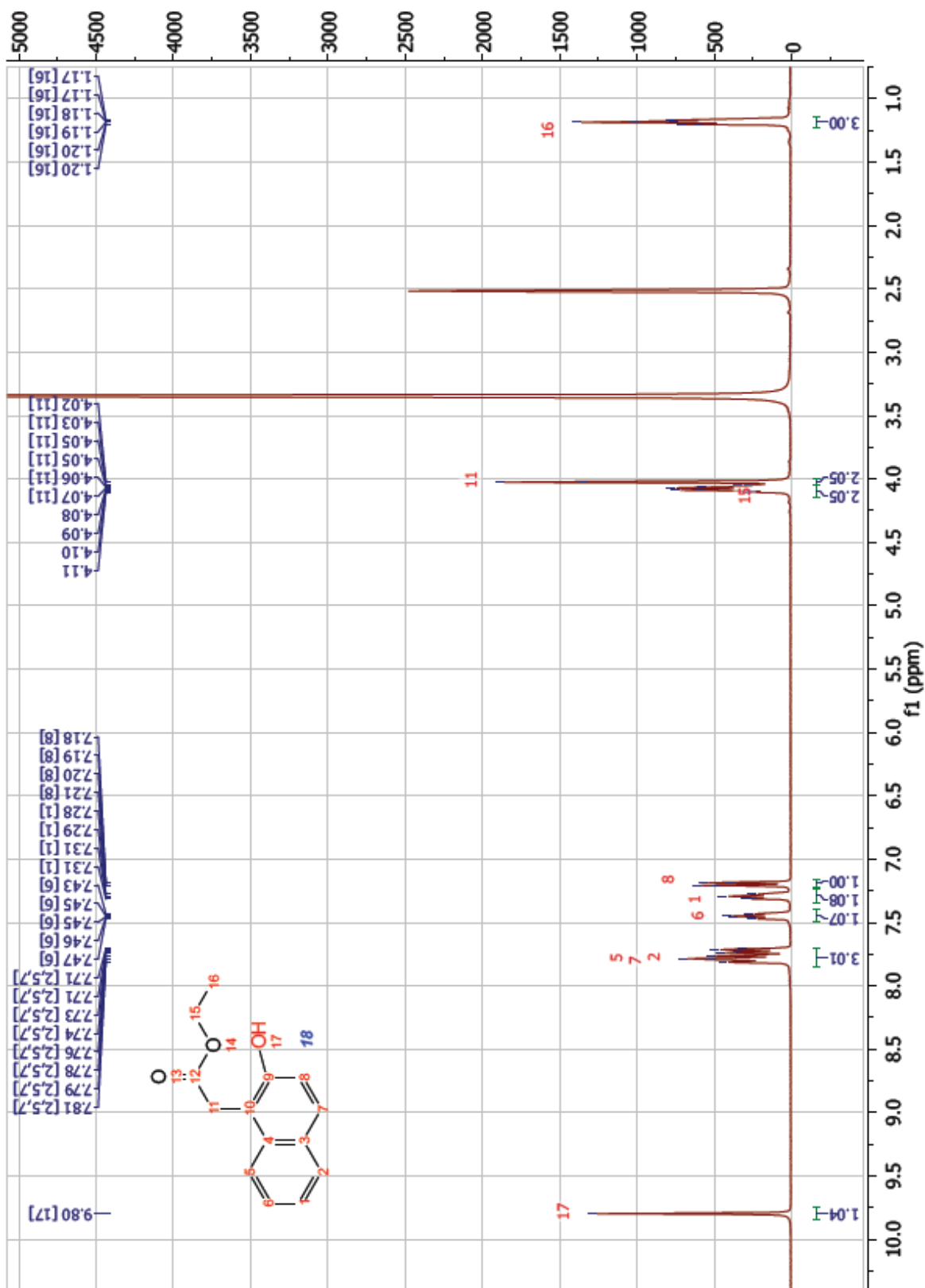


Figure 54: <sup>1</sup>H-NMR of Ethyl 2-(2-hydroxynaphthalen-1-yl)acetate

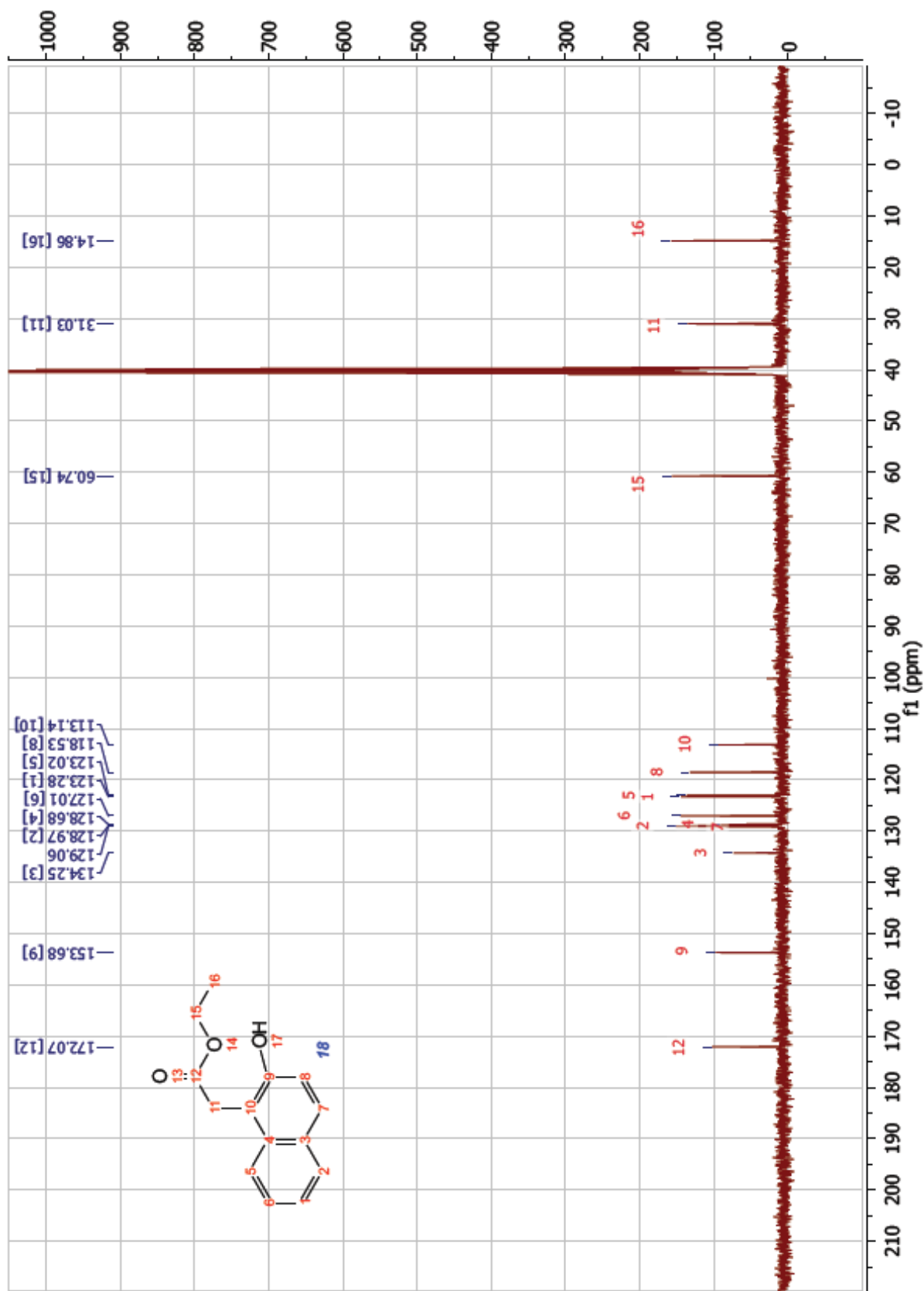


Figure 55: <sup>13</sup>C-NMR of Ethyl 2-(2-hydroxynaphthalen-1-yl)acetate

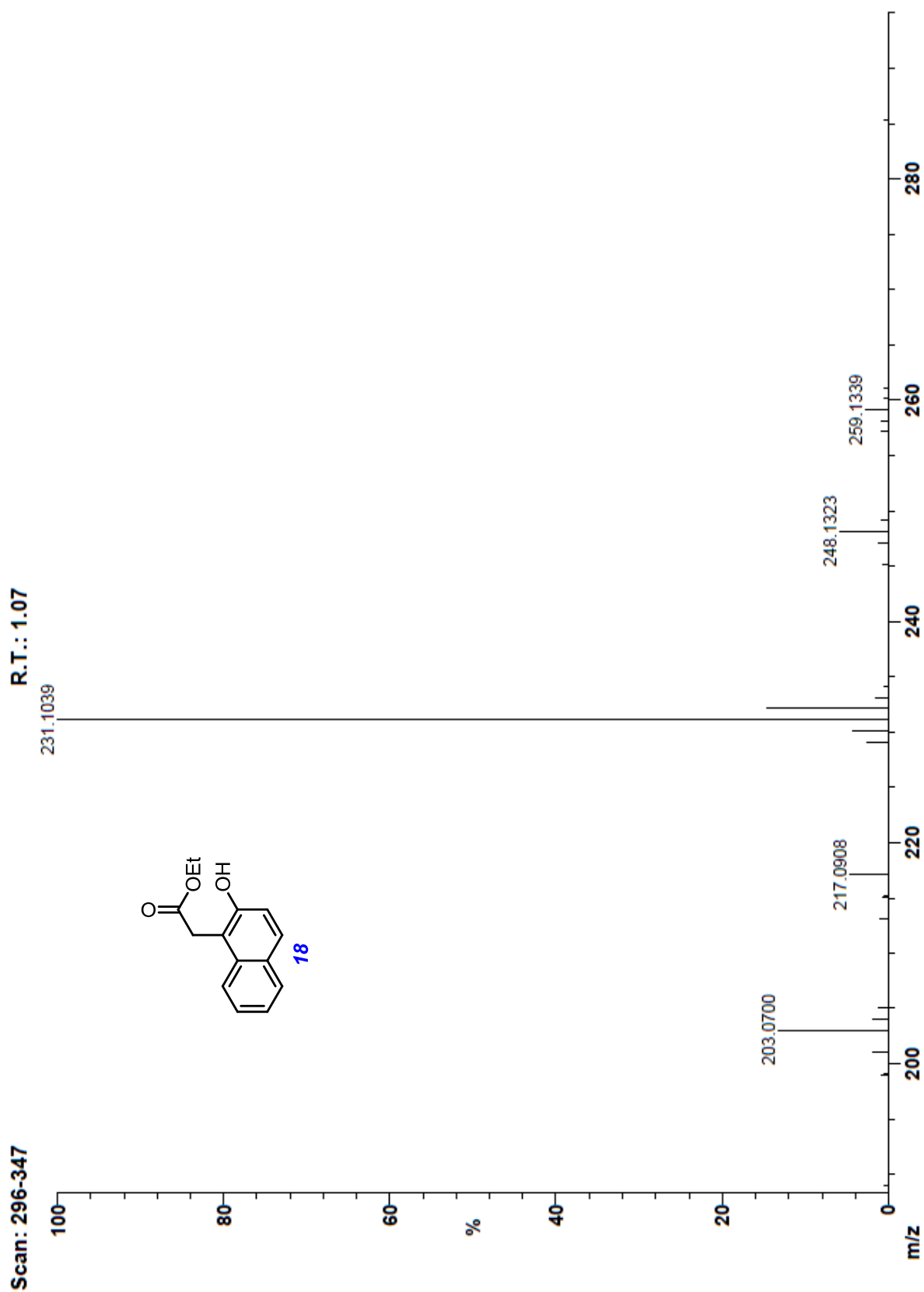


Figure S6: Mass Spectrum of Ethyl 2-(2-hydroxynaphthalen-1-yl)acetate

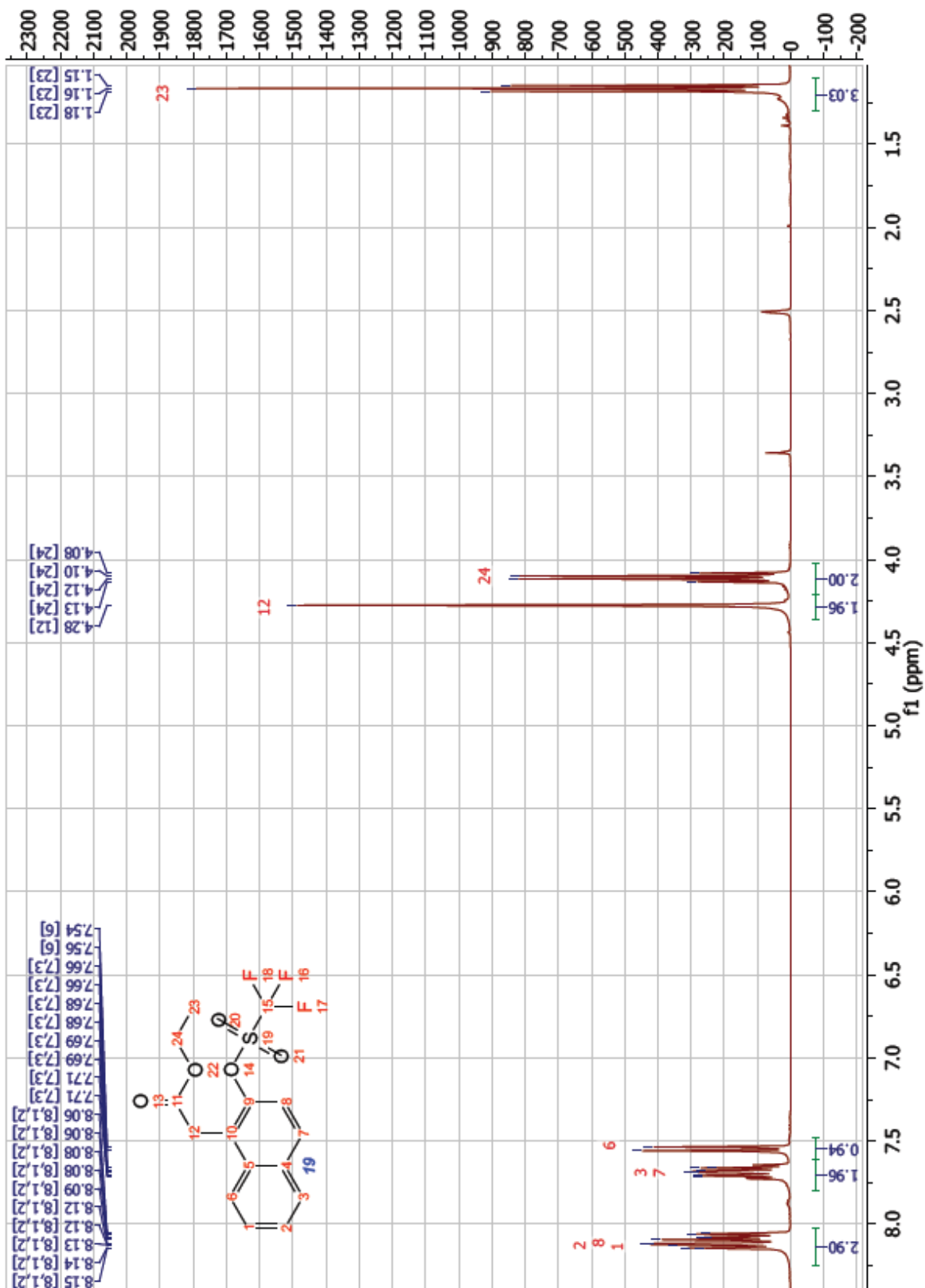


Figure 57: <sup>1</sup>H-NMR of Ethyl 2-(2-(((trifluoromethyl)sulfonyl)oxy)naphthalen-1-yl)acetate

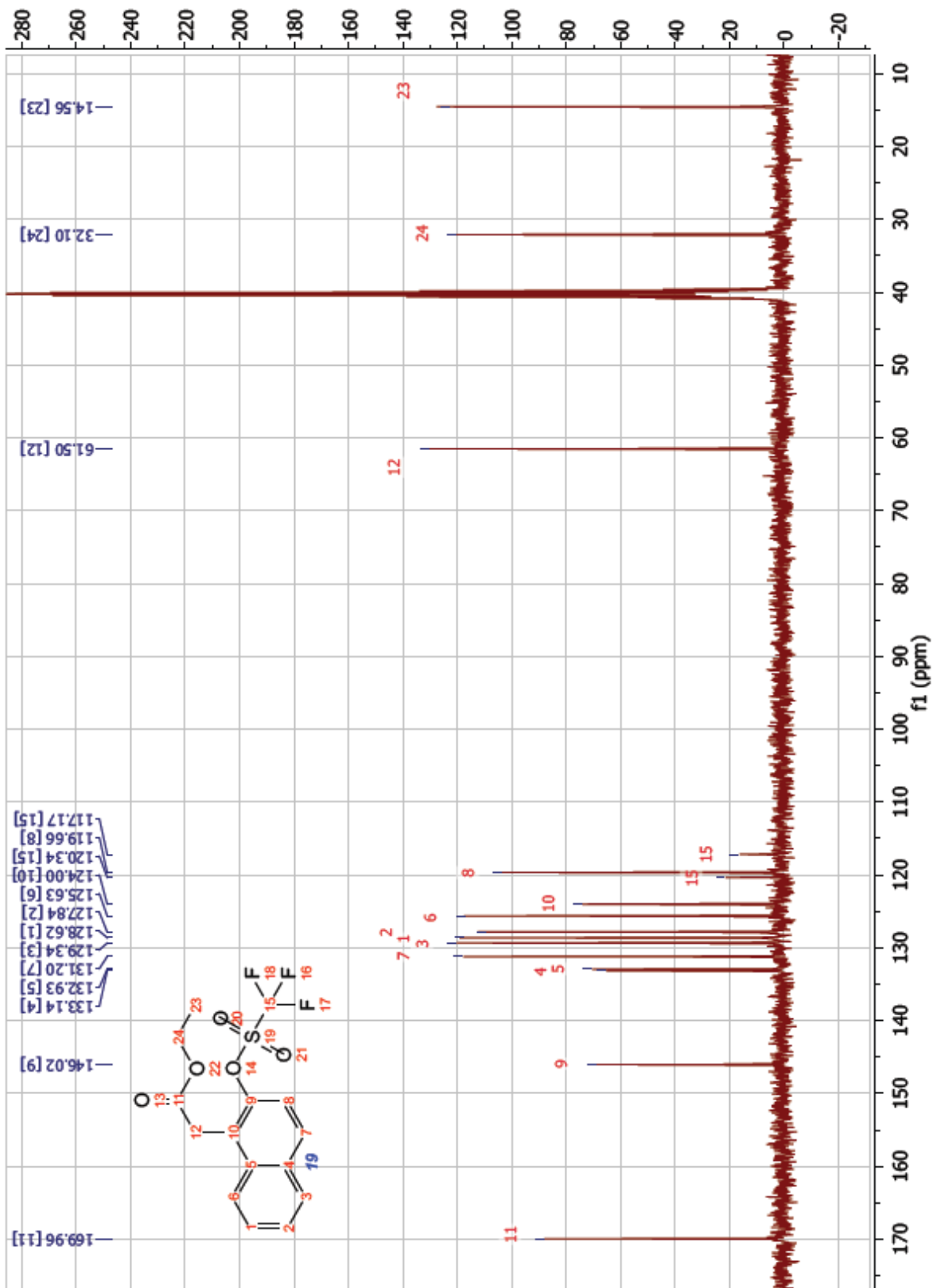


Figure 58: <sup>13</sup>C-NMR of Ethyl 2-(2-(((trifluoromethyl)sulfonyl)oxy)naphthalen-1-yl)acetate

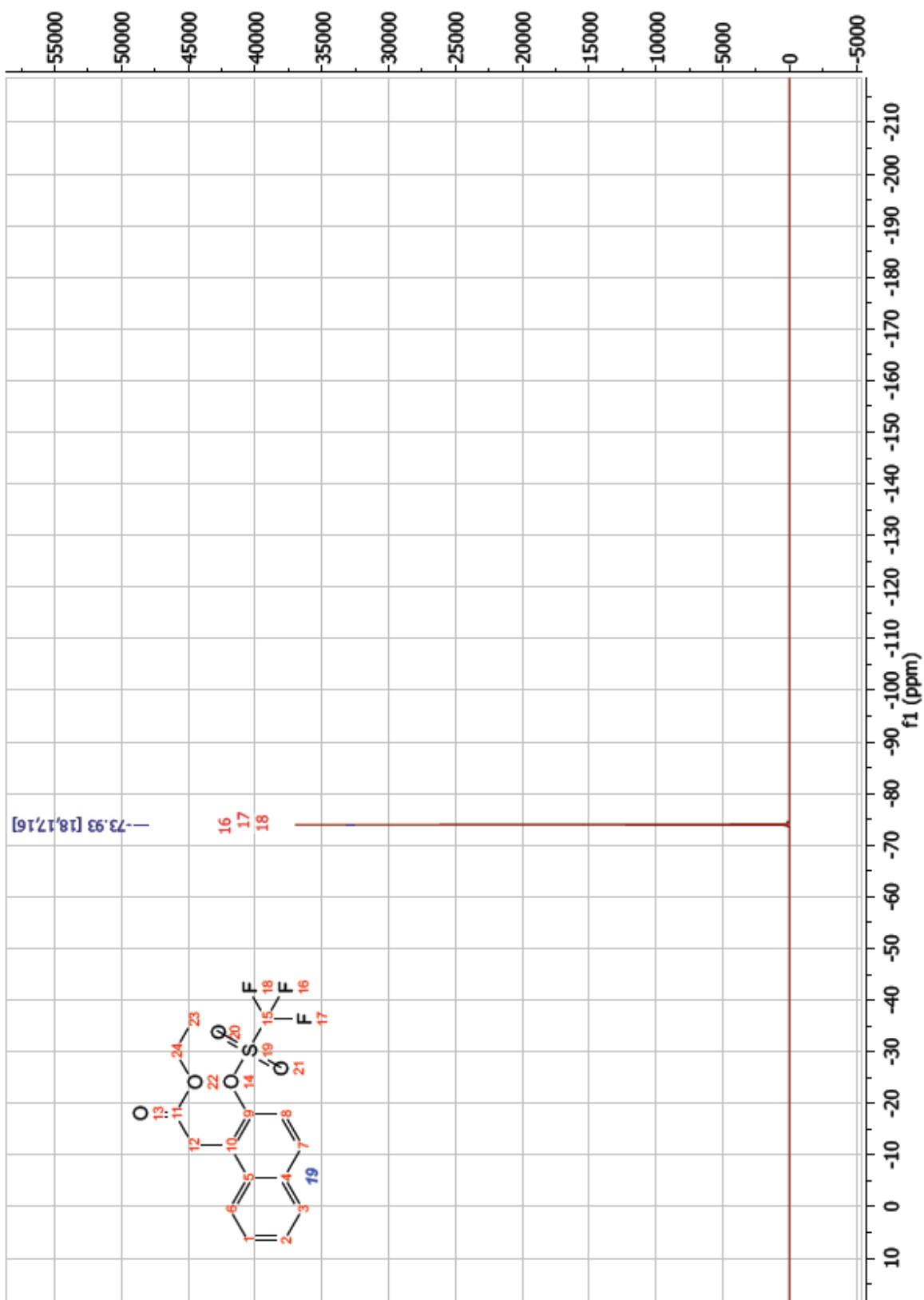


Figure 59:  $^{19}\text{F}$ -NMR of Ethyl 2-((2-(((trifluoromethyl)sulfonyl)oxy)naphthalen-1-yl)acetate

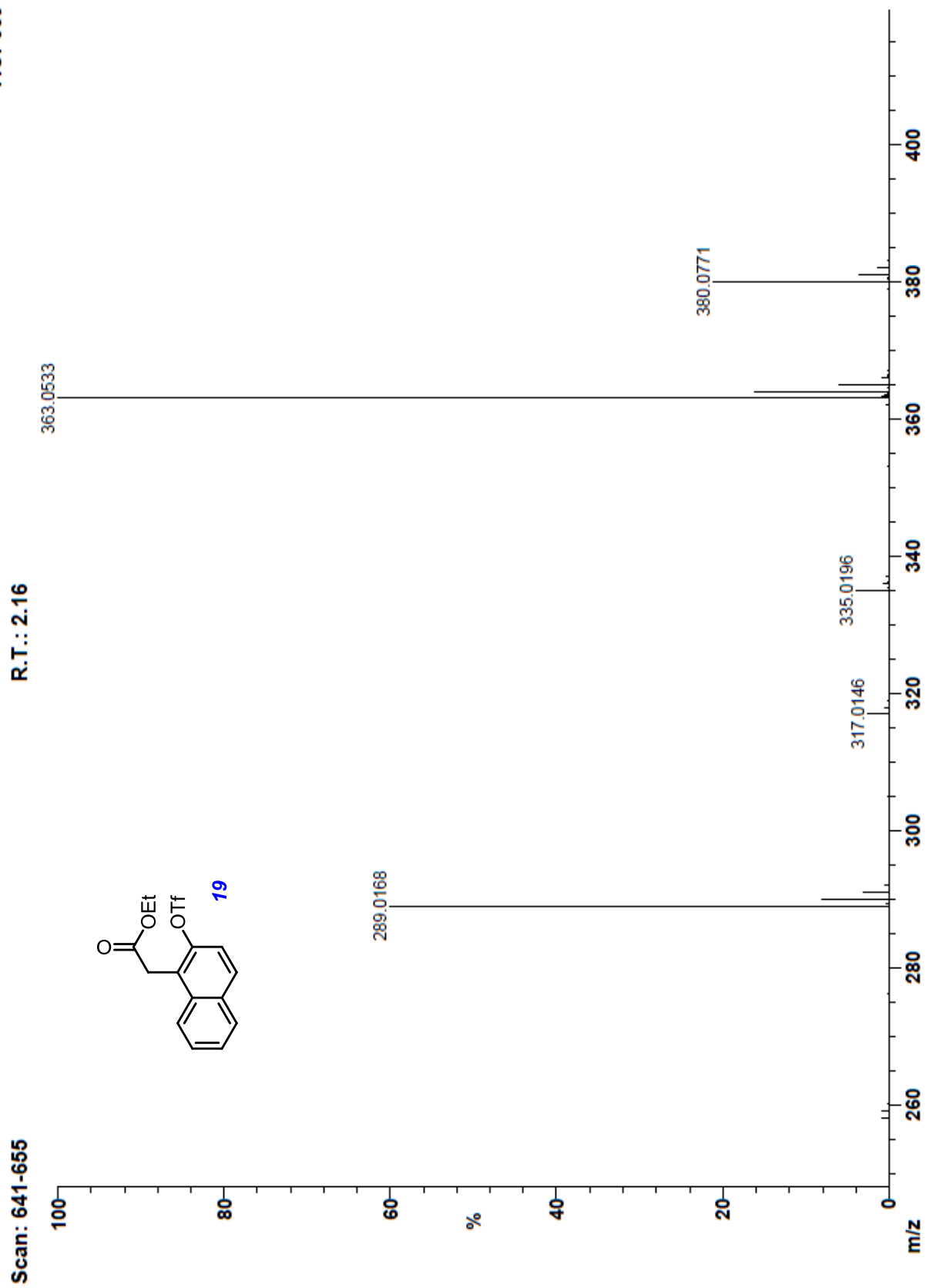


Figure 60: Mass Spectrum of Ethyl 2-(2-(((trifluoromethyl)sulfonyl)oxy)naphthalen-1-yl)acetate



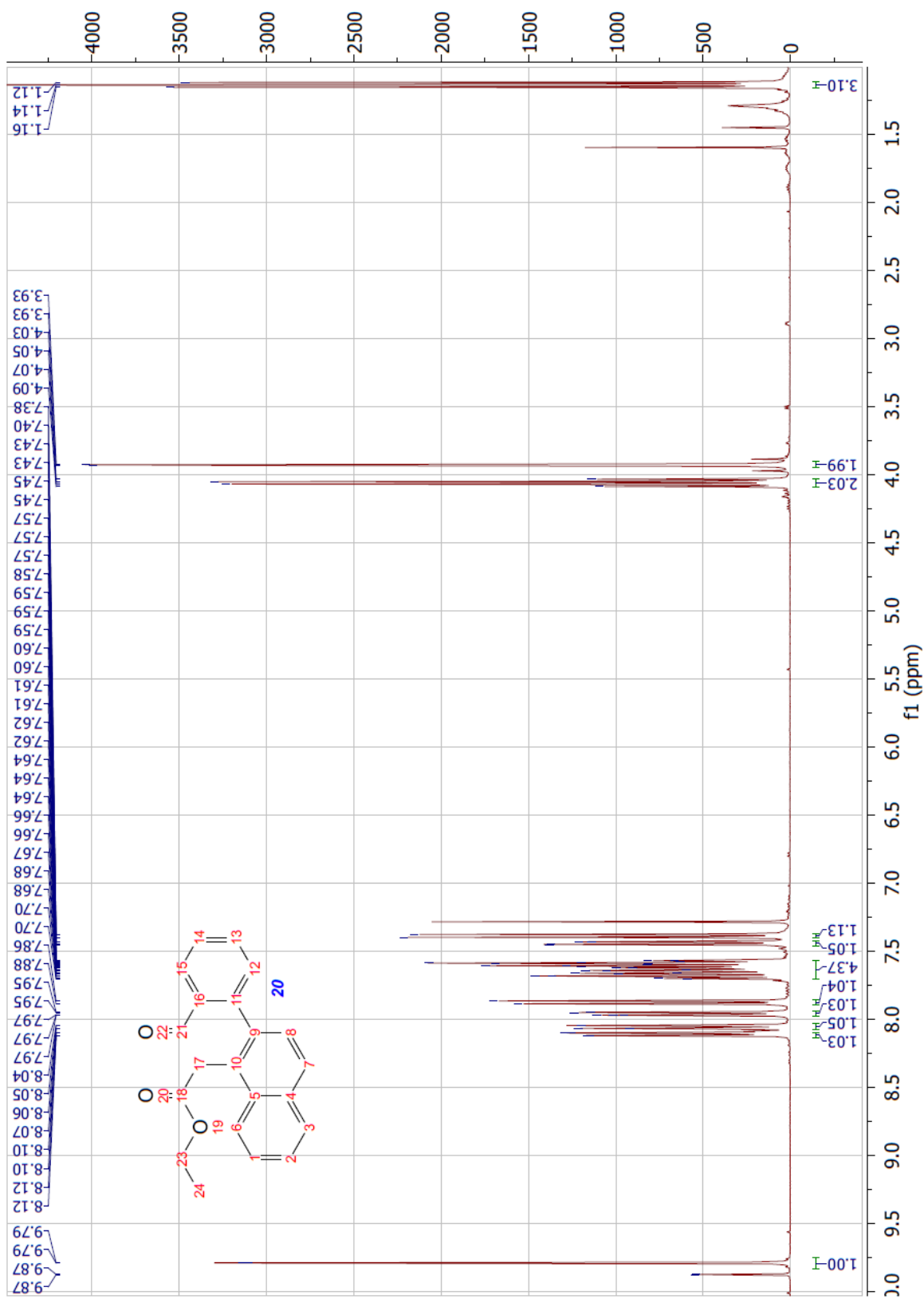


Figure 61:  $^1\text{H}$ -NMR of Ethyl 2-(2-(2-formylphenyl)naphthalen-1-yl)acetate

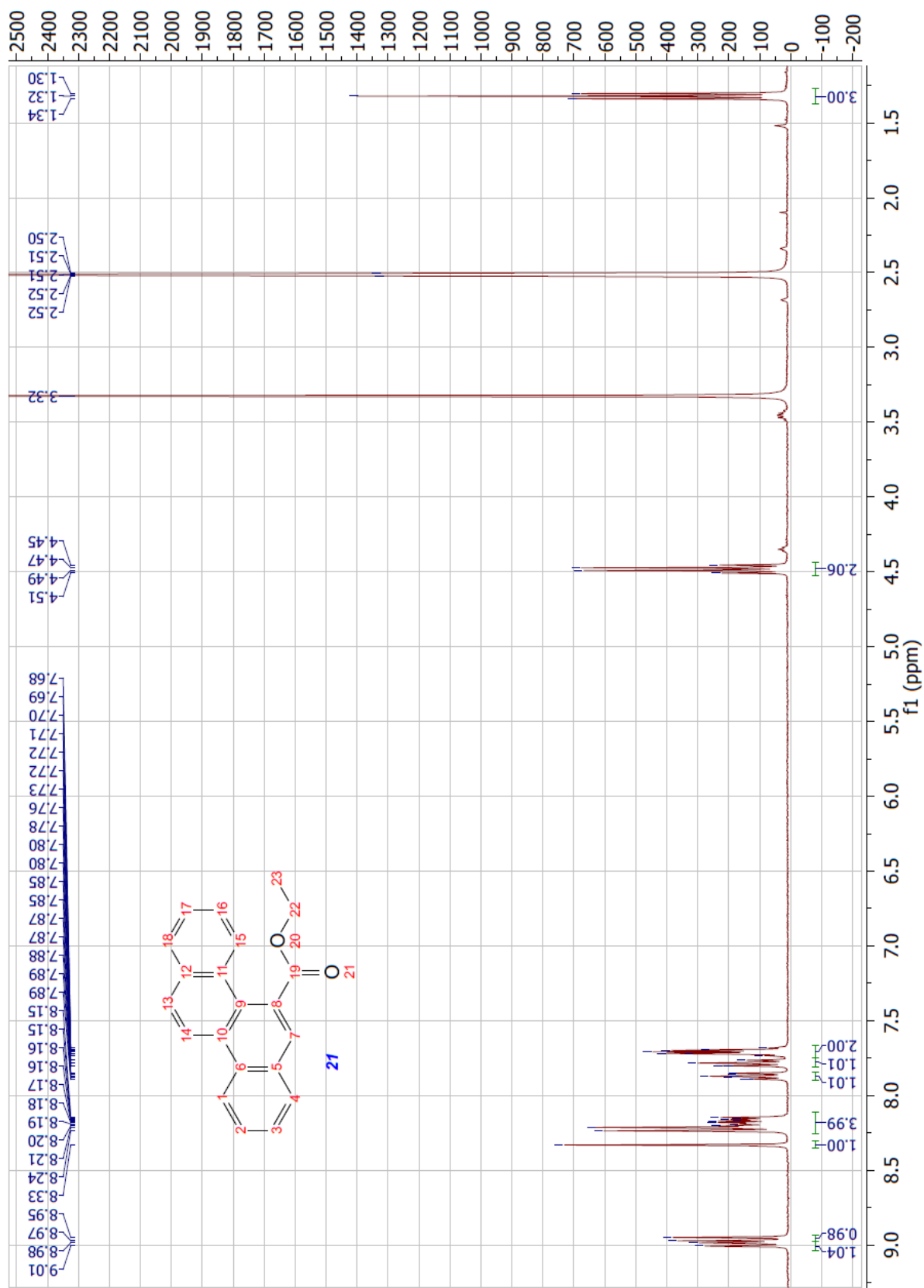


Figure 62:  $^1\text{H}$ -NMR of Ethyl chrysene-5-carboxylate

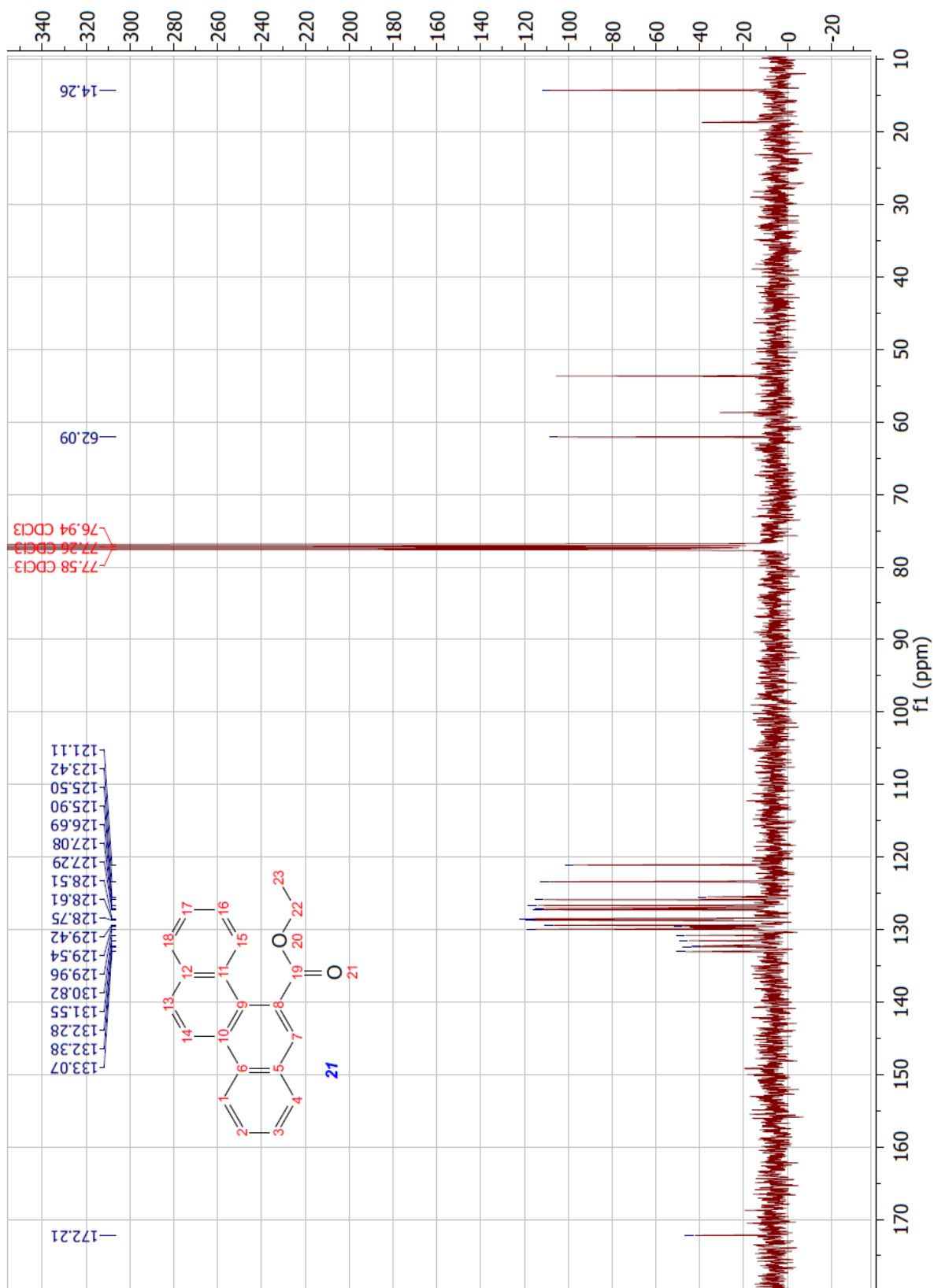


Figure 63:  $^{13}\text{C}$ -NMR of Ethyl chrysene-5-carboxylate

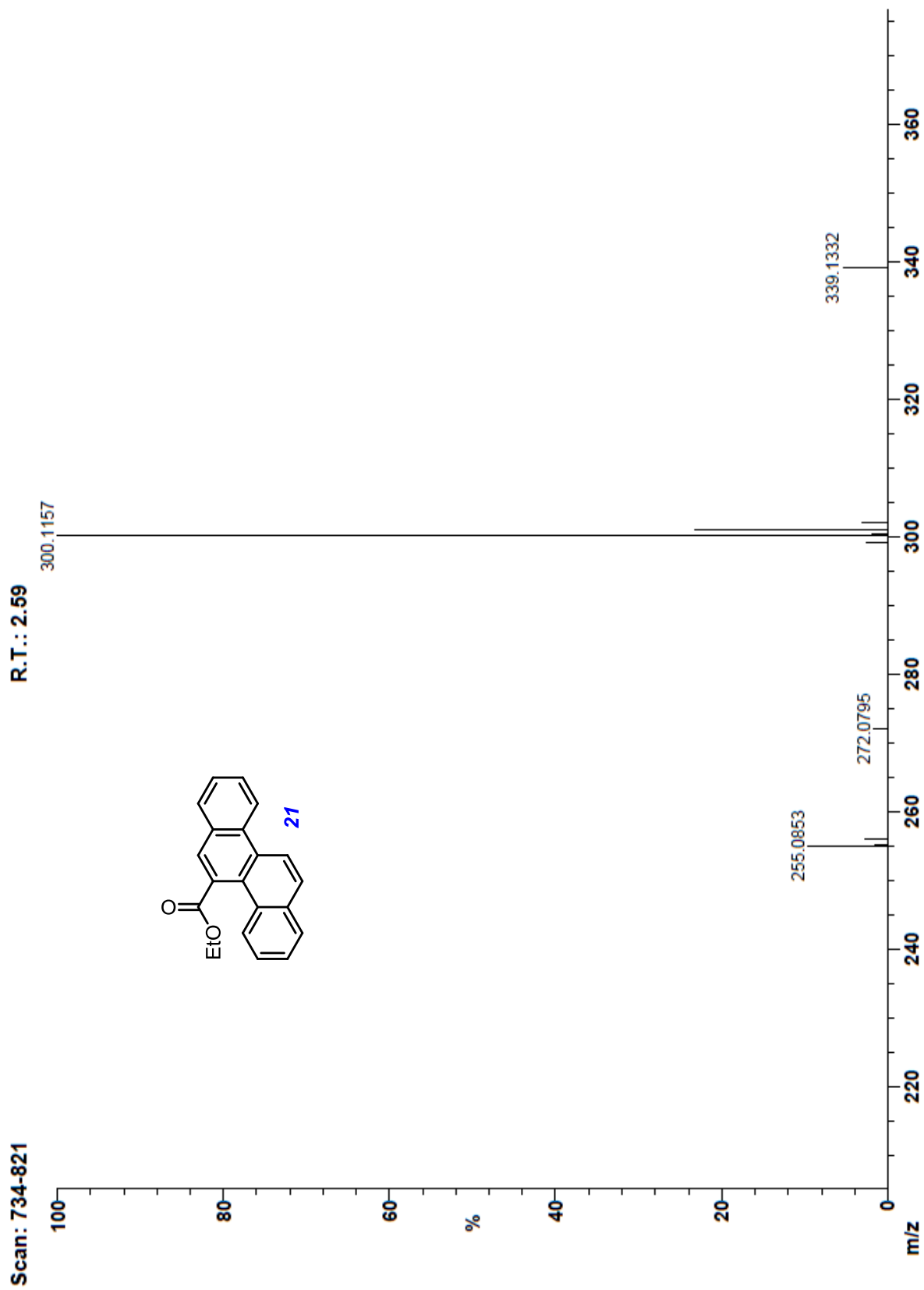


Figure 64: Mass Spectrum of Ethyl chrysene-5-carboxylate

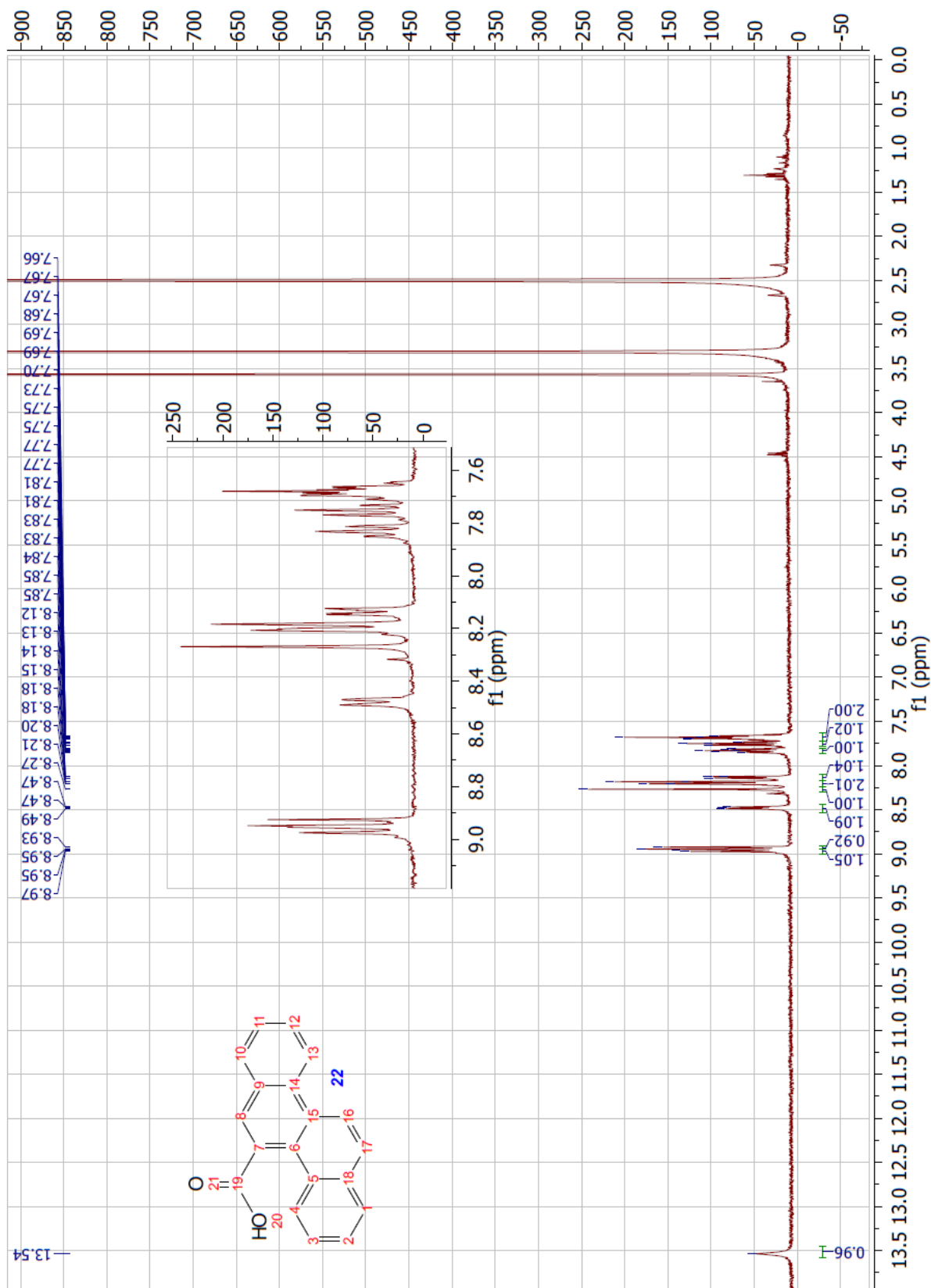


Figure 65:  $^1\text{H}$ -NMR of Chrysene-5-carboxylic acid

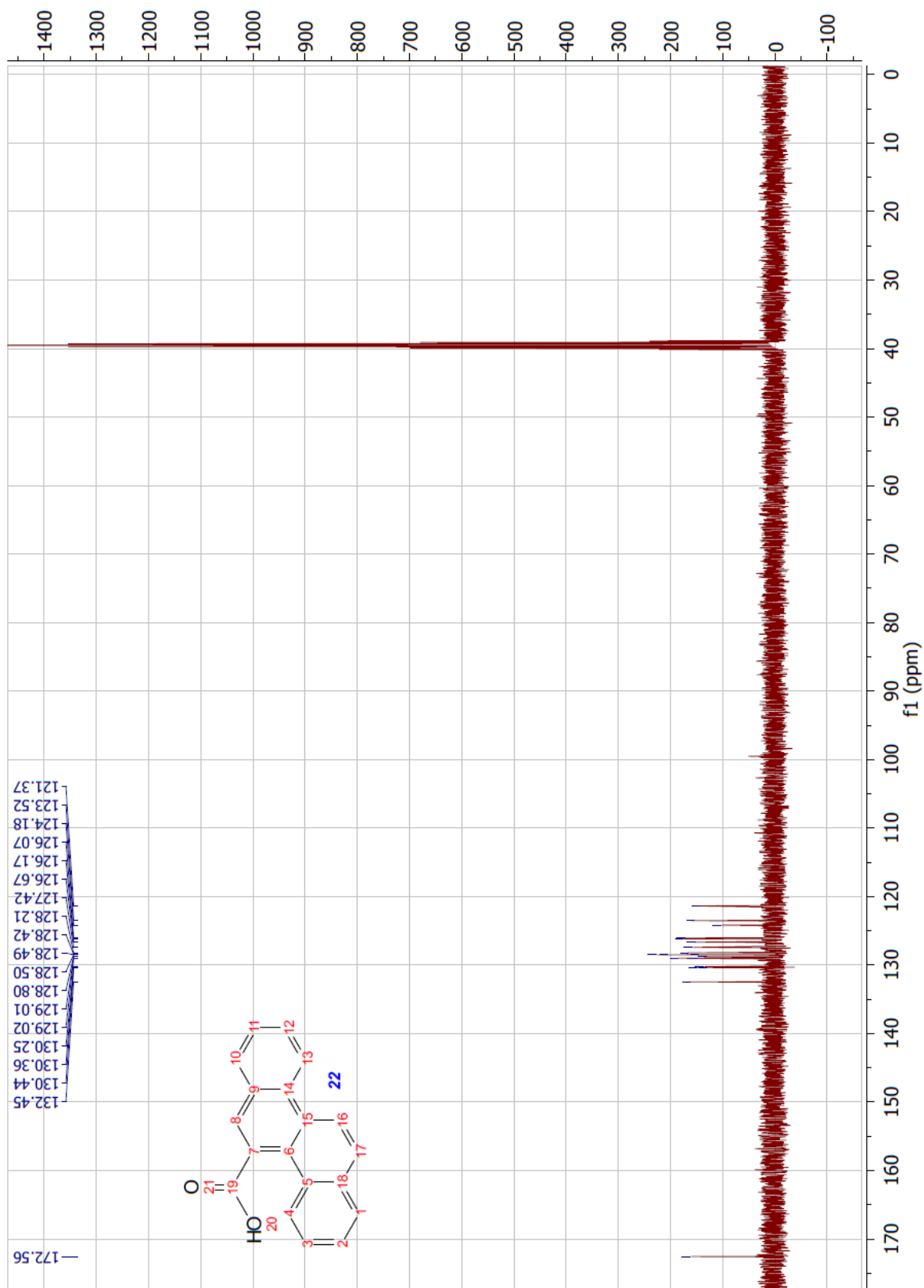


Figure 66:  $^{13}\text{C}$ -NMR of Chrysene-5-carboxylic acid

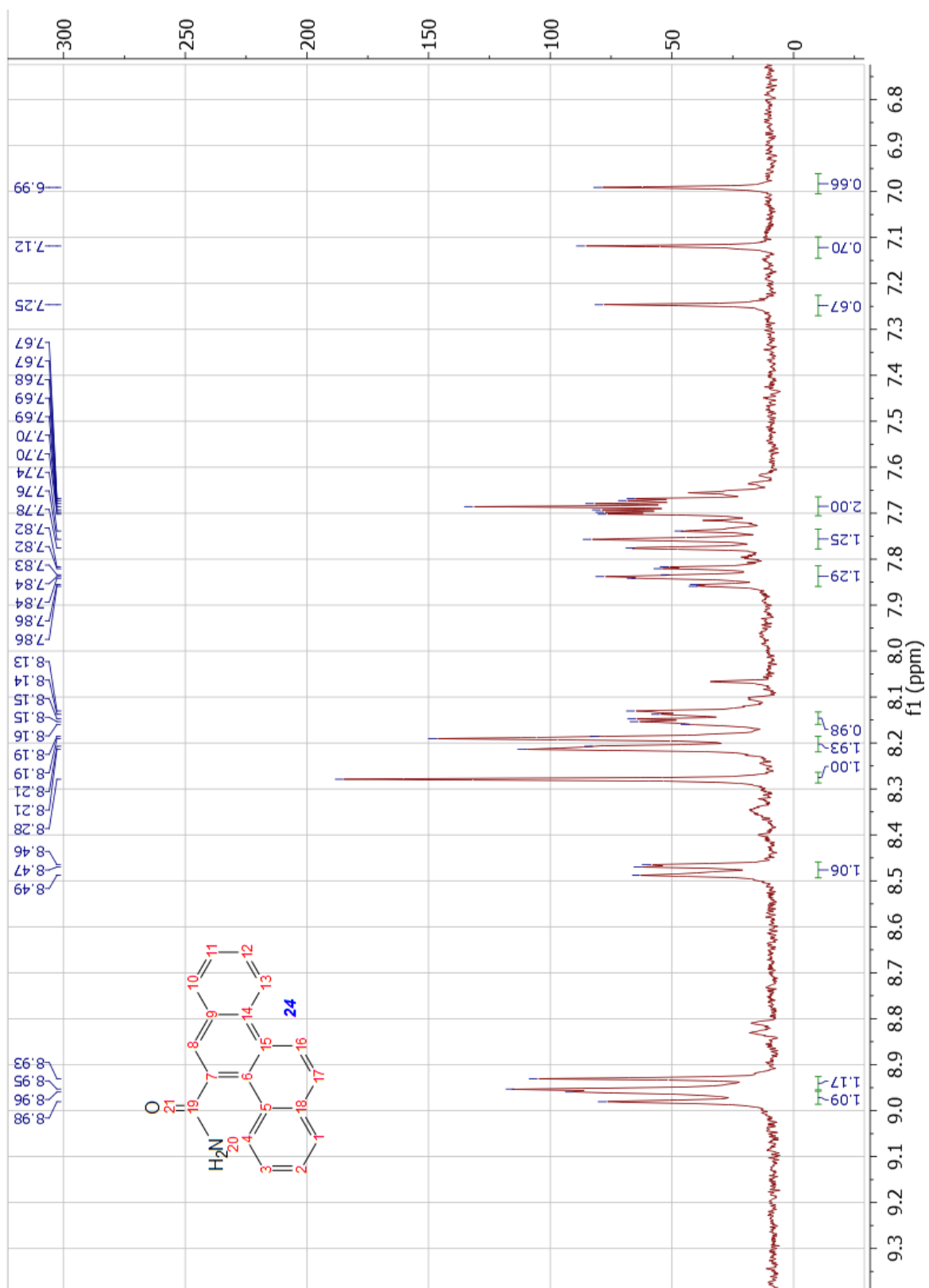


Figure 67:  $^1\text{H}$ -NMR of Chrysene-5-carboxamide

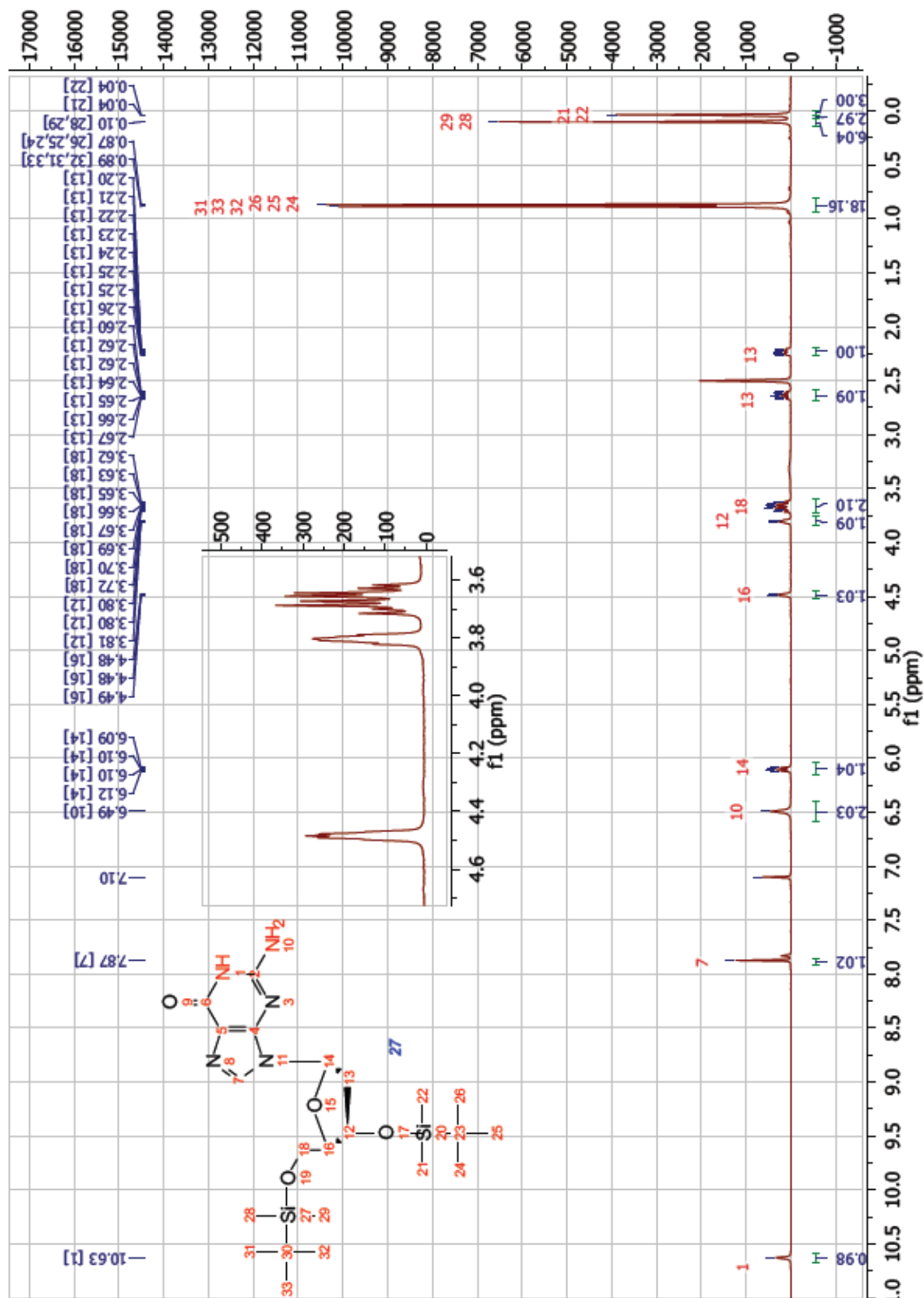


Figure 68: <sup>1</sup>H-NMR of 3',5'-O-Bis(*tert*-butyldimethylsilyl)-2'-deoxyguanosine



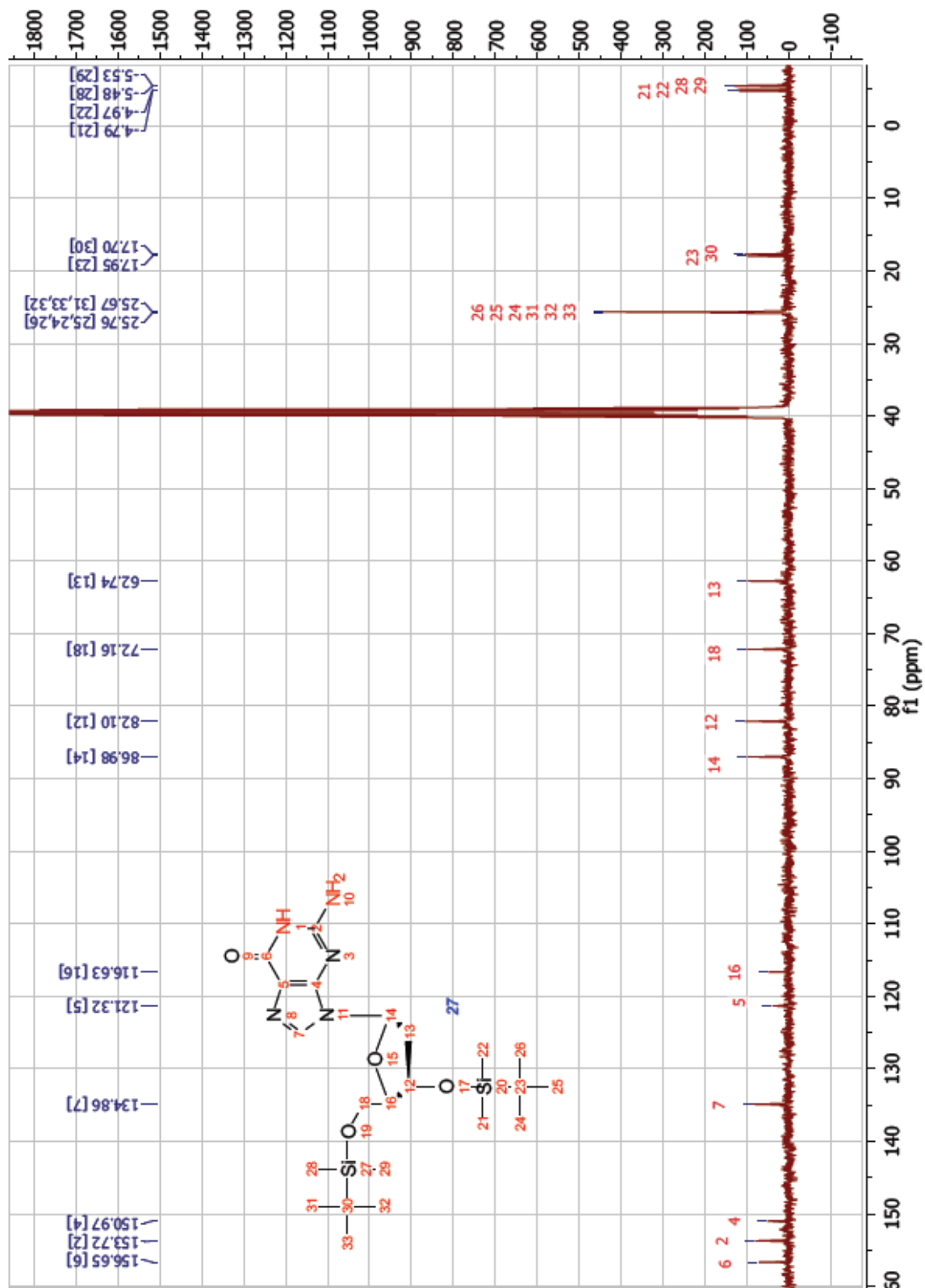


Figure 69: <sup>13</sup>C-NMR of 3',5'-O-Bis(*tert*-butyldimethylsilyl)-2'-deoxyguanosine

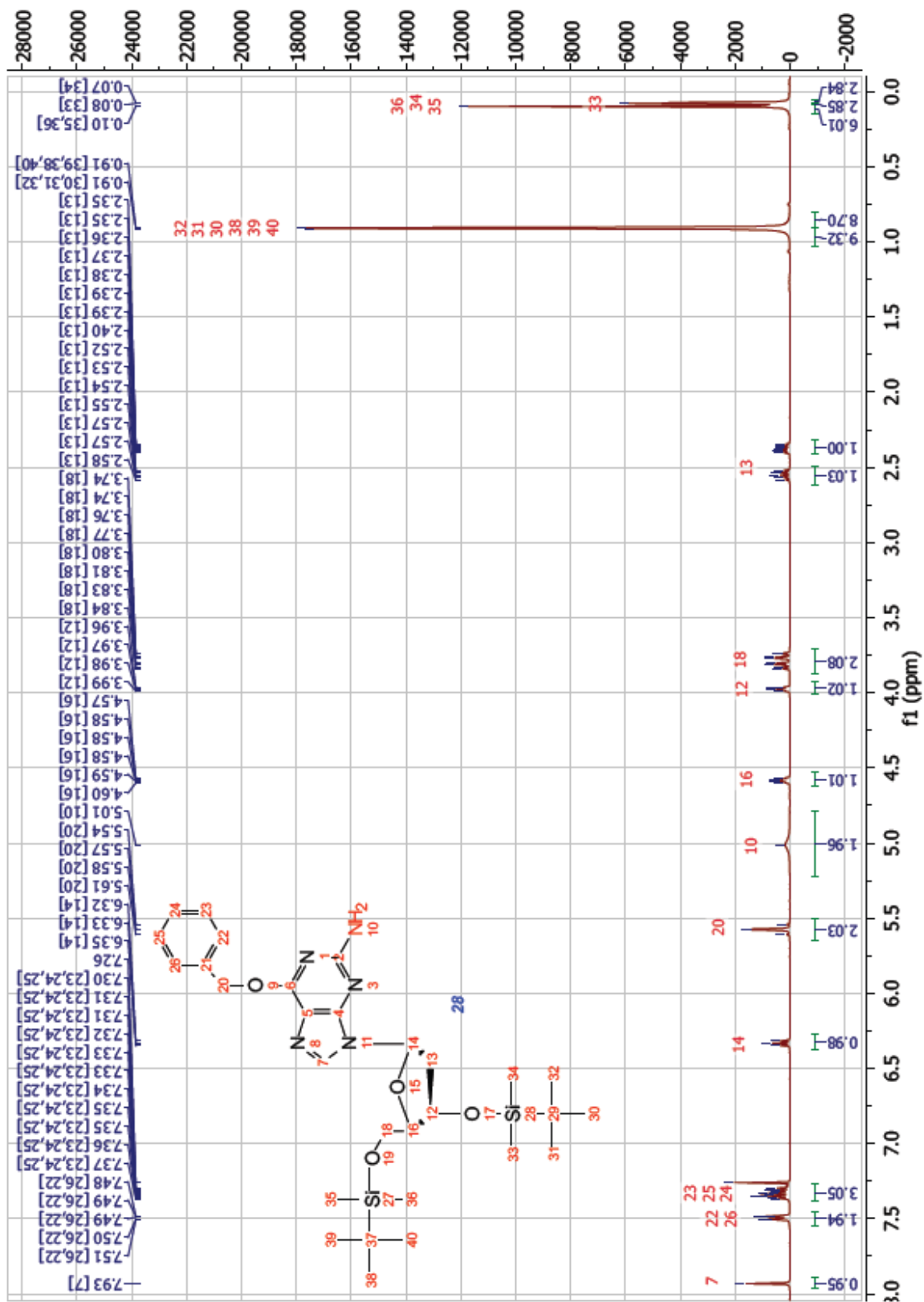
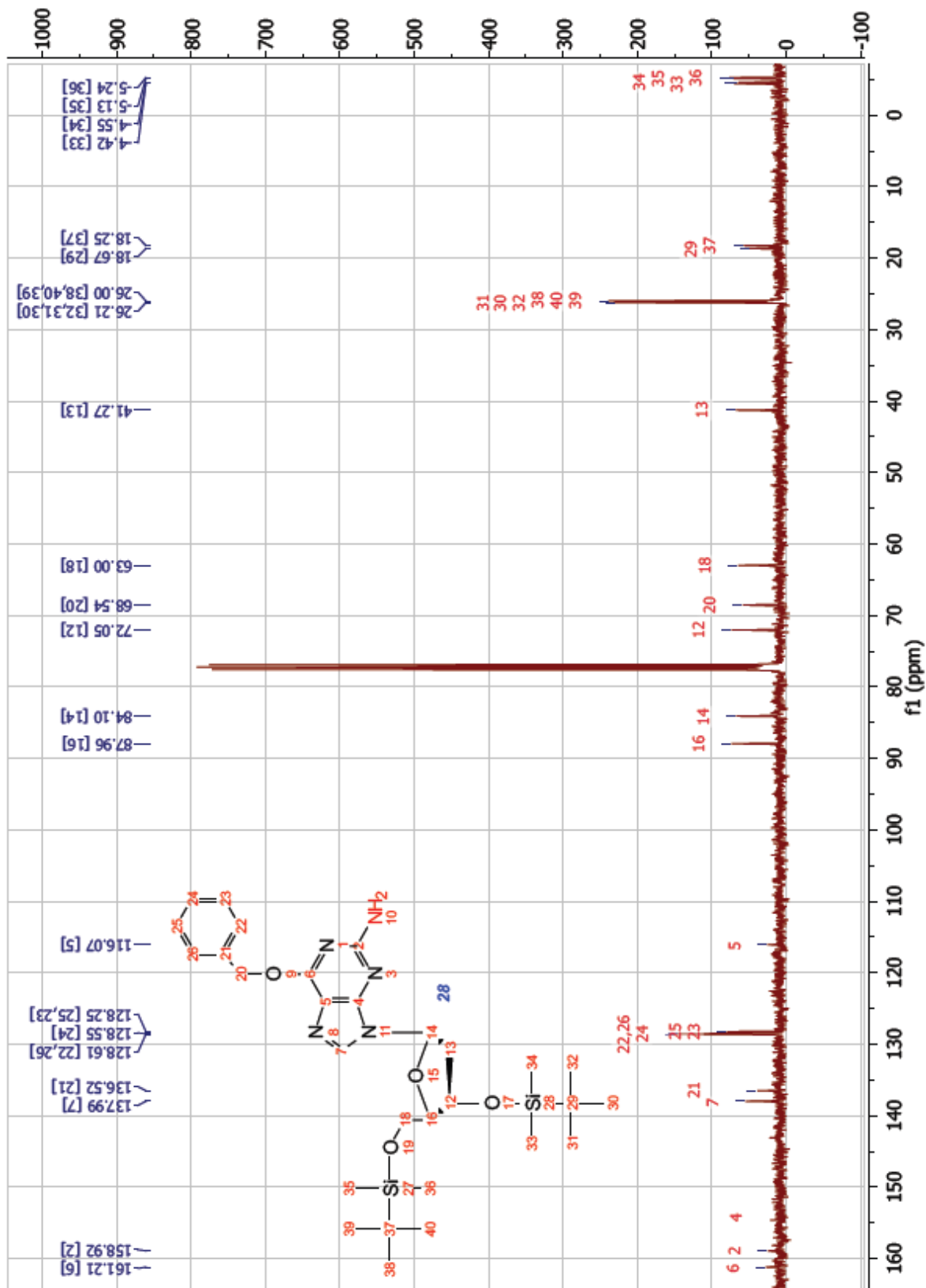


Figure 70:  $^1\text{H}$ -NMR of  $\text{O}^6$ -Benzyl-3',5'-O-bis(*tert*-butyldimethylsilyl)-2'-deoxyguanosine



**Figure 71:**  $^{13}\text{C}$ -NMR of O<sup>6</sup>-Benzyl-3',5'-O-bis(*tert*-butyldimethylsilyl)-2'-deoxyguanosine

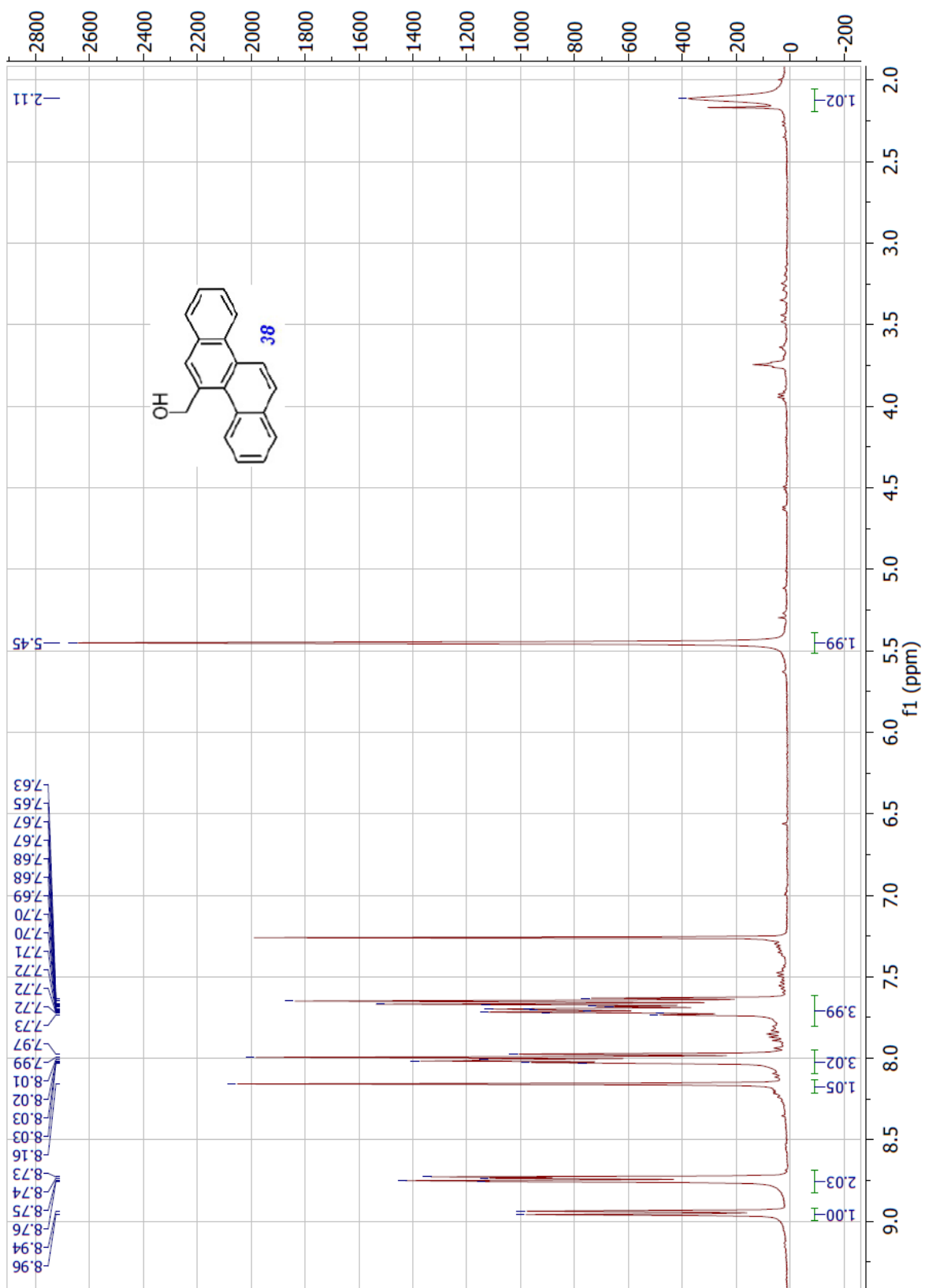


Figure 72:  $^1\text{H}$ -NMR of Chrysen-5-ylmethanol

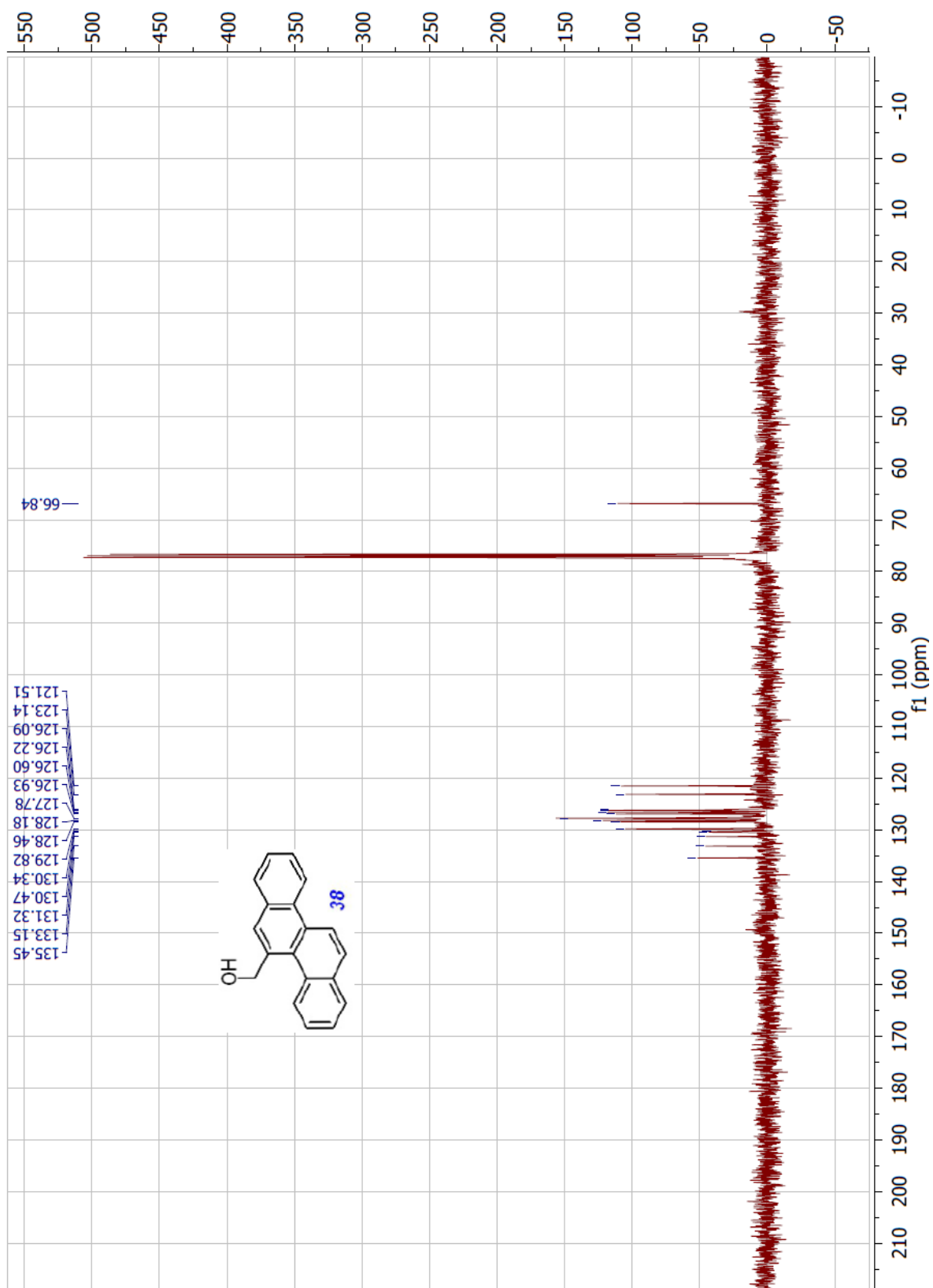


Figure 73:  $^{13}\text{C}$ -NMR of Chrysen-5-ylmethanol

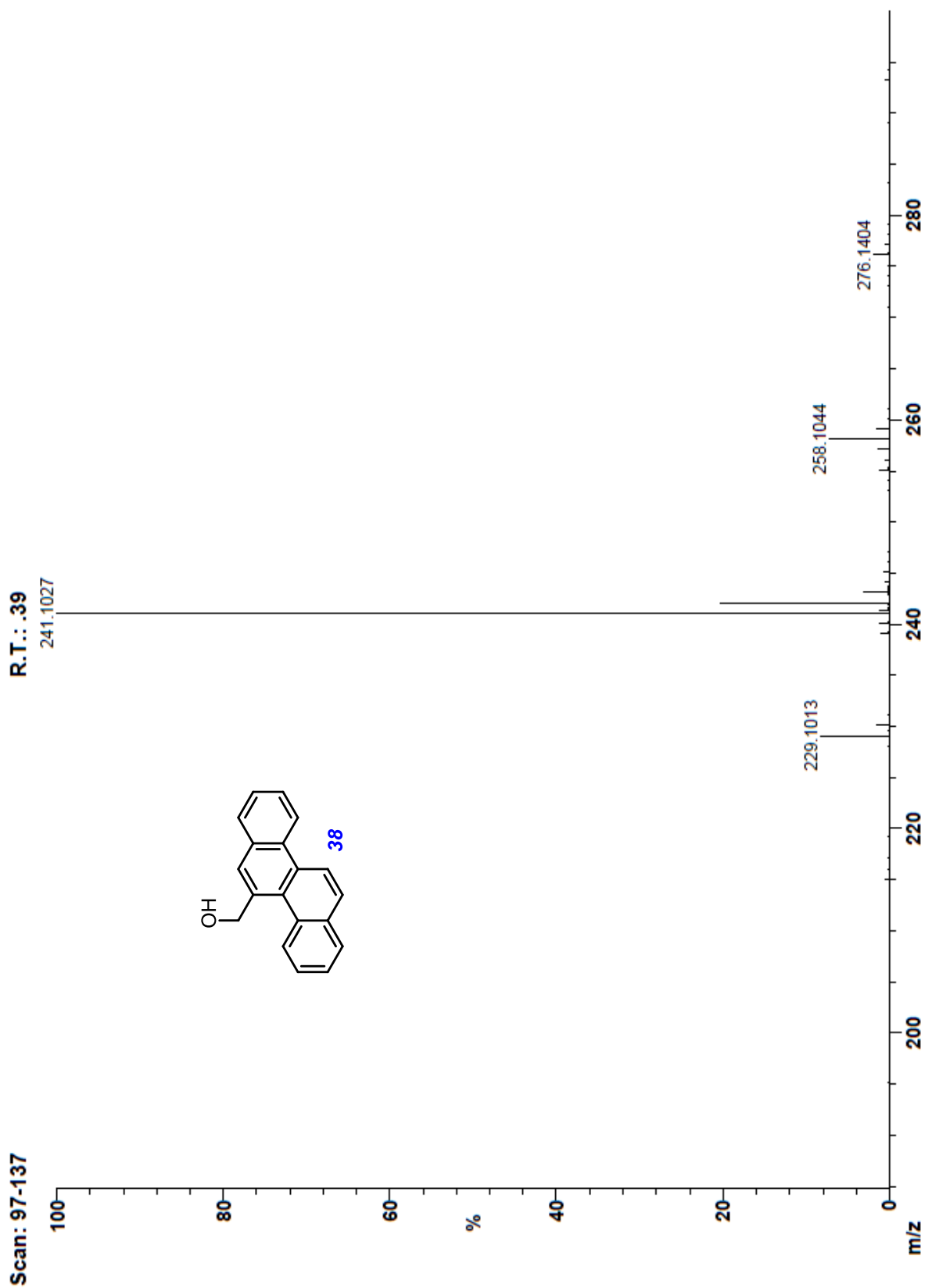


Figure 74: Mass Spectrum of Chrysen-5-ylmethanol

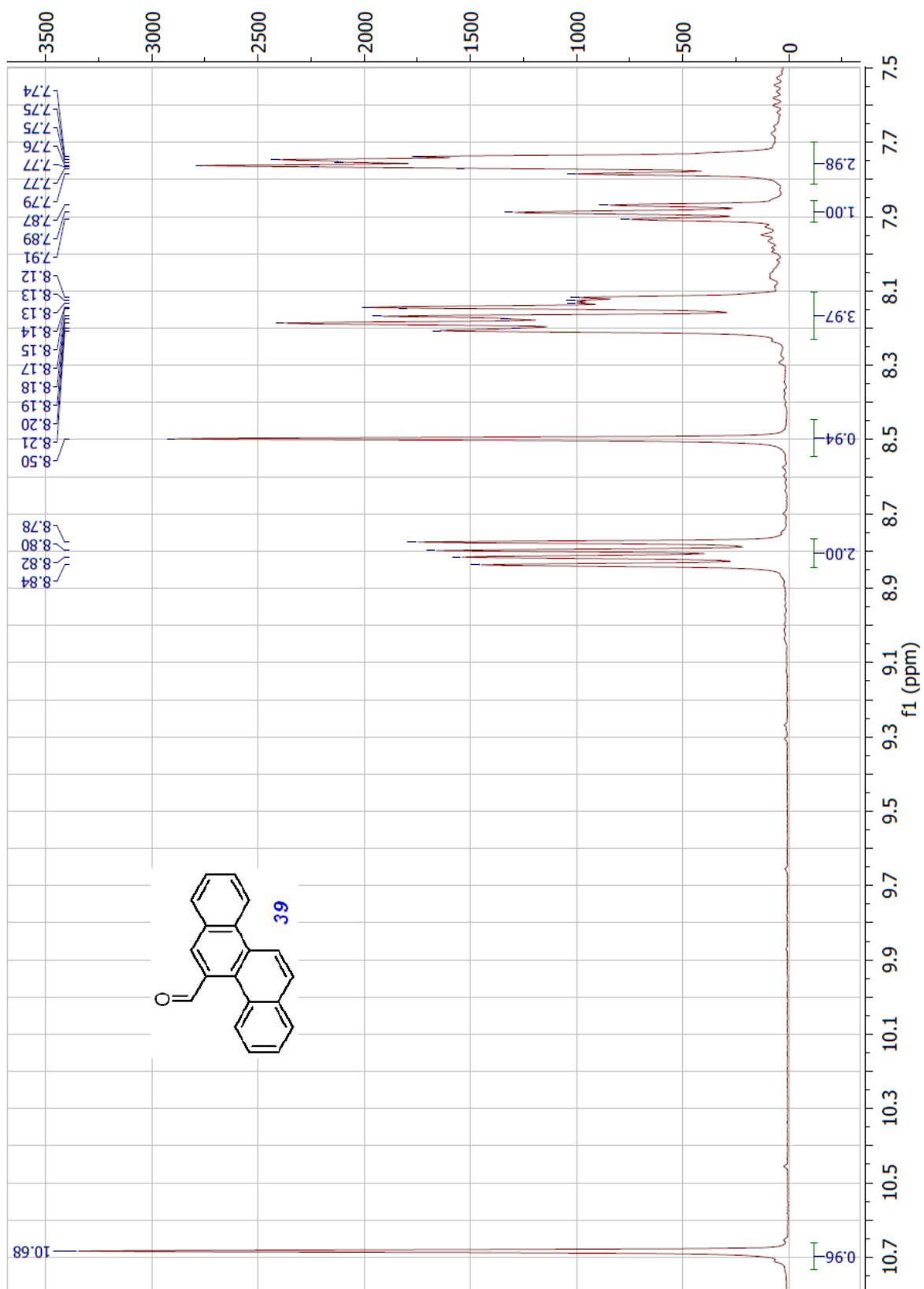


Figure 75:  $^1\text{H}$ -NMR of Chrysene-5-carbaldehyde